

**Reducing the risk for water biota by adsorption of pharmaceuticals and heavy metals
using a fixed-bed column with a novel biochar**

Mehdi Heidari

A Thesis

In the

Department of

Building, Civil, and Environmental Engineering

Presented in Partial Fulfillment of the Requirements

for the Degree of Master of Applied Science (Civil Engineering) at

Concordia University,

Montreal, Quebec, Canada

June 2020

© Mehdi Heidari, 2020

CONCORDIA UNIVERSITY

School of Graduate Studies

This is to certify that the thesis prepared

By: Mehdi Heidari

Entitled: Reducing the risk for water biota by adsorption of pharmaceuticals and heavy metals using a fixed-bed column with a novel biochar

and submitted in partial fulfillment of the requirements for the degree of

Master of Applied Science (Civil Engineering)

complies with the regulations of the University and meets the accepted standards with respect to originality and quality.

Signed by the final Examining Committee:

_____ Chair
Dr. F. Nasiri

_____ External to program
Dr. K. Schmitt

_____ Examiner
Dr. C. An

_____ Examiner
Dr. F. Nasiri

_____ Co-Supervisor
Dr. M. Elektorowicz

_____ Co-Supervisor
Dr. J. Hadjinicolaou

Approved by _____
Dr. Michelle Nokken, Graduate Program Director

July 07, 2020 _____
Dr. Amir Asif, Dean

Gina Cody School of Engineering and Computer Science

Abstract

Reducing the risk for water biota by adsorption of pharmaceuticals and heavy metals
using a fixed-bed column with a novel biochar

Mehdi Heidari, 2020

Pharmaceuticals and heavy metals derived from point sources and non-point sources find their ways into water bodies. One of the important sources of such pollutants is wastewater or effluents from wastewater treatment plants. The presence of pharmaceuticals and heavy metals in the water bodies causes irreversible damages to flora, fauna and human health. Risk assessment plays a vital role in identifying the pollution intensity. The adsorption process is one of the most appropriate processes in eliminating such pollutants from wastewater. In this study, a fixed-bed column is used to verify the feasibility of using a novel biochar material to remove organic (pharmaceuticals) and inorganic (heavy metals) compounds. This study was conducted in 3 phases. In the first phase, the pollution intensity of pollutants in wastewater effluent was evaluated by risk assessment formulas. In the second phase, the impact of the initial concentration, flow rate and bed depth on the laboratory-scale adsorption column performance were investigated. In the third phase, the Adam-Bohart model was used to design the large-scale fixed-bed column. Moreover, the pollution intensity of pollutants was determined. The results clearly indicated that the presence of venlafaxine and heavy metals in wastewater effluent poses adverse effects on aquatic and marine organisms. The adsorption of venlafaxine, Ni, Pb and Cu on biochar in a laboratory-scale column was observed as well as in the larger-scale column. Increasing the initial concentration and bed depth along with decreasing the flow rate caused the adsorption capacity to be on the rise. The removal over 90% of venlafaxine, Ni, Pb and Cu was found at the breakthrough point where the adsorption capacity was increased from 0.8 to 5.4 mg/g for venlafaxine, from 1.92 to 18.24 $\mu\text{g/g}$ for Ni, from 3.84 to 30.72 $\mu\text{g/g}$ for Pb, and from 2.88 to 24 $\mu\text{g/g}$ for Cu. The large-scale column, tested on real effluent at wastewater treatment plant, confirmed the feasibility of using biochar to eliminate 95% of venlafaxine and 90% of Ni, Pb and Cu at the breakthrough point. The adsorption capacity at the breakthrough point was 3051.406 ng/g for venlafaxine, 24.364 $\mu\text{g/g}$ for Ni, 0.1296 $\mu\text{g/g}$ for Pb, and 7.115 $\mu\text{g/g}$ for Cu. The pollution intensity of venlafaxine, Ni, Pb and Cu to aquatic and marine organisms decreased from a high to low risk due to the utilization of novel biochar in the fixed-bed column.

Acknowledgment

Foremost, I am deeply grateful to my supervisor Professor Maria Elektorowicz for her attention, time and support. Not only has Professor Maria Elektorowicz given aid to me as a mother in being faced with abrupt and unexpected changes during such a project, more importantly but she also has conveyed worthwhile knowledge, experience, guidance and proposals to me in conducting such a project in an accurate manner.

I am deeply grateful to my co-supervisor Professor John Hajinicolaou for his time, attention and support.

Also, I wish to acknowledge the financial support from Environment and Climate Change Canada (ECCC) [grant number EDF-PQ-2017G005].

Dedication

To:

My beloved mother: Fatemeh

For nursing me with affection and love and her endless support in my life

Table of contents

List of Figures	viii
List of Tables	xi
List of abbreviations and symbols	xiv
Chapter 1: Introduction	
1.1. Problem statement	1
1.2. Research objectives	2
1.3. Organization of thesis.....	2
Chapter 2: Literature review	
2.1. Pharmaceuticals.....	4
2.2. Heavy metals	8
2.3. Adsorption process.....	20
2.4. Breakthrough curve	23
Chapter 3: Methods and materials	
3.1. Sampling	30
3.2. Production of a novel biochar.....	30
3.2.1. Laboratory-scale.....	30
3.2.2. Large-scale	30
3.3. Analyzing	32
3.4. Column study	32
3.4.1. Laboratory-scale column study	32
3.4.2. MultiVariate Statistical Package (MVSP).....	34
3.4.3. Large-scale column study.....	34
3.5. Risk assessment.....	35
3.5.1. Pharmaceuticals.....	35
3.5.2. Heavy metals	37
Chapter 4: Results and discussions	
4.1. Risk assessment.....	39

4.1.1. Pharmaceuticals.....	39
4.1.2. Heavy metals.....	40
4.2. Laboratory-scale fixed-bed adsorption column (venlafaxine).....	41
4.2.1. Effect of the initial concentration.....	42
4.2.2. Effect of the flow rate.....	44
4.2.3. Effect of the bed height.....	46
4.2.4. Comparison the effect of different factors on the adsorption capacity.....	48
4.3. Design the large-scale PVC column (venlafaxine).....	50
4.4. Laboratory-scale fixed-bed adsorption column (Ni, Pb and Cu).....	54
4.4.1. Effect of the initial concentration.....	54
4.4.2. Effect of the flow rate.....	59
4.4.3. Effect of the bed depth.....	63
4.4.4. Comparison the effect of different factors on the adsorption capacity.....	67
4.5. Design the large-scale PVC column (Ni, Pb and Cu).....	72

Chapter 5: Conclusion and future work

5.1. Conclusion.....	80
5.2. Contribution.....	81
5.3. Future work.....	82
References.....	83

List of Figures

Fig. 1 Conceptual model of the fate of pharmaceuticals in the water bodies.....	4
Fig. 2 Conceptual model of the heavy metals fate in the water bodies.....	8
Fig. 3 Breakthrough curve of adsorption process.....	23
Fig. 4 Methodological approach	29
Fig. 5 Primary materials for biochar production.....	31
Fig. 6 Sustainable process to produce novel biochar on-site.....	31
Fig. 7 Schematic diagram of column system.....	32
Fig. 8 Large-scale PVC column.....	34
Fig. 9 Breakthrough curve at the initial concentration of 10 mg/L.....	42
Fig. 10 Breakthrough curve at the initial concentration of 20 mg/L.....	43
Fig. 11 Breakthrough curve at the initial concentration of 30 mg/L.....	43
Fig. 12 Breakthrough curve at the volumetric flow rate of 2 mL/min.....	45
Fig. 13 Breakthrough curve at the volumetric flow rate of 5 mL/min.....	45
Fig. 14 Breakthrough curve at the volumetric flow rate of 10 mL/min.....	45
Fig. 15 Breakthrough curve at the bed depths of 3 cm.....	47
Fig. 16 Breakthrough curve at the bed depths of 4 cm.....	47
Fig. 17 Cluster analysis of the initial concentration variations at the breakthrough point.....	48
Fig. 18 Cluster analysis of the flow rate variations at the breakthrough point.....	48
Fig. 19 Cluster analysis of the bed depth variations at the breakthrough point.....	48
Fig. 20 Cluster analysis of the initial concentration variations at the exhaustion point.....	49
Fig. 21 Cluster analysis of the flow rate variations at the exhaustion point.....	49
Fig. 22 Cluster analysis of the bed depth variations at the exhaustion point.....	49
Fig. 23 Bed-depth service time (BDST) curve at the removal efficiency of 90%.....	50
Fig. 24 Breakthrough curve for large-scale PVC column.....	52
Fig. 25 Breakthrough curve of Ni at the initial concentration of 60 µg/L.....	56
Fig. 26 Breakthrough curve of Ni at the initial concentration of 70 µg/L.....	56
Fig. 27 Breakthrough curve of Ni at the initial concentration of 80 µg/L.....	56

Fig. 28 Breakthrough curve of Pb at the initial concentration of 60 $\mu\text{g/L}$	56
Fig. 29 Breakthrough curve of Pb at the initial concentration of 70 $\mu\text{g/L}$	57
Fig. 30 Breakthrough curve of Pb at the initial concentration of 80 $\mu\text{g/L}$	57
Fig. 31 Breakthrough curve of Cu at the initial concentration of 60 $\mu\text{g/L}$	57
Fig. 32 Breakthrough curve of Cu at the initial concentration of 70 $\mu\text{g/L}$	57
Fig. 33 Breakthrough curve of Cu at the initial concentration of 80 $\mu\text{g/L}$	58
Fig. 34 Breakthrough curve of Ni at the volumetric flow rate of 2 mL/min.....	60
Fig. 35 Breakthrough curve of Ni at the volumetric flow rate of 5 mL/min.....	61
Fig. 36 Breakthrough curve of Ni at the volumetric flow rate of 10 mL/min.....	61
Fig. 37 Breakthrough curve of Pb at the volumetric flow rate of 2 mL/min.....	61
Fig. 38 Breakthrough curve of Pb at the volumetric flow rate of 5 mL/min.....	61
Fig. 39 Breakthrough curve of Pb at the volumetric flow rate of 10 mL/min.....	62
Fig. 40 Breakthrough curve of Cu at the volumetric flow rate of 2 mL/min.....	62
Fig. 41 Breakthrough curve of Cu at the volumetric flow rate of 5 mL/min.....	62
Fig. 42 Breakthrough curve of Cu at the volumetric flow rate of 10 mL/min.....	62
Fig. 43 Breakthrough curve of Ni at the bed depth of 3 cm	65
Fig. 44 Breakthrough curve of Ni at the bed depth of 4 cm	65
Fig. 45 Breakthrough curve of Pb at the bed depth of 3 cm	65
Fig. 46 Breakthrough curve of Pb at the bed depth of 4 cm	65
Fig. 47 Breakthrough curve of Cu at the bed depth of 3 cm	66
Fig. 48 Breakthrough curve of Cu at the bed depth of 4 cm	66
Fig. 49 Cluster analysis of the initial concentration variations at the breakthrough point of Ni	67
Fig. 50 Cluster analysis of the initial concentration variations at the breakthrough point of Pb	67
Fig. 51 Cluster analysis of the initial concentration variations at the breakthrough point of Cu	67
Fig. 52 Cluster analysis of the flow rate variations at the breakthrough point of Ni	68
Fig. 53 Cluster analysis of the flow rate variations at the breakthrough point of Pb	68
Fig. 54 Cluster analysis of the flow rate variations at the breakthrough point of Cu	68
Fig. 55 Cluster analysis of the bed depth variations at the breakthrough point of Ni	68

Fig. 56 Cluster analysis of the bed depth variations at the breakthrough point of Pb	69
Fig. 57 Cluster analysis of the bed depth variations at the breakthrough point of Cu	69
Fig. 58 Cluster analysis of the initial concentration variations at the exhaustion point of Ni	70
Fig. 59 Cluster analysis of the initial concentration variations at the exhaustion point of Pb	70
Fig. 60 Cluster analysis of the initial concentration variations at the exhaustion point of Cu	70
Fig. 61 Cluster analysis of the flow rate variations at the exhaustion point of Ni	70
Fig. 62 Cluster analysis of the flow rate variations at the exhaustion point of Pb	71
Fig. 63 Cluster analysis of the flow rate variations at the exhaustion point of Cu	71
Fig. 64 Cluster analysis of the bed depth variations at the exhaustion point of Ni	71
Fig. 65 Cluster analysis of the bed depth variations at the exhaustion point of Pb	71
Fig. 66 Cluster analysis of the bed depth variations at the exhaustion point of Cu	72
Fig. 67 Bed-depth service time (BDST) curve at the 90% removal of Ni	73
Fig. 68 Bed-depth service time (BDST) curve at the 90% removal of Pb	73
Fig. 69 Bed-depth service time (BDST) curve at the 90% removal of Cu	74
Fig. 70 Breakthrough curve of Ni for large-scale PVC column.....	76
Fig. 71 Breakthrough curve of Pb for large-scale PVC column.....	76
Fig. 72 Breakthrough curve of Cu for large-scale PVC column.....	77

List of Tables

Table 1 Effects of pharmaceuticals on marine organisms	5
Table 2 Effects of arsenic.....	9
Table 3 Effects of cadmium.....	10
Table 4 Effects of cobalt.....	11
Table 5 Effects of copper.....	12
Table 6 Effects of lead.....	13
Table 7 Effects of mercury.....	13
Table 8 Effects of vanadium.....	15
Table 9 Effects of zinc.....	16
Table 10 Effects of nickel.....	17
Table 11 Effects of chromium.....	17
Table 12 Effects of manganese.....	18
Table 13 Different methods of preparing biochar.....	21
Table 14 Different stages of Pyrolysis process.....	22
Table 15 Mathematical models in describing the fixed-bed adsorption.....	24
Table 16 Column tests for venlafaxine adsorption at the various experimental conditions.....	33
Table 17 Column tests for Ni, Pb and Cu adsorption at the various experimental conditions.....	33
Table 18 Classification of risk quotient (RQ).....	36
Table 19 Assessment factors.....	36
Table 20 Risk assessment of heavy metals.....	40
Table 21 Effects of different factors on breakthrough time and exhaustion time	41
Table 22 Breakthrough and exhaustion points at the initial concentration of 10 mg/L.....	42
Table 23 Breakthrough and exhaustion points at the initial concentration of 20 mg/L.....	42
Table 24 Breakthrough and exhaustion points at the initial concentration of 30 mg/L.....	42
Table 25 Breakthrough and exhaustion points at the flow rate of 2 mL/min.....	44
Table 26 Breakthrough and exhaustion points at the flow rate of 5 mL/min.....	44
Table 27 Breakthrough and exhaustion points at the flow rate of 10 mL/min.....	44

Table 28 Breakthrough and exhaustion points at the bed depth of 3 cm.....	46
Table 29 Breakthrough and exhaustion points at the bed depth of 4 cm.....	46
Table 30 Bed-depth service time (BDST) for at the removal efficiency of 90%.....	50
Table 31 Removal efficiency of venlafaxine in the large-scale column	51
Table 32 Breakthrough and exhaustion points of venlafaxine in the large-scale column	52
Table 33 Breakthrough and exhaustion points of Ni at the initial concentration of 60 µg/L	54
Table 34 Breakthrough and exhaustion points of Ni at the initial concentration of 70 µg/L	54
Table 35 Breakthrough and exhaustion points of Ni at the initial concentration of 80 µg/L	54
Table 36 Breakthrough and exhaustion points of Pb at the initial concentration of 60 µg/L	55
Table 37 Breakthrough and exhaustion points of Pb at the initial concentration of 70 µg/L	55
Table 38 Breakthrough and exhaustion points of Pb at the initial concentration of 80 µg/L	55
Table 39 Breakthrough and exhaustion points of Cu at the initial concentration of 60 µg/L	55
Table 40 Breakthrough and exhaustion points of Cu at the initial concentration of 70 µg/L	55
Table 41 Breakthrough and exhaustion points of Cu at the initial concentration of 80 µg/L	55
Table 42 Breakthrough and exhaustion points of Ni at the flow rate of 2 mL/min.....	59
Table 43 Breakthrough and exhaustion points of Ni at the flow rate of 5 mL/min.....	59
Table 44 Breakthrough and exhaustion points of Ni at the flow rate of 10 mL/min.....	59
Table 45 Breakthrough and exhaustion points of Pb at the flow rate of 2 mL/min.....	59
Table 46 Breakthrough and exhaustion points of Pb at the flow rate of 5 mL/min.....	60
Table 47 Breakthrough and exhaustion points of Pb at the flow rate of 10 mL/min.....	60
Table 48 Breakthrough and exhaustion points of Cu at the flow rate of 2 mL/min.....	60
Table 49 Breakthrough and exhaustion points of Cu at the flow rate of 5 mL/min.....	60
Table 50 Breakthrough and exhaustion points of Cu at the flow rate of 10 mL/min.....	60
Table 51 Breakthrough and exhaustion points of Ni at the bed depth of 3 cm	64
Table 52 Breakthrough and exhaustion points of Ni at the bed depth of 4 cm	64
Table 53 Breakthrough and exhaustion points of Pb at the bed depth of 3 cm	64
Table 54 Breakthrough and exhaustion points of Pb at the bed depth of 4 cm	64
Table 55 Breakthrough and exhaustion points of Cu at the bed depth of 3 cm	64

Table 56 Breakthrough and exhaustion points of Cu at the bed depth of 4 cm	64
Table 57 Bed-depth service time (BDST) for Ni at the removal efficiency of 90%.....	72
Table 58 Bed-depth service time (BDST) for Pb at the removal efficiency of 90%.....	72
Table 59 Bed-depth service time (BDST) for Cu at the removal efficiency of 90%	73
Table 60 Equation of Bed-depth service time (BDST) curve at the removal efficiency of 90%	75
Table 61 Adsorbent utilization in the large-scale PVC column	75
Table 62 Removal efficiency of Ni in the large-scale column	75
Table 63 Removal efficiency of Pb in the large-scale column	75
Table 64 Removal efficiency of Cu in the large-scale column	75
Table 65 Breakthrough and exhaustion points of Ni in the large-scale column	77
Table 66 Breakthrough and exhaustion points of Pb in the large-scale column	77
Table 67 Breakthrough and exhaustion points of Cu in the large-scale column	77
Table 68 Risk assessment of heavy metals.....	78

List of abbreviations and symbols

BDST	Bed depth service time
C_0	Initial concentration
C_t	Effluent concentration
Cu	Copper
EC ₅₀	The median concentration
HCL	Hydrochloric acid
HPI	Heavy metal pollution index
KOH	Potassium hydroxide
Ni	Nickel
NOEC	No observed effect concentration
Pb	Lead
PNEC	Predicted no-effected concentration
PVC	Polyvinyl chloride
Q	Flow rate
q	Adsorption capacity
Q _i	Sub-index
RQ	Risk quotient
S _i	Standard value
t	Time
V	Loading rate
W _i	Unit weight
Y	Removal efficiency
Z	Bed depth

Chapter 1: Introduction

1.1. Problem statement

Pharmaceuticals and heavy metals derived from different point sources and non-point sources are eventually carried by rivers into water bodies including oceans, seas and lakes (Fakhraee et al. 2015; Heidari 2019; Karbassi and Heidari 2015; Vaezi 2016). The accumulation of such pollutants in the aquatic and marine environments has been on the increase which poses a serious threat to the flora, fauna and human health (Heidari 2019; Karbassi et al., 2013; Valikhani Samani et al., 2014). Pharmaceuticals and heavy metals have been detected in the liver, kidney and gill of fishes. DNA damage, impairment of reproductive capacity, oxidative stress, cell death, hair cell death, delay in maturation, reduction in fecundity, mortality etc. are considered as deleterious impacts of pharmaceuticals and heavy metals (Duarte et al., 2020; Gautam et al., 2018; Ghosh et al., 2018; Li et al., 2018; Liu et al., 2018; Mezzelani et al., 2020; Nunes et al., 2020). One of the important sources of pharmaceuticals and heavy metals is wastewater or effluent of wastewater. As a result, the elimination of these pollutants from wastewater plays a vital role in enriching the condition of water bodies. There are diverse processes including adsorption process, biological process, filtration, advanced oxidation process and chlorination, and the combination of different processes which can be used for water purification and wastewater treatment (Abazari 2019; Fang et al., 2018; Liu et al., 2018a; Nasseh et al., 2019; Xu et al., 2018a; Zhang et al., 2019b; Zhu et al., 2017; Zhu et al., 2015). Among such methods, the adsorption process is well-known for simplicity of operation and cost-effectiveness (Ahmed et al., 2017a; Appavu et al., 2018; Mandal et al., 2019; Okoli and Ofomaja, 2019; Tien et al. 2018). Batch and column studies are considered as two ways to adsorption studies. The data gained from a batch study is limited to the laboratory scale and thus cannot be applied in industrial systems. Nevertheless, the column study provides data for direct applications in industrial systems. In the last few years, the adsorption of pharmaceuticals and heavy metals on the different adsorbents in the fixed-bed column has been conducted (Abdolali et al., 2017; Alimohammadi et al., 2016; Bakar et al., 2019; Guocheng et al., 2011; Hajilari et al., 2019). On the other hand, the results have indicated that the risk of such pollutants in water bodies is high. As a consequence, comprehensive investigations on utilizing appropriate adsorbent in the column and the column performance should be conducted in producing a pivotal remedy to eliminate pharmaceuticals and heavy metals from different types of wastewaters or effluent of wastewaters.

1.2. Research objectives

The main objective of this study was to assess the feasibility of using a novel biochar for the emerging pollutant removal at a wastewater treatment plant. The specific objectives were:

1. Assessing adsorption capacity of a representative pharmaceutical using fixed-bed column
2. Assessing adsorption of representative heavy metals on biochar in a fixed-bed column
3. Defining parameters affecting the adsorption efficiency
4. Designing a large-scale column based on a model
5. Conducting risk assessment to aquatic biota before and after treatment

1.3. Organization of thesis

The thesis consists of five chapters. The problem statement along with research objectives were described in chapter 1. A comprehensive literature review about the sources, effects, elimination method and column study of pharmaceuticals and heavy metals were provided in chapter 2. Sampling and analysis, installation of laboratory-scale column, design of large-scale column and risk assessment methods were explained as method and materials in chapter 3. The results of utilizing laboratory-scale column under various experimental conditions, designing of large-scale column and risk assessment of pollutants are explained and discussed in chapter 4. Conclusion of research novelty and recommendations for future work are provided in chapter 5.

Chapter 2: Literature review

2.1. Pharmaceuticals

Pharmaceuticals derived from various point sources and non-point sources are carried by rivers into water bodies including oceans, seas and lakes (Fakhraee et al. 2015; Heidari et al. 2015; Karbassi et al. 2016; Vaezi et al. 2014) (Fig. 1).

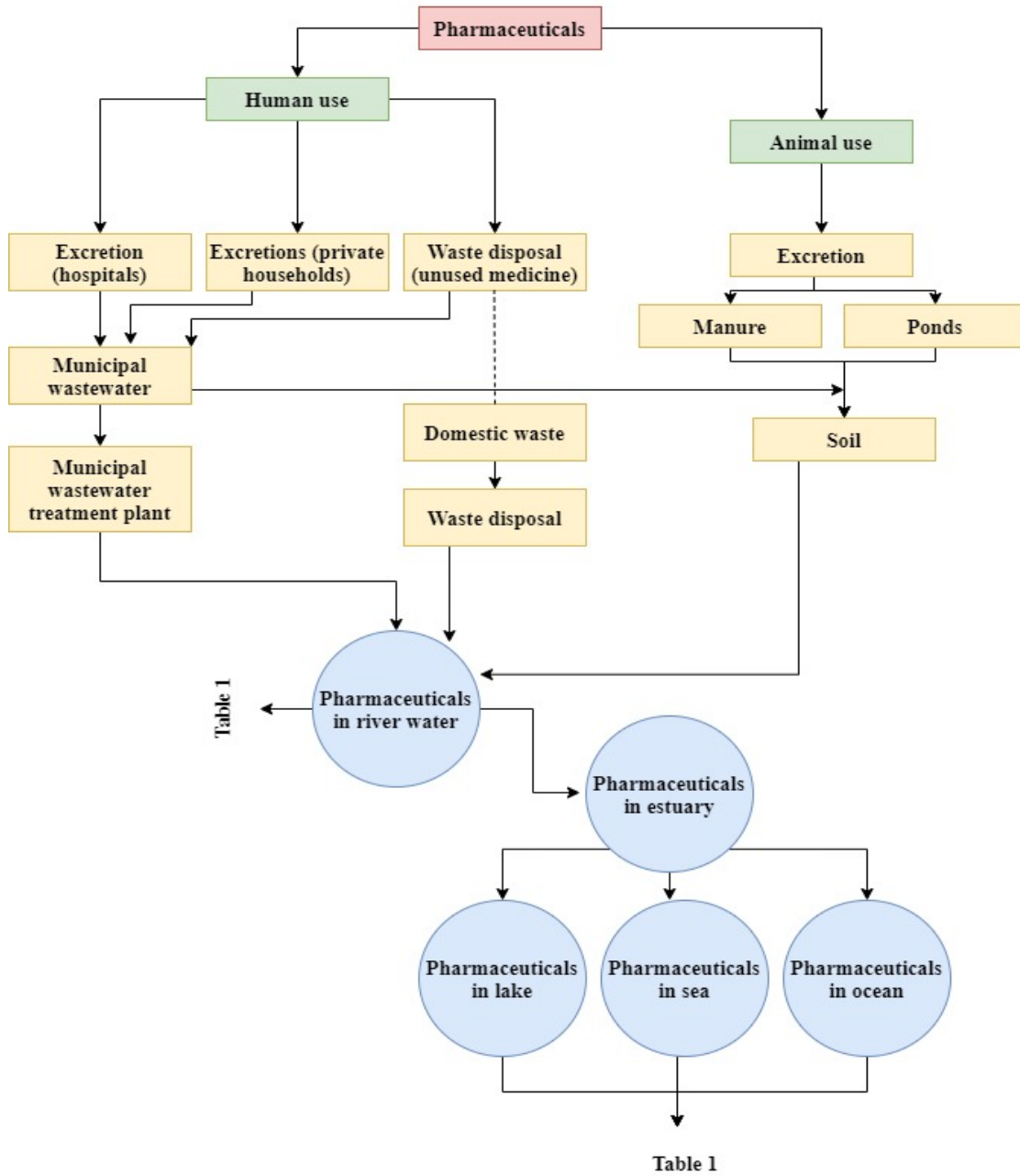


Fig. 1 Conceptual model of the fate of pharmaceuticals in the water bodies

Wastewater or effluent of wastewater is considered as one of the important sources of pharmaceuticals. Pharmaceuticals are detected in low ng/L to high µg/L concentrations in waste and surface water (Lonappan et al., 2019; Zhang et al., 2008). In the last few years the pollution intensity of such contaminants in marine and aquatic environments has been on the rise (Farajnejad et al. 2017; Heidari et al. 2017; Vaezi et al., 2016; Valikhani Samani et al., 2014). Pharmaceuticals have been detected in the liver, kidney, gill of fishes etc. The presence of such toxic pollutants in aquatic ecosystems has long lasting deleterious effects on flora, fauna and human health (Heidari 2019; Karbassi and Heidari 2015; Karbassi et al., 2014; Karbassi et al., 2013) (Table 1). As a result, such pollutants should be removed from the environmental compartments.

Table 1 Effects of pharmaceuticals on marine organisms

Pharmaceuticals	Utilization	Examples	Effects
Analgesics	Inhibition of individual pain pathways (local anesthesia), render a patient unconscious for surgical procedures (general anesthesia), etc.	Opioids, non-opioids etc.	DNA damage, alteration of immunological parameters (lysosomal membrane stability, granulocytes-hyalinocytes content, phagocytosis activity), Inhibition of striking prey efficiency, Inhibition of final biomass, growth inhibition, mortality, Foot detachment, Spawning induction, immobility, inhibition fertilization, oxidative stress, genotoxic damage, transcriptional changes in genes, Inhibition of striking prey efficiency, impairment of endocrine system, impairment of reproductive capacity, decrement of byssus strength and energy, inhibition of synthesis of proteins, inhibition of synthesis of nucleic acids, disruption of mitotic spindle, cell death, inhibition of DNA replication etc.
Antibacterials	An antibacterial as a type of antimicrobial substance destroys bacteria and suppresses the growth of bacteria.	Ciprofloxacin, Spectinomycin, etc.	
Anticonvulsants	Anticonvulsant as a drug can be used to the treatment of epileptic seizure, bipolar disorder and borderline personality disorder.	Brivaracetam, Carbamazepine etc.	
Antidementia agents	Antidementia drugs as a pharmaceutical agent are approved for treatment of dementia.	Donepezil, Galantamine etc.	
Antidepressants	An antidepressant drug can be used in the treatment of depressive disorder, anxiety disorders, chronic pain conditions and some addictions.	Venlafaxine, Citalopram etc.	
Antidotes and antitoxins	Treatment of some poisoning	Acetylcysteine, activated charcoal etc.	
Antiemetics	Antiemetic as a heterogeneous group of drugs can be used to treat various nausea and vomiting caused by motion sickness, severe cases of the stomach flu (gastroenteritis) etc.	Aprepitant, dexamethasone etc.	
Antifungals	The antifungals as a large and diverse group of drugs are used in treatment of fungal infections.	Clotrimazole, econazole etc.	

Pharmaceuticals	Utilization	Examples
Anti-inflammatory agents	Anti-inflammatory drugs give aid to treat treating multisystem inflammatory disorders.	Aspirin, ibuprofen etc.
Antimigraine agents	Treatment of severe cases of migraine attack.	Methysergide, zolmitriptan etc.
Antimyasthenic agents	Treatment of myasthenia gravis	Mestinon Timespan etc.
Antimycobacterials	Treatment of mycobacteria infections	Rifampin, isoniazid etc.
Antineoplastics	Treatment of cancer	Azacitidine, capecitabine etc.
Antiparasitics	Treatment of parasitic infections	Ivermectin etc.
Antiparkinson agents	Treatment of Parkinson's disease	Ropinirole, benzatropine etc.
Antipsychotics	Treatment of psychosis, principally in schizophrenia and bipolar disorder.	Risperidone, olanzapine etc.
Antivirals	Treatment of viral infections	Abacavir, amplitgen etc.
Anxiolytic (anti-anxiety) agents	Inhibition of inhibits anxiety	Amitriptyline, Doxepin etc.
Bipolar agents	Treatment of bipolar disorder	Olanzapine, aripazole etc.
Blood glucose regulators	Treatment of diabetes mellitus	Insulin, biguanides etc.
Blood products	Treatment of hemophilia	blood components, plasma derivatives etc.
Cardiovascular agents	Treatment of different heart disorders or diseases of the vascular system	Chlorothiazide, amiloride etc.
Central nervous system agents	Treatment of anxiety and insomnia	Anesthetics, anticonvulsants etc.
Dental and oral agents	Treatment of a variety of diseases involving the oral cavity (mouth)	Fluorides, benzodiazepines etc.
Dermatological (skin) agents	Treatment of skin conditions	Ketoconazole, anthralin etc.
Enzyme replacement agent	Treatment of lysosomal storage diseases	Velaglucerase alfa etc.
Gastrointestinal agents	Treatment of gastrointestinal disorders	Antidiarrheals, laxatives etc.
Genitourinary agents	Treatment of conditions of the reproductive organs and excretory system or urinary tract	Darifenacin, solifenacin etc.
Hormonal agents (adrenal)	Treatment of cancers	Aldosterone, cortisol etc.

Pharmaceuticals	Utilization	Examples
Immunological agents	Preventing graft rejection	Immune globulins, immunostimulants etc.
Inflammatory agents	Reduction in inflammation	Celecoxib, diclofenac etc.
Antimetabolite drugs	Treatment of leukemia, cancers of the breast, ovary, and the gastrointestinal tract, as well as other types of cancers	Floxuridine, fludarabine etc.
Ophthalmic (eye) agents	Treatment of eye infections	Moxifloxacin, besifloxacin etc.
Otic (ear) agents	Treatment of outer ear infections	Ciprofloxacin, hydrocortisone etc.
Respiratory tract agents	Preventing respiratory diseases	Antiasthmatic combinations
Sedatives and hypnotics	Treatment of insomnia	Barbiturates, benzodiazepines etc.
Skeletal muscle relaxants	Reducing tension in muscles	Baclofen, methocarbamol etc.
Therapeutic nutrients, minerals, and electrolytes	Preventing vitamin deficiency, renal problems, diarrhea and vomiting	Magnesium sulfate, calcium carbonate etc.

Note: data generated based on (Bebiano and da Fonseca 2020; Bonnefille et al., 2018; Byeon et al., 2020; Estévez-Calvar et al., 2017; Fabbri and Franzellitti 2016; Fong et al., 2015; Fong and Hoy 2012; Halm-Lemeille and Gomez 2016; Hodkovicova et al., 2020; Ikert and Craig 2020; Klatte et al., 2017; Nunes et al., 2020; Duarte et al., 2020; Malve 2016; Menon et al., 2020; Minguez et al., 2015; Prichard and Granek 2016; Renault 2015; Sangion and Gramatica 2016)

Among the pharmaceuticals measured in RABEL wastewater treatment plant effluent, the concentration of venlafaxine was particularly high (Zojaji 2020). Venlafaxine is considered as an antidepressant drug for treatment of major depressive disorder, anxiety and panic disorder (Olver et al., 2004). Moreover, venlafaxine is a subclass of norepinephrine reuptake inhibitor (SNRI) (Hodkovicova et al., 2020). Venlafaxine derived from a wide variety sources (e.g. domestic, hospital and industrial effluents etc.) finds its way into water bodies (Gros et al., 2012; Valcárcel et al., 2011; Maulvault et al., 2018). In the last few years the pollution intensity of such an antidepressant drug in water bodies has been on the increase which have posed a serious threat to marine and aquatic organisms even at low concentrations (Bueno et al., 2014; Halm-Lemeille and Gomez 2016; Maulvault et al., 2019). In other words, increasing the accumulation of pharmaceuticals, especially venlafaxine in marine environments might causes serious ecological and human health risks (Maulvault et al., 2018).

2.2. Heavy metals

Conceptual model gives aid to possess a profound thought about the heavy metals fate in water bodies (Heidari 2019). Conceptual model of the heavy metals is shown in Fig. 2 (Heidari 2019).

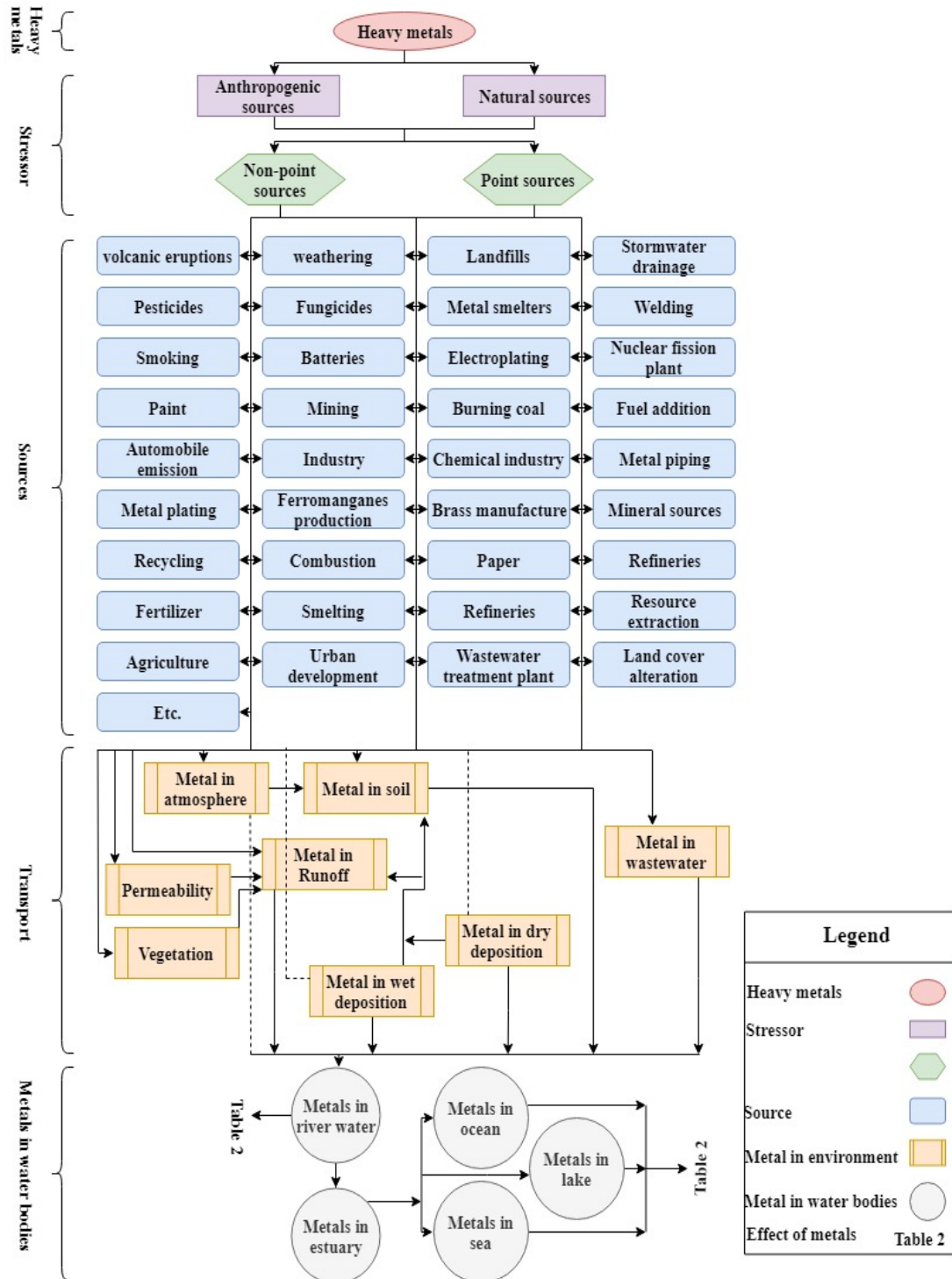


Fig. 2 Conceptual model of the heavy metals fate in the water bodies

Heavy metals derived from different natural and anthropogenic sources are eventually carried by rivers into oceans, seas and lakes (Heidari 2019; Fakhraee et al., 2015; Vaezi et al., 2016; Vaezi et al., 2014). The presence of heavy metals as dangerous environmental pollutants in marine ecosystems poses serious ecological risk concerns for aquatic organisms (Billah et al., 2017; Fu et al., 2017; Naifar et al., 2018). Due to rapid population growth, industrialization, urbanization and economic development in a wide variety of countries all across the world, high concentration of essential elements in conjunction with low concentration of non-essential elements have become a serious problem in marine ecosystems (Cipro et al., 2018; Frontalini et al., 2018; Fuentes-Gandara et al., 2018; Souza et al., 2018; Stankovic et al., 2014). The characteristics of heavy metals including toxicity, bio-concentration and non-degradation play an important role in posing irreversible damages to marine organisms, especially fish (Green et al., 2018; Rajeshkumar et al., 2018). Moreover, the human health condition can be impacted by exposure to toxic elements (Ding et al., 2018; Fuentes-Gandara et al., 2018; Wang et al., 2018). As a consequence, such pollutants should be removed from water bodies. Deleterious impacts of heavy metals on human health, marine and aquatic organisms are indicated in Tables 2 to 12.

Table 2 Effects of arsenic

Detrimental effects on human health	Detrimental effects on marine and aquatic organisms
Disordering nervous system	Reducing the innate immune system
Cardiovascular diseases	Bulging of tip of gill filaments
Skin cancer	Oxidative stress
Lung cancer	Reducing embryonic development
Urinary bladder cancer	Cell death
Skin lesions	Reducing growth
Melanosis	DNA damage
Leucomelanosis	Decreasing metabolism
Breast cancer	Protein inactivation
Keratosi	Enzyme inactivation
Liver cancer	Impairment of ATP synthesis
Perturbation of cell membrane stability	Impairment of the endocrine system
Perturbation of energy cycle	Impairment of the cortisol response
Perturbation of methylation processes	Death
Substitution of zinc	Distortion of the shape gill filament

DNA damage	Disturbing the transcriptional levels of antioxidant related genes
Loss of protein action	
Diabetes	
Kidney dysfunction	

Note: data were generated based on (Abadi et al., 2018; Adeyemi et al., 2015; Bhowmick et al., 2018; Coppola et al., 2018; Dong et al., 2018; Elia et al., 2018; Khairul et al., 2017; Moreira et al., 2018; Moreira et al., 2016; Moslen and Miebaka 2016; Mukherjee 2017; Olivares et al., 2016; Osborne et al., 2017; Rodríguez-Moro et al., 2018; Sarkar et al., 2017; Zuo et al., 2018)

Table 3 Effects of cadmium

Detrimental effects on human health	Detrimental effects on marine and aquatic organisms
Kidney dysfunction	Respiration imbalance
Renal cancer	Osmoregulation imbalance
Prostate cancer	Delay in maturation
Breast cancer	Reducing fecundity
Lung cancer	Inhibition of activation and sperm motion
Liver cancer	Impairment of social and escape behavior
Bladder cancer	Hypocalcaemia
Skin cancer	Cellular stress
Skin lesions	Cell death
Keratosis	Neuronal cell death
Pigmentation	Oxidative stress
Nausea	Immunotoxicity
Vomiting	Impairing steroidogenesis
Reducing production of erythrocytes	Lipid peroxidation
Reducing leukocytes	DNA damage
Reproductive system damage	Reducing the uptake of essential nutrients
Abnormal heartbeat	Abnormality in body size
Skeletal system damage	Increasing heart rate
Blood vessels damage	Imbalance regulation of ion
Pricking sensation in body	Imbalance regulation of copper
Neurological disorders	Inhibiting enzyme activity
Pulmonary disease	
Peripheral vascular disease	
Cardiovascular disease	
Hypertension	

Diabetes	
----------	--

Note: data were generated based on (Benaduce et al., 2008; Biswas et al., 2018; Cazan and Klerks 2015; de Angelis et al., 2017; Faucher et al., 2008; Hayati et al., 2017; Komjarova and Bury 2014; Kumar and Singh 2010; McGeer et al., 2000; Nair et al., 2013; Naseri et al., 2018; Noor et al., 2018; Nordberg et al., 2018; Pastorelli et al., 2018; Paul and Small 2018; Pereira et al., 2016; Philippe et al., 2018; Qi et al., 2017; Witeska et al., 1995; Wold et al., 2017; Yu et al., 2016; Zhao et al., 2015; Zheng et al., 2016)

Table 4 Effects of cobalt

Detrimental effects on human health	Detrimental effects on marine and aquatic organisms
Increasing the RBC count (polycythemia)	Inhibiting the growth
Increasing hematocrit level	Reducing cell viability
Increasing hemoglobin level	Reproductive damage
Inducing pathogenesis	Hair cell death
Skin damage	Blocking lateral line hair cells
Acne	Increasing intracellular reactive oxygen species (ROS) levels
Skin rashes	
Flares of dermatitis	
Lung cancer	
Chronic thyroiditis	
Disturbing the thyroid hormone metabolism	
Reducing thyroid volume	
Neurologic deficit	
Hearing impairment	
Tinnitus	
Vertigo/dizziness	
Nausea	
Vomiting	
Visual impairment	
Reducing visual acuity	
Complete blindness	
Retinal dysfunction	
Poor color vision	
Blurred vision	
Irregular cortical visual responses	
Cognitive impairment	
Reduction in memory and thinking skills	

Disorientation	
Cardiovascular disease	
Reduction in left ventricular systolic function	
Damaging the myocardial function	
Reversible electrocardiographic alterations	

Note: data were generated based on (Alinovi et al., 2015; AnvariFar et al., 2018; Bozich et al., 2017; Chen et al., 2018; Fox et al., 2016; Gautam et al., 2018; Goodnough et al., 2018; Leyssens et al., 2017; Li et al., 2018; Melby et al., 2018; Mohan and Kasprovicz 2016; Sonnack et al., 2018; Stewart et al., 2017)

Table 5 Effects of copper

Detrimental effects on human health	Detrimental effects on marine and aquatic organisms
Altering glutathione levels	Hair cell death
Lipid peroxidation	Respiratory dysfunction
Inducing oxidative stress	Disruption of migration
Inducing cytotoxicity	Alteration of the swimming behaviour
Reducing cell viability	Oxidative stress
Lysosomal damage	Disruption of osmoregulation structure
Mitochondrial damage	Increasing operculum movements
Cell death	Decreasing swimming ability
Anemia	Decreasing food intake
Gastric upset	Alteration of glucose level
Nausea	Increasing gluconeogenic enzyme activity
Vomiting	Reduction in level of protein
Leucopenia	Alteration in appetite
Myeloneuropathy	Alteration in navigation
Wilson's diseases	Alteration in awareness of surroundings
Alzheimer's disease	Reducing sperm production
Inducing the production of ROS	Reducing egg production
DNA damage	Reduction in survival rate
Hepatobiliary disease	Increasing abnormality incidences
Increasing vascularity of the mucous membrane inside the nose	Inhibiting growth
	Cell death

Note: data were generated based on (Assadian et al., 2018; Elbeshti et al., 2018; Ingle et al., 2018; Khan et al., 2018; Khoshdel et al., 2016; Sonnack et al., 2018; Wazir et al., 2017; Xu et al., 2017)

Table 6 Effects of lead

Detrimental effects on human health	Detrimental effects on marine and aquatic organisms
Neurological disorder	Learning disability
Mental retardation	Embryonic toxicity
Hypertension	Behavioral alteration
Reducing cognitive function	Memory deficit
Vascular damage	Impairing nervous system functions
Genetic damage	Oxidative stress
Brain damage	Muscular degeneration and destruction
Red blood cells damage	Inhibiting growth
Behavioral changes	Cell membrane damage
Learning deficit	Lipid peroxidation
Disrupting skeletal hematopoietic function	Mortality
Disrupting digestive system	Reproductive disorders
Disrupting reproductive system	Disturbing the protein metabolism
Renal disease	Alteration of the number of genes
Death	Alteration of color preference
Colic	Reduction in axon length
Anemia	Reduction in locomotion
Headache	Inducing overproduction of reactive oxygen species (ROS)
Convulsions	
Chronic nephritis	

Note: data were generated based on (Biswas et al., 2018; Fuentes-Gandara et al., 2018; Green et al., 2018; Hamilton et al., 2017; Kohzadi et al., 2018; Kumar et al., 2018; Meng et al., 2018; Monastero et al., 2018; Singh et al., 2017; Yin et al., 2018; Zhong et al., 2018)

Table 7 Effects of mercury

Detrimental effects on human health	Detrimental effects on marine and aquatic organisms
Neurodegenerative disorder	Central nervous system morbidity
Headache	Swim behavior alteration
Memory loss	Sensory deficits
Epilepsy	Behavioral impairment
Depression	Anxiety status alteration
Abrupt burst of anger	Decreasing number of optic tectum cells
Abrupt burst of rage	Reducing foraging efficiency
Abrupt burst of violence	Reducing prey capture speed

Abrupt burst of self-effacement	Inhibiting membrane adenosine deaminase
Abrupt burst of suicide thoughts	Hyperactivity
Abrupt burst of lack of strength	Reduction in dopamine
Abrupt burst of anxiety	Reduction in hatching time
Abrupt burst of resist	Reduction in serotonin
Obsession	Increasing mortality
Compulsion	Histopathological alterations
Erethism	Brain mitochondrial respiration
Infectious disease	Mitochondrial disease
Schizophrenia	Neurotoxicity
Bipolar disorder	Gastrointestinal tract dysfunction
Dementia	Renal disease
Parkinson	Reproductive disorder
Twitching	Oxidative stress
Visual impairment	Lipid damage
kidney impairment	DNA damage
Lymphoproliferative disorders	Altering proteins associated with gap junction signaling
Hypergammaglobulinemia	
Systemic Hypertension	
Hyporeactivity	
Heart arrhythmia	
Cardiomyopathy	
Chest pains	
Fast heartbeat	
High blood pressure	
Myocardial infarction (heart attack)	
Coronary heart disease	
Atherosclerosis	
Fatigue	
Coordination impairment	
Muscle atrophy	
Movement difficulties	
Impotency	
Reducing sperm mobility	

Reducing sperm count	
Reducing libido	
Miscarriage	
Impairment of fertility	
Impairment of pregnancy	
Impairment of newborn development	
Menstrual cycle dysfunction	
Necrotizing bronchitis	
Pneumonitis	
Respiratory disorder	
Inhibiting protein synthesis	
Microtubule disruption	
Blocking enzymes	
Blocking cofactors	
Blocking hormones	

Note : data were generated based on (Beckers and Rinklebe 2017; Bosch et al., 2016; Castro et al., 2018; Green et al., 2018; Monastero et al., 2018; Officioso et al., 2018; Okpala et al., 2018; Paz et al., 2017; Rasinger et al., 2017; Rodríguez et al., 2018; Wahlberg et al., 2018; Xu et al., 2018)

Table 8 Effects of vanadium

Detrimental effects on human health	Detrimental effects on marine and aquatic organisms
Irritating skin	Increasing increase in cortisol level
Irritating throat	Increasing cholesterol level
Irritating nasal	Reducing growth rate
Cough	Reduction in body weight
Discoloration of tongue	Reduction in haemoglobin
Discoloration of oral mucosa	Reduction in hematocrit
Chest pain	Increasing cholesterol
Genotoxicity	Increasing alkaline phosphate
Reproductive toxicity	Reproductive toxicity
Sperm motility	Increasing alanine aminotransferase enzyme
Decreasing the weight of testicular	Increasing urea
Increasing abnormal spermatozoa	Increasing creatinine
DNA damage	Neurologic toxicity

Kidney disease	Hematologic toxicity
Cardiovascular disease	Renal toxicity
Thyroid cancer	Hepatic toxicity
Cell damage	Increasing oxidative stress
Impairing fetal growth	Increasing aspartate aminotransferase enzyme
Early pregnancy	
Late pregnancy	

Note: data were generated based on (Authman et al., 2015; Bikkini and Nanda 2016; Çanlı 2018; Carson 2018; Costigan et al., 2001; Filler et al., 2017; Hu et al., 2018; Liu et al., 2018; Malandrino et al., 2016; Schiffer and Liber 2017; Schlesinger et al., 2017; Vijaya Bharathi et al., 2015; Wang et al., 2018; Wilk et al., 2017; Zwolak and Gołębiowska 2018)

Table 9 Effects of zinc

Detrimental effects on human health	Detrimental effects on marine and aquatic organisms
Inducing cytotoxic	DNA damage
Genotoxicity	Necrosis
Infertility	Apoptosis
Kidney disease	Hyperplasia
Central nervous system disease	Respiratory disorder
	Inducing oxidative stress
	Inducing antioxidant defence mechanism
	Genotoxicity
	Gill damage
	Reducing growth
	Mortality
	Damaging cytoplasmic proteins of skeleton cells
	Inducing oxidative stress
	Inducing overproduction of reactive oxygen species
	DNA damage
	Histological alterations
	Retardation in growth
	Retardation in feed utilization
	Inhibition of hatching
	Hypoplasia
	Oedema

Note: data were generated based on (Abdel-Tawwab et al., 2018; adel Abdel-Khalek et al., 2015; Kaya et al., 2015; Li et al., 2018; Ratn et al., 2018; Shahzad et al., 2018; ; ur Rehman et al., 2018)

Table 10 Effects of nickel

Detrimental effects on human health	Detrimental effects on marine and aquatic organisms
Cardiovascular diseases	Reducing growth
Kidney diseases	Nephrotoxicity
Pulmonary fibrosis	Hepatotoxicity
Lung inflammation	Teratogenesis
Contact dermatitis	Respiratory distress
Emphysema	Inhibiting cellular antioxidant defenses
Tumours	DNA damage
Chronic inflammatory airway diseases	Protein molecules damage
Bronchitis	Lipids damage
Proteinosis	Oxidative stress
Pulmonary edema	Inducing reactive oxygen species (ROS)
Asthma	Skeletal impairment
Apoptosis	Alteration of cellular homeostasis
Inducing oxidative stress	Inducing gene expression
Inducing reactive oxygen species (ROS)	Neurotoxicity
DNA damage	Olfactory toxicity
Transcriptome alterations	Ionoregulatory impairment
	Inhibiting respiration

Note: data were generated based on (Blewett et al., 2017; Blewett et al., 2016; Boran et al., 2018; Buekers et al., 2015; Chiou et al., 2014; da Silva Aires et al., 2018; Dew et al., 2014; Fuentes-Gandara et al., 2018; Ghosh et al., 2018; Jose et al., 2018; Kim et al., 2015; Lari et al., 2018; Panneerselvam et al., 2018; Saquib et al., 2018)

Table 11 Effects of chromium

Detrimental effects on human health	Detrimental effects on marine and aquatic organisms
DNA adduct formation	Alteration of behavioral patterns
Oxidative stress	Cytotoxicity
DNA damage	Reducing cell viability
Cellular proteins damage	Increasing ROS production
Cellular lipids damage	Inducing oxidative stress
Cardiovascular disease	Lipid peroxidation
Impairment of fertility	Decreasing serum lysozyme activity
Impairment of glucose tolerance	DNA damage
Maturity-onset diabetes	Oxidative deterioration of proteins
Cytotoxicity	Reduction in antibody production

Sister chromatid exchanges	Decreasing lymphocyte count
Respiratory cancer	Reducing spleen weight
Oxidative stress	Reducing growth rate
Lung cancer	Reducing survival rate
Bone cell disorder	Diminishing humoral responses
	Increasing lactic acid of blood
	Increasing lactic acid of muscle
	Reduction in glycogen content
	Inhibition of LDH (Lactate dehydrogenase) activity
	Inhibition of PDH (pyruvate dehydrogenase) activity
	Inhibition of SDH (succinate dehydrogenase) activities
	Hyperplasia or hypergenesis
	Necrosis of hepatic cells
	Cellular disorganization
	Reducing nucleus to cytoplasm ratio
	Degrading Inner epithelial layers
	Loosening of muscle fibre
	Increasing space between fibres
	Degrading Lamellar
Thickening of blood vessels	

Note: data were generated based on (Abbas and Javed 2016; Aslam and Yousafzai 2017; Azmat et al., 2018., Bakshi et al., 2018; Biswas et al., 2018; Borgia et al., 2018; Chen et al., 2018; Fuentes-Gandara et al., 2018; Song and Li, 2015; Swiatkowska et al., 2018; Xia et al., 2016)

Table 12 Effects of manganese

Detrimental effects on human health	Detrimental effects on marine and aquatic organisms
Hepatic cirrhosis	Oxidative stress induction
Polycythemia	Inducing reactive oxygen species (ROS) production
Hyper manganeseemia	Altering haematological parameters
Dystonia	Impairment of immunological functions
Parkinsonism	Disturbing the sodium balance
Neurological dysfunction	Reduction in the absorption of calcium
Growth disorder	Reduction in the absorption of phosphorus
Impairing cellular function	Disturbing the metabolism of carbohydrates
Depression	Reducing the total protein concentration

Anxiety	Alteration of antioxidant defense system
Dementia	Reducing embryo survival
Parkinson's disease	Reducing hatching rates
Alzheimer's disease	Neurological disorders
Stroke	Fin abnormalities
Mitochondrial dysfunction	DNA damage
Oxidative stress	Lipid peroxidation
Changing polyamine	Mitochondrial diseases
Changing methionine	Disrupting the normal physiological process
Disrupting the brain maturation processes	Growth disorders
Dopaminergic dysfunction	Genotoxicity
Changing the function of astrocytes	Hydromineral imbalance
	Impairing gill epithelium function
	Metabolic system damage
	Alteration of antioxidant system

Note: data were generated based on (Chen et al., 2018; Chin and Vora 2014; de Water et al., 2018; Fernandes et al., 2018; Fernandes et al., 2016; Lee et al., 2018)

Among above listed pollutants, Ni, Pb and Cu were often present in the effluent of wastewater treatment plants as it has been demonstrated by Hasan (2011). Nickel derived from anthropogenic and natural sources enters water bodies. Nickel is considered as an essential metal for biota. Nevertheless, the high concentration of nickel can be toxic to aquatic and marine organisms (Al-Ghanim 2011; Ololade and Oginni 2010; Wu and Kong 2020). Moreover, nickel can be considerably carcinogenic in humans (Ermolli et al., 2001; Fu and Xi 2020).

Diverse anthropogenic activities (e.g. vehicular exhaust, leaded paint, industrial emissions etc.) give aid to release of lead into water bodies substantially (Espejo et al., 2019; Jin et al., 2019). Pb is considered as a non-essential metal which can cause irreversible damages to aquatic organisms even in low concentration (Has-Schön et al., 2015; Jaishankar et al., 2014; Jin et al., 2019; Nourouzi et al., 2018). A huge number of studies have indicated that occupational and environmental exposures to lead have deleterious impacts on human health (Assi et al., 2016; Machoń-Grecka et al., 2020).

Copper finds its way to marine ecosystems because of domestic and industrial activities (Corcoll et al., 2019; Edosa et al., 2019; Misson et al., 2016). Copper is considered as an essential micronutrient, whereas it might be toxic to aquatic and marine organisms at exceeded available levels (Kim et al., 2018; Wang et al., 2020; Zimmer et al., 2012). Copper is one of the first metals used by humans, while at high concentration might be lethal for living beings (de Namor et al., 2012; Izah et al., 2016).

2.3. Adsorption process

There are diverse processes including adsorption, biological, filtration, advanced oxidation and chlorination, as well as the combination of different processes, which can be used for water purification and wastewater treatment (Abazari 2019; Fang et al., 2018; Liu et al., 2018; Nasseh et al., 2019; Xu et al., 2018; Zhang et al., 2019b; Zhu et al., 2017; Zhu et al., 2015). Among such methods, the adsorption process is well-known for simplicity of operation and cost-effectiveness (Ahmed et al., 2017; Appavu et al., 2018; Mandal et al., 2019; Okoli and Ofomaja, 2019; Tien et al. 2018).

Adsorption is a process by which an adsorbate moves from the liquid phase to the surface of a solid across some boundaries (Blair Crawford and Quinn 2017). During such a mass transfer process liquid-solid intermolecular forces of attraction give aid to some of the solute molecules from the solution to be concentrated or deposited at the solid surface due to interaction between a solution containing absorbable solute and a highly porous solid material (Thomas et al. 2018). The molecule or pollutant adsorbed on the solid surface is defined as an adsorbate, whereas, the surface on which the process of adsorption takes place is defined as an adsorbent (Rashed 2013). Moreover, the surface accumulation of pollutants (adsorbate) on the solid surface (adsorbent) can be referred to as the adsorption process (Tareq et al., 2019).

The degree as to which adsorption occurs can be determined by analyzing the physiochemical properties of an adsorbate (Apul and Karanfil 2015). Occurring the adsorption process through chemisorption is far more stable in comparison with physisorption (Das et al., 2018). Physisorption involves the intermolecular forces and a substantial change in the electronic orbital patterns of the species, whereas, chemisorption is a chemical process in which a reacting molecule forms a

definite chemical bond with an unsaturated atom, or a group of atoms on an adsorbent surface, and electron transfer is included (Das et al., 2018; Tareq et al., 2019).

Carbon-based materials, clay and minerals, polymeric resins, chitosan and gels etc. have been utilized as adsorbents (Ahmed and Theydan, 2012; Ashiq et al., 2019; Erşan et al., 2013; Fakhri and Behrouz, 2015; Wang et al., 2015; Wu et al., 2016; Xing et al., 2016; Yi et al., 2018; Yu et al., 2016). Carbon-based materials such as activated carbon, biochar etc. have been widely used due to characteristics including abundant pore structures, high specific surface areas, and tunable surface functionality (Ashiq et al., 2019; Xiang et al., 2019; Yi et al., 2018). Among such adsorbents, biochar as a type of carbonaceous material is well-known for adsorption of organic and inorganic contaminants (Lonappan et al., 2019).

Biochar has exhibited a greater potential for eliminating pollutants from wastewater in comparison with other adsorbents (activated carbon, clay and minerals etc.) (Deng et al., 2017; Shaheen et al., 2019). Since biochar contains micro- and/or meso-porous structures, diverse surface functional groups (carboxylic, hydroxyl etc.), and the stable molecular structure, biochar is considerably capable of eliminating pollutants from wastewater (Deng et al., 2017; Yargicoglu et al., 2015). Recently, biochar has received an attention for eliminating pharmaceuticals and heavy metals from wastewater due to high surface area, large pore volume, plentiful functional groups, and environmental stability (Beesley et al., 2011; Rosales et al., 2017; Zama et al., 2017). A huge number of studies utilized different types of biochar in eliminating pollutants (Afzal et al., 2018; Ahmed et al., 2017b; Ahmed et al., 2017c; Boni et al., 2020; Chen et al., 2018a).

However, the biochar cost-effectiveness is related to cost of primary products. Biochar can be produced from a variety of biomass by pyrolysis under oxygen-limited conditions at an appropriate temperature (Jing et al., 2014) (Table 13).

Table 13 Different methods of preparing biochar

Method	Heating rate	Residence time
Slow pyrolysis	10–30 °C/min	Several hours or more
Fast pyrolysis	100–800 °C/s	Less than 2 s
Instantaneous carbonization	103-104 °C/s	0 .5s or less

Note: data were generated based on (Li et al. 2010; Manyà et al. 2018; Meyer et al. 2011; Wang et al. 2018).

Pyrolysis is necessary for the chemical decomposition of a carbon-based material by heating (Dai et al., 2019). Under oxygen-free or limited conditions, biochar can be prepared in different methods including slow pyrolysis, fast pyrolysis and instantaneous carbonization. Increasing the temperature in such methods causes the surface area, pore volume and stability of biochar to be on the increase (Agrafioti et al., 2013; Zama et al., 2017; Kim et al., 2012). Different stages of Pyrolysis process are summarized in Table 14.

Table 14 Different stages of Pyrolysis process

Stages	Description
Drying	In such a stage, moisture in the biomass is evaporated. Physical changes occur in the material, whereas, the chemical composition does not change.
Preheating	In such a stage, thermal reaction of materials is obvious, and the chemical composition begins to change. Unstable components in biomass, such as hemicellulose, decompose into carbon dioxide, carbon monoxide and a small amount of acetic acid, etc.
Solid decomposition	In such a stage, material decomposed by heat under the condition of hypoxia. The liquid products include acetic acid, wood tar, methanol etc. The gas products include CO ₂ , CO, CH ₄ , H ₂ , etc.
Carbonization	In such a stage, biomass depends on the external supply of heat for charcoal combustion, which reduces the volatile matter in charcoal and increases the carbon content.

Note: (Dai et al. 2019)

For producing biochar, chemical decomposition of materials is conducted in diverse stages including drying, preheating, solid decomposition and carbonization (Dai et al. 2019). Wood-based biochars have larger surface area and lower ash in comparison with other biochars because of possessing the higher proportions of lignin, cellulose, and hemicellulose (Rehrah et al., 2016; Shaheen et al., 2019). The biochar produced from hardwood has higher microporosity, negative charge density, cation exchange capacity, alkalinity, and electrostatic capacity compared with the softwood biochar (Huggins et al., 2016; Inyang et al., 2016). However, the usage of wood as a primary material for activated carbon productions is too expensive to be applied at full scale for effluent treatment at a wastewater treatment plant. Therefore, using some wasted biomass might decrease the costs. Furthermore, the most sustainable solution is to use onsite produced waste, for example, biosolids, which are produced at each wastewater treatment plant at a huge volume. The biochar produced from sludge has an appropriate surface area (Agrafioti et al., 2013). Zojaji (2020) clearly showed that biochar resulting from a mixture of sludge and hardwood is the most appropriate alternative for the commercially available activated carbons in tertiary treatments of

the wastewater treatment industry. In the present study, the novel biochar was produced from the sustainable combination of municipal sludge, hardwood waste and KOH.

Batch and column studies are considered as two ways to adsorption studies. The data gained from a batch study is limited to the laboratory scale and thus cannot be applied in industrial systems. Nevertheless, perform column studies play a vital role in providing data for direct applications in industrial systems. In such an investigation, the performance of the fixed-bed column was studied.

2.4. Breakthrough curve

Loading behavior of adsorbate to be eliminated from the solution in a fixed-bed column can be indicated by the breakthrough curve. Such a curve is obtained by plotting C_t / C_0 (where C_0 and C_t are the inlet and outlet (at time t) concentrations of adsorbate, respectively) for a given mass of adsorbent (bed height) (Gupta et al., 2016; Qian et al., 2019). The breakthrough curve of adsorption process is indicated in Fig. 3 (Gupta et al., 2016; Qian et al., 2019).

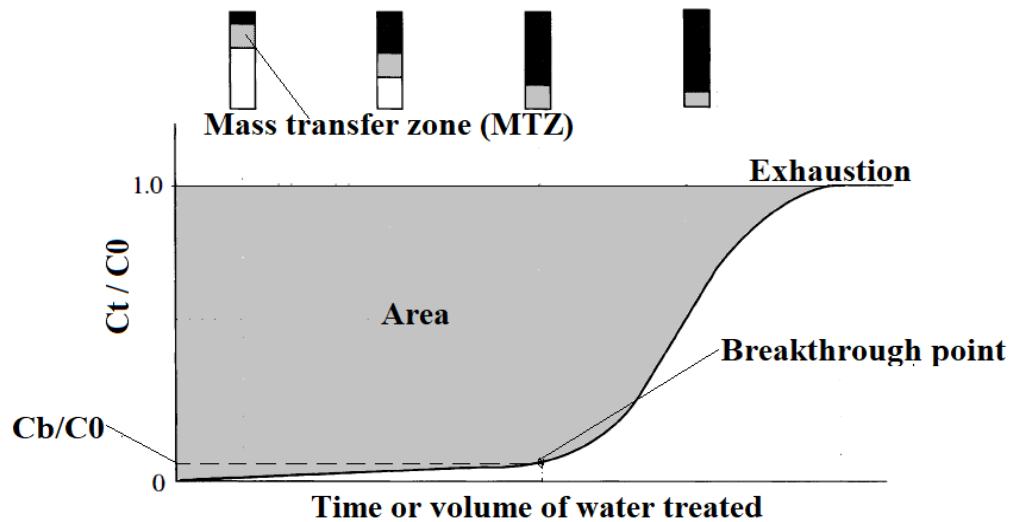


Fig. 3 Breakthrough curve of adsorption process (Gupta et al., 2016; Qian et al., 2019)

The area under the breakthrough curve is calculated by integrating the plot of adsorbed concentration ($C_{\text{adsorption}} = C_0 - C_t$) versus time (Mojiri et al., 2019). In a breakthrough curve, the breakthrough point is a point where the effluent concentration reaches a determined percentage comparatively to the influent concentration ($C_t/C_0 = 0.05$ or 0.1). Nevertheless, exhaustion or saturation point is a point where the column is entirely saturated and thereafter, adsorption does not occur ($C_t/C_0 = 1$).

The volume within the adsorbent bed where adsorption takes place is defined as mass transfer zone (MTZ) (Beji et al., 2018; Mojiri et al., 2019; Shahid et al., 2019). MTZ starts moving down the column when adsorbent becomes exhausted (Nidheesh et al., 2013). At $V = V_1$ or $t = t_1$, a small portion of the adsorbent at the top is exhausted (dark shading) and MTZ (light shading) is near the top of the column due to low concentration of effluent. At breakthrough point ($V = V_b$, $t = t_b$ and $C = C_b$), MTZ reaches the bottom of the fixed-bed column.

The adsorption rate of adsorbate can be evaluated by applying Thomas, Yoon and Nelson, Adams–Bohart, Yan et al., Wolborska, Bed depth–service time (BDST) and Modified dose-response models at starting ratio $C_t/C_0 > 0.1$ (10 percent of breakthrough) until $C_t/C_0 > 0.9$ (90 percent of breakthrough) to predict the dynamic behaviour of the fixed-bed column in an accurate manner (Table 15) (Doufene et al., 2019; Georgin et al., 2019; Marzbali and Esmaili 2017; Saadi et al., 2019; Wang et al., 2019).

Table 15 Mathematical models in describing the fixed-bed adsorption

Model	Equation	Parameters
Thomas model	$\ln \left[\frac{C_0}{C_t} - 1 \right] = \frac{k_{th} q_0 M}{Q} - k_{th} C_0 t$	C_0 (mg mL ⁻¹) (influent concentration) C_t (mg mL ⁻¹) (effluent concentration) k_{th} (mL mg ⁻¹ min ⁻¹) (Thomas model rate constant) $q_0 = q_{eq}$ (mg g ⁻¹) (equilibrium uptake or maximum mass of adsorbate adsorbed at saturation per gram of adsorbent) m (g) Total dry weight of adsorbent in the fixed-bed column at the end of process (adsorbent used) Q (mL min ⁻¹) (volumetric flow rate) t (min) (service time)
Yoon and Nelson model	$\ln \left[\frac{C_t}{C_0 - C_t} \right] = k_{YN} t - \tau k_{YN}$	C_0 (mg mL ⁻¹) (influent concentration) C_t (mg mL ⁻¹) (effluent concentration) k_{YN} (min ⁻¹) (Yoon–Nelson model rate constant) t (min) (service time) τ (min) (the time required for 50% adsorbate breakthrough) ($C_t / C_0 = 0.5$)
Adam-Bohart model	$\ln \left[\frac{C_t}{C_0} \right] = k_{AB} C_0 t - k_{AB} N_0 \frac{Z}{U_0}$	C_0 (mg mL ⁻¹) (influent concentration) C_t (mg mL ⁻¹) (effluent concentration)

		<p>k_{AB} (mL mg⁻¹min⁻¹) (Adams-Bohart model rate constant)</p> <p>t (min) (service time)</p> <p>N_0 (mg mL⁻¹) (equilibrium volumetric sorption capacity or saturation concentration)</p> <p>Z (cm) (bed depth)</p> <p>U_0 (cm min⁻¹) (linear velocity of influent solution that can be calculated by dividing flow rate by the column cross-sectional area)</p>
Yan et al. model	$\ln\left(\frac{C_t}{C_0 - C_t}\right) = \frac{K_Y C_0}{Q} \ln\left(\frac{Q^2}{K_Y q_Y m}\right) + \frac{K_Y C_0}{Q} \ln t$	<p>C_0 (mg mL⁻¹) (influent concentration)</p> <p>C_t (mg mL⁻¹) (effluent concentration)</p> <p>K_Y (mL mg⁻¹min⁻¹) (Yan et al. model rate constant)</p> <p>Q (mL min⁻¹) (volumetric flow rate)</p> <p>q_Y (mg/g) (maximum adsorption capacity)</p> <p>m (g) total dry weight of adsorbent in the fixed-bed column at the end of process (adsorbent used)</p> <p>t (min) (service time)</p>
Wolborska model	$\ln\left(\frac{C_t}{C_0}\right) = \frac{\beta C_0 t}{N_0} - \frac{\beta Z}{U_0}$	<p>C_0 (mg mL⁻¹) (influent concentration)</p> <p>C_t (mg mL⁻¹) (effluent concentration)</p> <p>B (min⁻¹) (external mass transfer kinetic coefficient of Wolborska model)</p> <p>t (min) (service time)</p> <p>N_0 (mg mL⁻¹) (equilibrium volumetric sorption capacity or saturation concentration)</p> <p>Z (cm) (bed depth)</p> <p>U_0 (cm min⁻¹) (linear velocity of influent solution that can be calculated by dividing flow rate by the column cross-sectional area)</p>
Bed depth service time (BDST) model	$t = \left(\frac{N_0 Z}{C_0 U_0}\right) - \left(\frac{1}{K_0 C_0}\right) \ln\left(\frac{C_0}{C_t} - 1\right)$	<p>t (min) (service time)</p> <p>N_0 (mg mL⁻¹) (equilibrium volumetric sorption capacity or saturation concentration)</p> <p>Z (cm) (bed depth)</p> <p>C_0 (mg mL⁻¹) (influent concentration)</p> <p>U_0 (cm min⁻¹) (linear velocity of influent solution)</p> <p>K_0 (mL mg⁻¹min⁻¹) (BDST model rate constant)</p> <p>C_t (mg mL⁻¹) (effluent concentration)</p>

Modified dose–response model	$\ln \left(\frac{C_t}{C_0 - C_t} \right) = a \ln \left(\frac{Q}{b} \right) + a \ln(t)$	<p>C_0 (mg mL⁻¹) (influent concentration)</p> <p>C_t (mg mL⁻¹) (effluent concentration)</p> <p>a (modified dose-response rate constant that can be obtained from the plot $\ln \left(\frac{C_t}{C_0 - C_t} \right)$ vs $\ln(t)$)</p> <p>b (modified dose-response rate constant that can be obtained from the plot $\ln \left(\frac{C_t}{C_0 - C_t} \right)$ vs $\ln(t)$)</p> <p>Q (mL min⁻¹) (volumetric flow rate)</p> <p>t (min) (service time)</p> <p>m (g) Total dry weight of adsorbent in the fixed-bed column at the end of process (adsorbent used)</p>
-------------------------------------	--	--

Note: data were generated based on (Hanbali et al., 2014; La et al., 2019; Shanmugam et al., 2016; Xu et al., 2013; Yan et al., 2001; Zhang et al., 2019)

Thomas model can be used to characterize dynamic adsorption curves along with computing the maximum concentration of adsorbate on the adsorbent surface and adsorption rate constant for an adsorption process (Kumpanenko et al., 2019; Niu et al., 2019). According to second-order reversible reaction kinetics and the Langmuir adsorption isotherm, Thomas model assumes that diffusion constraints (both external and internal) are remarkably low in the adsorption process (Abdolali et al., 2017; Duan et al., 2016; Kumpanenko et al., 2019; Niu et al., 2019).

The Yoon–Nelson model as a relatively simple breakthrough model is independent of the characteristics of adsorbate, type of adsorbent and physical properties of sorption bed (Baker et al., 2017; Majumdar et al., 2019; Wang et al., 2019b). Such a mathematical model is based on the hypothesis that the rate of decreasing in the probability of adsorption for each adsorbate molecule is directly proportional to the probability of adsorbate adsorption and the probability of adsorbate breakthrough on the adsorbent (Ahmed and Hameed 2018a; Fadzil et al., 2016; Gong et al., 2015; Niasar et al., 2019; Singh et al., 2015).

Adams-Bohart model considers the rate of adsorption is proportional to both the sorbate concentration and the sorption capacity of the sorbent (Basu et al., 2019; Chen et al., 2012; Hu et al., 2019; Romero-Cano et al., 2019). In other words, the adsorption rate is controlled by external mass transfer (Du et al., 2019; Niasar et al., 2019; Wang et al., 2015).

The erroneous of Thomas model in predicting the effluent concentration at time zero can be eradicated by Yan et al. model (de Franco et al., 2017; Hadavifar et al., 2014; Liu et al., 2019; Su et al., 2012; Wu et al., 2010). The quantity adsorbed cannot be predicted by Yan et al. model.

The Wolborska model has some similarities with Adams–Boharts model and considers mass transfer phenomenon for the inner diffusion mechanism at low concentration range of influents (Lau et al., 2016; Mitra et al., 2019; Nag et al., 2019). The first period of the breakthrough curve can be described by Wolborska model in an accurate manner (Alalwan et al., 2019; Swapna Priya and Radha 2016; Ye et al., 2019).

Bed depth service time (BDST) model as an empirical model can be used to predict the relationship between bed height (Z , cm) and service time (t , h), in terms of process concentrations and adsorption parameters (Brassesco et al., 2019; Dabbagh et al., 2019; Jain et al., 2013; Zulfadhly et al., 2001). In such a model, the rate of adsorption is properly controlled by the surface reaction between adsorbate and the residual capacity of the adsorbent (Igberase and Osifo 2019; Jang et al., 2018; Metwally et al., 2019). The deficiencies of the Thomas model can be overcome using the modified dose-response model to predict the breakthrough curve at higher and lower periods (Banerjee et al., 2019; Palágyi 2019; Shanmugam et al., 2016; Yan et al., 2001). In the present study, adsorption of pharmaceuticals on biochar in a fixed-bed column has been investigated.

Chapter 3: Methods and Materials

Adsorption of pharmaceutical (venlafaxine) and heavy metals (Ni, Pb and Cu) on biochar in a fixed-bed column were conducted in three phases (Fig. 4).

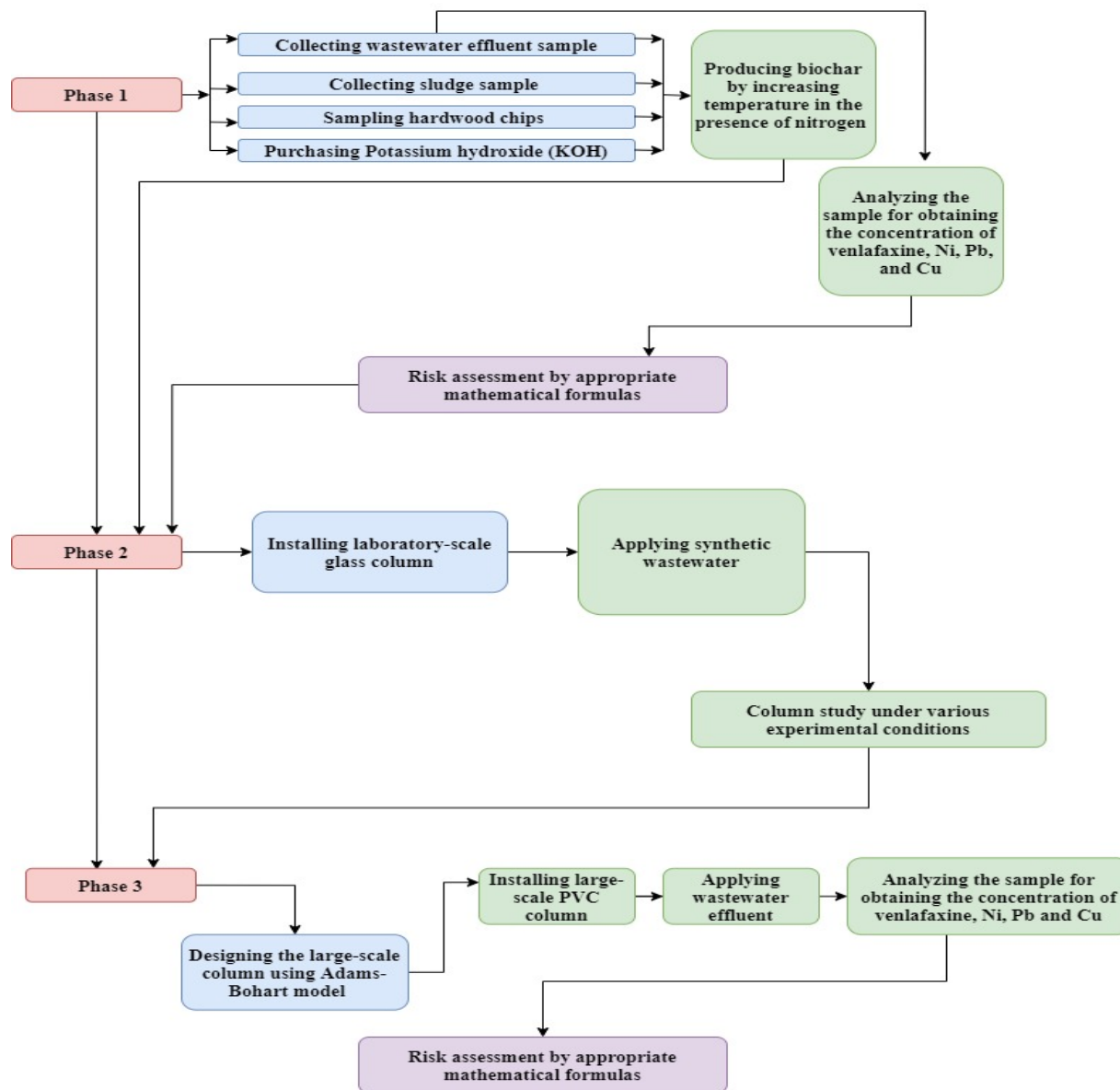


Fig. 4 Methodological approach

Previous study (Zojaji et al., 2019a, 2019b) revealed a very high occurrence of psychiatric compounds (e.g. venlafaxine) and their by-products in the wastewater treatment effluents and in the vicinity of outflow in Saint Lawrence River. Subsequently, venlafaxine was used as a representative compound of pharmaceuticals in this study. Other pilot study (Hasan 2011) showed that Ni, Pb and Cu are present in sewage redirected to wastewater treatment plants in Quebec. Subsequently, the above-mentioned metals were considered in this study.

3.1. Sampling

The proportional composite wastewater effluent samples were collected for three consecutive days (i.e. 3 samples) from RAEBL wastewater treatment plant, Montreal, Quebec, Canada by ISCO refrigerated autosampler. After every 24 hours, 50 mL aliquot was sampled and filtered using a Chromafil syringe microfilter. The filtered samples were kept in a 50 mL amber pre-cleaned glass bottle inside the cooler. Moreover, the rest of the unfiltered composite samples were transferred to a HDPE container and kept at the temperature of 4°C. Blank samples were also collected in the place. The stabilized/dewatered sludge was collected inside the wastewater treatment plant at the place where it was loaded onto the trucks. The sludge was transferred into the HDPE buckets and kept at the temperature of 4°C. Moreover, wood residue (hardwood) samples were collected from a wood mill located in the City of Mirabel, Quebec, Canada. KOH was purchased from COOP COCO, Montreal, Quebec, Canada.

3.2. Production of a novel biochar

3.2.1. Laboratory-scale

Biochar was produced based on the previous study (Zojaji 2020). Experiments were conducted in the environmental laboratory of Concordia University. For production of biochar, primary material ratio of Sludge-hardwood-KOH (2:1:2) was mixed at 750 ± 1 °C by increasing the temperature of biomass at the rate of 10 °C/min in the presence of nitrogen for 60 minutes. The sample obtained was washed with HCl (3 M) to remove any activator residues. Subsequently, it was washed with a sufficient amount of distilled water. The sample was dried overnight inside an oven at 105 °C. The final product (10 g) was ground and sieved through ASTM no: 200 sieves (corresponds to 75 µm mesh size) to get a uniform size distribution.

3.2.1. Large-scale

The sustainable combination of municipal sludge, hardwood waste and KOH (Fig. 5) played a vital role in producing a novel biochar with adequate developed pore structure, the high specific surface area, and the stable molecular structure. Utilization of the waste materials as the primary materials along with the availability of materials onsite led to sustainable, novel and cost-effective technology. Therefore, biochar for large-scale tests was produced from the mixture of sludge-hardwood-KOH (2:1:2) at 550 ± 1 °C by increasing the temperature of biomass at the rate of

10 °C/min in the presence of nitrogen for 60 minutes (Fig. 6). The sample obtained was washed with HCl (3 M) to remove any activator residues. Subsequently, it was washed with a sufficient amount of distilled water. The sample was dried. The final product (2000 g) was ground and sieved through ASTM no: 200 sieves (corresponds to 75 µm mesh size) to get a uniform size distribution.



Fig. 5 Primary materials for biochar production

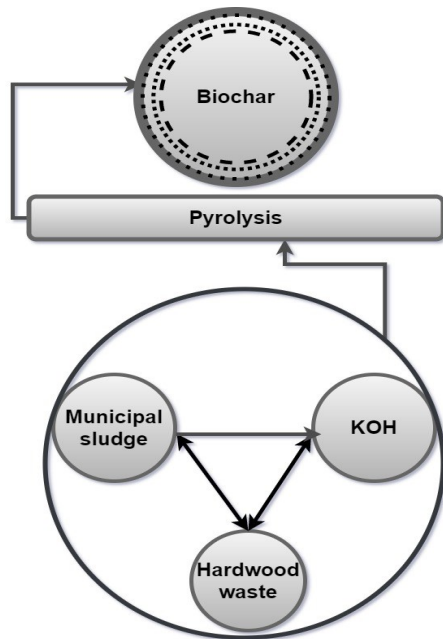


Fig. 6 Sustainable process to produce novel biochar on-site

3.3. Analyzing

Analysis of pharmaceutical (venlafaxine) was performed using automated solid-phase extraction coupled to liquid chromatography tandem mass spectrometry (on-line SPE LC-MS/MS). Moreover, the concentration of heavy metals (Zn, Cu and Ni) was measured by inductively coupled plasma mass spectroscopy (ICP-MS) (Agilent Technologies 7700 Series ICP-MS).

3.4. Column study

The feasibility of utilizing a novel biochar material to elimination of organic (pharmaceuticals) and inorganic (heavy metals) compounds were evaluated in laboratory-scale column and large-scale column.

3.4.1. Laboratory-scale column study

The column study was conducted in a glass column (height and inner diameter of 10 and 1 cm, respectively) (Fig. 7).

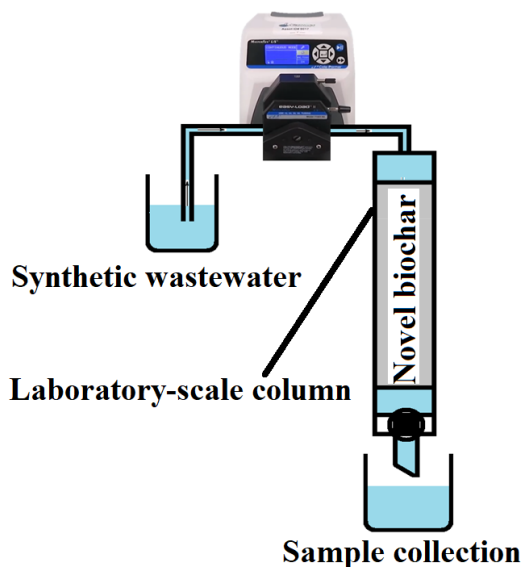


Fig. 7 Schematic diagram of column system

In this stage, the synthetic wastewater was applied with known concentrations of pollutants. The column was packed with biochar and sealed with glass wool below and above and then filled with a layer of glass balls to compact the mass of adsorbent and avoid dead volumes. The adsorption of pharmaceuticals on the glass is negligible (Mizutani and Mizutani 1978). As a result, the column was created by glass. The column study was conducted under various initial concentrations,

volumetric flow rates and bed depths. Divers values of such factors were derived from the results of other compressive studies (Ahmed et al., 2018; Dubey et al., 2014; Khobragade et al., 2016; Liao et al., 2013; Mondal et al., 2016; Nazari et al., 2016; Patel 2019; Reynel-Avila et al., 2015; Sancho et al., 2012; Zhang et al., 2016). Different concentrations of pollutants, flow rate of pollutants and amount of biochar were applied in obtaining various initial concentrations (10 to 30 mg/L for venlafaxine and 60 to 80 µg/L for Ni, Pb and Cu), volumetric flow rates (2-10 mL/min) and bed depths (2-4 cm), respectively (Tables 16 and 17).

Table 16 Column tests for venlafaxine adsorption at the various experimental conditions

Factor		
C ₀ (mg/L)	Q (mL/min)	Z (cm)
10	2	4
20	2	4
30	2	4
10	5	4
10	10	4
10	2	3

Table 17 Column tests for Ni, Pb and Cu adsorption at the various experimental conditions

Factor		
C ₀ (µg/L)	Q (mL/min)	Z (cm)
60	2	4
70	2	4
80	2	4
60	5	4
60	10	4
60	2	3

The formula for designing the column is as follows:

$$(3-1) \quad q = \frac{Q}{m \times 1000} \int_{t=0}^{t=t_{\text{total}}} (C_0 - C_t) dt$$

where q (mg/g), C₀ (mg/mL), C_t (mg/mL), t_{total} (min) and m(g) are adsorption capacity, influent concentration, effluent concentration, the time of exhaustion and total dry weight of adsorbent, respectively (Deokar and Mandavgane 2015; Ferreira et al., 2017; Jaria et al., 2019; Lawal and Moodley 2018; Lima et al., 2017; Lonappan et al., 2019; Marzbali and Esmaili 2017).

3.4.2. MultiVariate Statistical Package (MVSP)

MVSP is a proper program which can be utilized in performing a number of multivariate numerical analyses for diverse scientific fields (Kovach 1999; Heidari 2019). MVSP program can be defined based on the Pearson Coefficient which shows the data between -0.45 to 0.45 are undefined (Kovach 1999; Karbassi et al., 2013). MVSP program was used to comparison the effects of initial concentration, flow rate and bed depth on the adsorption capacity.

3.4.3. Large-scale column study

Based on obtained results from laboratory-scale, the large-scale column was designed using Adams–Bohart model (Fig. 8).

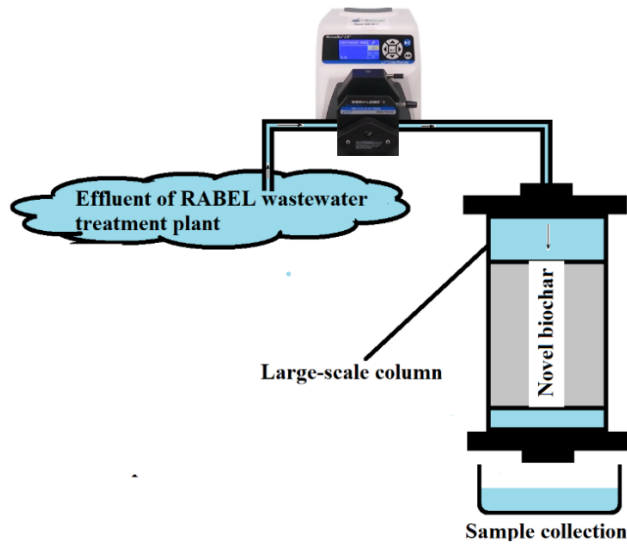


Fig. 8 Large-scale PVC column

The column was packed with biochar and sealed with glass wool below and above and then filled with a layer of glass balls to compact the mass of adsorbent and avoid dead volumes. The Adams–Bohart model was used to evaluate the efficiency and applicability of the novel biochar in the large-scale column (Doufene et al., 2019; Georgin et al., 2019; Marzbali and Esmaili 2017; Saadi et al., 2019; Wang et al., 2019). The Bed-depth service time curve was described by Adams–Bohart formula as follows (LaGrega et al., 2010):

$$(3-2) \quad t = aX + b$$

where X = depth in column (m)

$$(3-3) \quad a = \frac{F_1 N}{C_{in} V}$$

where a = slope (h/m)

F₁ = conversion factor for units = 10³ for metric units

N = adsorptive capacity of adsorbent (mass of contaminant removed per volume of adsorbent in the column, kg/m³)

C_{in} = influent contaminant concentration (mg/L)

V = superficial velocity through column (m/h) (m³/h per m² of column)

$$(3-4) \quad b = (F_2 / K C_{in}) \times \ln [(C_n / C_{out}) - 1]$$

where b = intercept (h)

F₂ = conversion factor = 10³ for metric units

K = adsorption rate constant required to move an adsorption zone through the critical depth [m³ / (kg. h)] (m³ of liquid treated per kg impurity fed per hour)

C_{out} = contaminant concentration at breakthrough (mg / L)

The rate of adsorbent utilization can be determined by using this velocity:

$$(3-5) \quad \text{Adsorbent utilization} = \text{area} \times (1/a) \times \text{unit weight}$$

where a = slope (h/m)

3.5. Risk assessment

Based on the obtained concentration of pollutants in wastewater effluent before and after utilizing large-scale column, risk assessment can be calculated in identifying the pollution intensity of pollutants.

3.5.1. Pharmaceuticals

The detrimental effects of pharmaceutical compounds on marine and aquatic ecosystems can be evaluated through risk assessment measurements. Based on the guidelines issued by the European

Agency for Evaluation of Medicinal Products, the potential risk posed by pharmaceuticals can be evaluated by the risk quotient (RQ). Risk quotient (RQ) as an appropriate index for determining the pollution intensity can be described as follows (Ashfaq et al., 2017; Hernando et al., 2006; Kosma et al., 2014):

$$(3-6) \quad RQ_{freshwater} = \frac{C_t}{PNEC_{freshwater}}$$

$$(3-7) \quad RQ_{freshwater} = \frac{C_t}{PNEC_{freshwater}}$$

where C_t is the effluent concentration. The PNEC is the predicted no-effect concentration and can be calculated as follows (Backhaus and Faust 2012; Minguez et al., 2016; Perrodin and Orias 2017):

$$(3-8) \quad PNEC_{freshwater} = \frac{EC_{50} (freshwater)}{Assessment\ factors}$$

$$(3-9) \quad PNEC_{marine\ water} = \frac{EC_{50} (marine\ water)}{Assessment\ factors}$$

The classification of Risk quotient (RQ) and assessment factors for calculation of PNEC are shown in Tables 18 and 19.

Table 18 Classification of risk quotient (RQ)

RQ class	Quality
$RQ \leq 0.01$	No risk to the aquatic community
$0.01 < RQ \leq 0.1$	Low risk to the aquatic community
$0.1 < RQ \leq 1$	Medium risk to the aquatic community
$RQ > 1$	High risk to the aquatic community

Note: (Ashfaq et al., 2017; Hernando et al., 2006; Kosma et al., 2014)

Table 19 Assessment factors

Arability toxicity data	Factor
At least one short-term EC50 from each of three trophic levels (algae, crustaceans and fish)	1000
Long-term NOEC from one trophic level (either fish or crustaceans)	100
Long-term NOEC from species representing two trophic levels (fish and/or crustaceans and/or algae)	50
Long-term NOEC from at least three trophic levels (fish, crustaceans and algae)	10

Note: (Backhaus and Faust 2012)

3.5.2. Heavy metals

A wide variety of pollution indexes have been used to evaluate the source and contamination extent of heavy metals in water system; e.g. Heavy metal pollution index (HPI). (Abdullah, 2013; Cengiz et al., 2017; Milivojević et al., 2016; Tiwari et al., 2017). Thus, heavy metal pollution index (HPI) is used to assess the quality of water with respect to the concentration of metals (Abdullah et al., 2013; Milivojević et al., 2016; Qu et al., 2018). The HPI as a proper index in evaluating the pollution intensity can be calculated by the following formula (Abdullah et al., 2013; Milivojević et al., 2016; Qu et al., 2018):

$$(3-9) \quad \text{HPI} = \frac{\sum_{i=1}^n W_i Q_i}{\sum_{i=1}^n W_i}$$

where Q_i (sub-index) and W_i (unit weight) are calculated by the given formulas (Wanda et al., 2012; Yang et al., 2015):

$$(3-10) \quad Q_i = \frac{C_t}{S_i} \times 100$$

$$(3-11) \quad W_i = \frac{1}{S_i}$$

where C_t and S_i are the monitored heavy metal and standard values, respectively. Three classes of heavy metal pollution index (HPI) are high risk ($\text{HPI} \geq 30$), medium risk ($15 < \text{HPI} < 30$) and low risk ($\text{HPI} \leq 15$) (Mahato et al., 2017).

Chapter 4: Results and discussions

4.1 Risk assessment

The results of risk assessment of organic (pharmaceuticals) and inorganic (heavy metals) compounds are summarized in sections 4.1.1 and 4.1.2.

4.1.1. Pharmaceutical

Analyzing the collected samples showed the concentration of venlafaxine in wastewater effluent is 2354 ng / L. The results of compressive studies clearly indicated that the EC₅₀ of venlafaxine in freshwater and marine water are 141 µg/L and 120 µg/L, respectively (Minguez et al., 2016; Perrodin and Orias 2017). Based on the formula 3-7, the PNEC can be calculated as follows:

$$PNEC_{freshwater} = \frac{141 \mu\text{g/L}}{1000} = 0.141 \mu\text{g/L}$$

$$PNEC_{marine\ water} = \frac{120 \mu\text{g/L}}{1000} = 0.12 \mu\text{g/L}$$

Based on formula 3-8, the Risk quotient (RQ) can be calculated as follows:

$$RQ_{freshwater} = \frac{2.354 \mu\text{g/L}}{0.141 \mu\text{g/L}} = 16.695 > 1$$

$$RQ_{marine\ water} = \frac{2.354 \frac{\mu\text{g}}{\text{L}}}{0.12 \frac{\mu\text{g}}{\text{L}}} = 18.108 > 1$$

The values of (RQ) revealed that the presence of venlafaxine in wastewater effluent poses toxic effects on various aquatic and marine organisms. As a result, an appropriate method should be utilized in producing a pivotal remedy to eliminate venlafaxine from wastewater.

Municipal wastewater treatment plants eliminate some of the pharmaceuticals and other complex substances. Nevertheless, a huge percentage of such pharmaceuticals can still be found in treatment plant final effluent, which is released into receiving waterways, especially Saint-Lowrance River (Blaise et al., 2006; Grill et al., 2016; Marcogliese et al., 2014). Grill et al. (2016) revealed that the MEC concentration of azithromycin is higher in comparison with the PNEC concentration of azithromycin, consequently, poses detrimental effects on various aquatic organisms. Moreover, results showed the high risk of diclofenac to the aquatic community (Grill et al. 2016). The

pollution intensity of pharmaceuticals was considered as high risk for sulfamethoxine, norfloxacin, ofloxacin, ciprofloxacin (Liu et al., 2018a). Ma et al., (2016) indicated that venlafaxine and diclofenac acid pose a high risk to aquatic organisms. Liu et al., (2019) showed that the value of RQ is lower than 0.01, and thus antibiotics do not have any risk to the aquatic community.

4.1.2. Heavy metal

Analyzing the collected samples showed the concentration of Ni, Pb and Cu in wastewater effluent is 18.8, 0.086 and 5.49 µg/L, respectively. The results of evaluating the risk of Ni, Pb and Cu to the aquatic community are shown in Table 20.

Table 20 Risk assessment of heavy metals

Metals	C _i (µg/L)	S _i (µg/L)	W _i	Q _i	W _i x Q _i	HPI	Class of risk
Cu	5.49	1000	0.001	0.55	0.00055	31.699	High
Ni	18.8	20	0.05	94	4.7		
Pb	0.086	10	0.1	0.86	0.086		
			Σ W_i = 0.151		Σ W_i x Q_i = 4.787		

Note: formulas 3-8, 3-9 and 3-10 and Table 19 were used to evaluate the pollution intensity of heavy metals

Based on the concentration of Ni, Cu, Pb and Zn, the overall HPI was 31.699 which is more than the critical threshold pollution index value of 30, indicating that the sample is critically contaminated with heavy metals.

In Montreal, where chemically enhanced primary treatment is utilized, municipal wastewater plays an important role in loading a huge percentage of heavy metals into the Saint Lawrence River and (Marcogliese et al., 2015). The significant role of urban effluents to the total metal fluxes carried into the sea by the Saint Lawrence River was demonstrated by measuring heavy metals at the Montreal wastewater treatment plant (Gobeil et al., 2005). The high risk of nickel in wild freshwater mussels of Grand River (Ontario) was observed due to high concentration of nickel in effluents from municipal wastewater treatment plants (Gillis 2012). Based on the heavy metal pollution index (HPI), the pollution of heavy metals in the collected water sample was considered as low (HPI < 15) (Abdullah et al., 2013). Ojekunle et al., (2016) and Milivojević et al. (2016) indicated that the overall HPI for the selected water samples is equal to 518.55, which is more than the critical threshold pollution index value of 30.

4.2. Laboratory-scale fixed-bed adsorption column (venlafaxine)

The adsorption column performance is influenced by a wide variety of factors including the initial concentration of adsorbate (C_0) (mg / mL), volumetric flow rate of adsorbate (Q) (mL / min) and bed depth (Z) (cm) (Ahmad and Hameed 2010; Cruz et al., 2020; Gokulan et al., 2019; Gouran-Orimi et al., 2018; Qian et al., 2019; Radhika et al., 2018; Zhang et al., 2019). The effects of such factors on breakthrough and exhaustion times are indicated in Table 21.

Table 21 Effects of different factors on breakthrough time and exhaustion time

Factor	Breakthrough time	Exhaustion time	Explanation
Initial concentration of adsorbate	Is decreased due to increasing initial concentration	Is decreased due to increasing initial concentration	Increasing the initial concentration provides a larger driving force to diffuse into the pore structure of adsorbent.
Volumetric flow rate of adsorbate	Is decreased due to increasing Volumetric flow rate of adsorbate	Is decreased due to increasing Volumetric flow rate of adsorbate	Increasing flow rate leads to the low duration of contact between adsorbate and adsorbent.
Bed depth or amount of adsorbent	Is increased due to increasing bed height or amount of adsorbent	Is increased due to increasing bed height or amount of adsorbent	Increasing bed height or amount of adsorbent leads to adequate contact for adsorbate molecules onto the adsorbent within the column. Such results are attributed to the availability of additional binding sites which increase the adsorption area of the adsorbent.

Note: data were generated based on (Abdolali et al., 2017; Alimohammadi et al., 2016; Bakar et al., 2019; Guocheng et al., 2011; Hajilari et al., 2019; Hethnawi et al., 2017; Jang and Lee 2019; Kumar et al., 2019; Majumdar et al., 2019; Nwabanne et al., 2012; Ocampo-Perez et al., 2011; Oladipo et al., 2016; Sivarajasekar et al., 2017; Soto et al., 2012)

According to Table 21, the breakthrough and exhaustion times are decreased due to increasing the initial concentration and flow rate of adsorbate. Nevertheless, increasing the bed height or amount of adsorbent causes the breakthrough and exhaustion times to be on the increase. Increasing the initial concentration of adsorbate and amount of adsorbent along with decreasing volumetric flow rate of adsorbate play a significant role in enriching the capacity of the adsorption process in eliminating pollutants.

4.2.1. Effect of the initial concentration

The initial concentration of adsorbate is an important factor which gives aid to provide an appropriate driving force for the transport of adsorbate molecules toward the adsorbent bed.

The impact of the initial venlafaxine concentration on the adsorption was studied by varying the concentration in the range of 10, 20 and 30 mg/L, while the bed depth and flow rate were kept constant at 4 cm and 2 mL/min, respectively. The results are shown in Tables 22 to 24.

Table 22 Breakthrough and exhaustion points at the initial concentration of 10 mg/L

Point	t (min)	q (mg/g)	Y (%)
Breakthrough	31	3.72	90
Exhaustion	170	2.266	10

Note: Q = 2 mL/min and Z = 4 cm

Table 23 Breakthrough and exhaustion points at the initial concentration of 20 mg/L

Point	t (min)	q (mg/g)	Y (%)
Breakthrough	21	5.04	90
Exhaustion	103	2.746	10

Note: Q = 2 mL/min and Z = 4 cm

Table 24 Breakthrough and exhaustion points at the initial concentration of 30 mg/L

Point	t (min)	q (mg/g)	Y (%)
Breakthrough	15	5.4	90
Exhaustion	88	3.52	10

Note: Q = 2 mL/min and Z = 4 cm

Loading behavior of different concentrations of venlafaxine to be eliminated from the solution in the laboratory-scale column is indicated by the breakthrough curves (Fig. 9, 10 and 11).

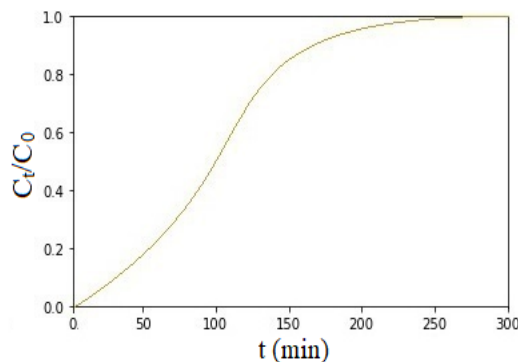


Fig. 9 Breakthrough curve at the initial concentration of 10 mg/L

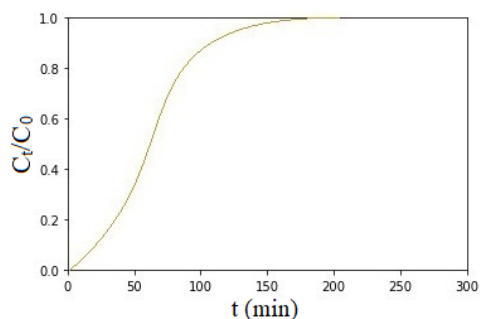


Fig. 10 Breakthrough curve at the initial concentration of 20 mg/L

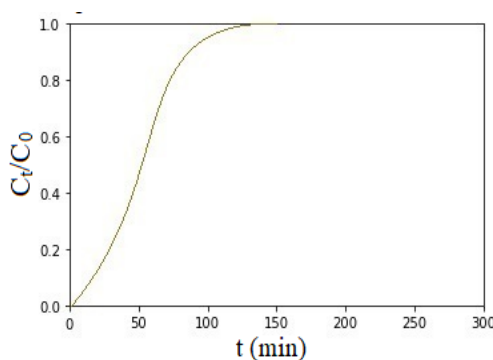


Fig. 11 Breakthrough curve at the initial concentration of 30 mg/L

According to Tables 22 to 24 and Fig. 9 to 11, increasing the initial concentration from 10 mg/L to 30 mg/L caused the breakthrough time and exhaustion time to decrease from 31 to 15 min and 170 to 88 min, respectively.

90% of venlafaxine was eliminated at the breakthrough point where the adsorption capacity was increased from 3.72 mg/g to 5.4 mg/g due to increasing the initial concentration. Moreover, the removal efficiency of 10% occurred at the exhaustion point in which the adsorption capacity of venlafaxine was increased from 2.266 mg/g to 3.52 mg/g due to increasing the initial concentration.

Such results are related to the enhancement of the concentration gradient for mass transfer across the liquid film along with the acceleration of the adsorption rate, which leads to an early saturation of the column. Increasing the initial concentration of adsorbate causes the adsorption capacity to be on the increase due to providing a larger driving force to diffuse into the pore structure of adsorbent. Since an increase in the initial concentration resulted in a larger driving force for the

adsorbate mass transfer, it caused saturation of the adsorbent bed quickly (Gupta and Garg 2019). Increasing the initial concentration caused the breakthrough and exhaustion time to be on the decline because of the quick saturation of the available binding sites for adsorbate (Tsai et al., 2016). The breakthrough and exhaustion occurred faster at higher C_0 (López-Cervantes et al., 2018).

4.2.2. Effect of the flow rate

The efficiency of the continuous adsorption system is substantially influenced by the flow rate. In other words, the flow rate as a significant factor determines the adequate contact between adsorbate and adsorbent.

The impact of the flow rate on the adsorption was studied by varying the flow rate in the range of 2, 5 and 10 mL/min, while the bed depth and initial concentration were kept constant at 4 cm and 10 mg/L, respectively. The results are shown in Tables 25 to 27.

Table 25 Breakthrough and exhaustion points at the flow rate of 2 mL/min

Point	t (min)	q (mg/g)	Y (%)
Breakthrough	31	3.72	90
Exhaustion	170	2.266	10

Note: $C_0 = 10$ mg/L and $Z = 4$ cm

Table 26 Breakthrough and exhaustion points at the flow rate of 5 mL/min

Point	t (min)	q (mg/g)	Y (%)
Breakthrough	11	3.3	90
Exhaustion	67	2.23	10

Note: $C_0 = 10$ mg/L and $Z = 4$ cm

Table 27 Breakthrough and exhaustion points at the flow rate of 10 mL/min

Point	t (min)	q (mg/g)	Y (%)
Breakthrough	4	2.4	90
Exhaustion	28	1.867	10

Note: $C_0 = 10$ mg/L and $Z = 4$ cm

Loading behavior of different concentrations of venlafaxine to be eliminated from the synthetic wastewater in the laboratory-scale column is indicated by the breakthrough curves (Fig. 12, 13, and 14).

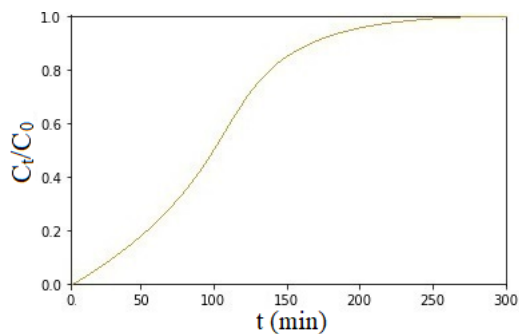


Fig. 12 Breakthrough curve at the volumetric flow rate of 2 mL/min

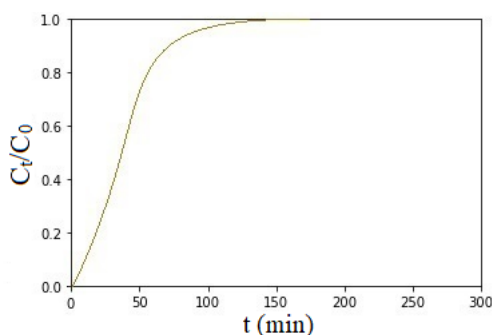


Fig. 13 Breakthrough curve at the volumetric flow rate of 5 mL/min

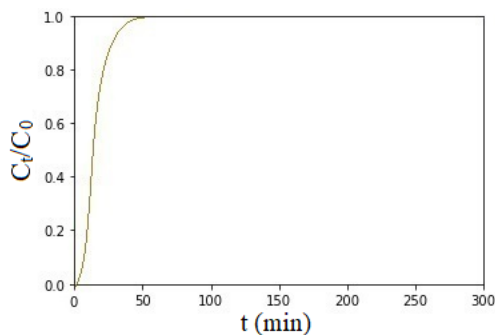


Fig. 14 Breakthrough curve at the volumetric flow rate of 10 mL/min

According to Tables 25 to 27 and Fig. 12 to 14, increasing the flow rate from 2 mg/L to 10 mg/L caused the breakthrough time and exhaustion time to decrease from 31 to 4 min and 170 to 28 min, respectively.

90% of venlafaxine was eliminated at the breakthrough point where the adsorption capacity was decreased from 3.72 mg/g to 2.4 mg/g due to increasing the flow rate. Moreover, the removal

efficiency of 10% occurred at the exhaustion point in which the adsorption capacity of venlafaxine was decreased from 2.226 mg/g to 1.867 mg/g due to increasing the flow rate.

Such results are related to the inadequate contact between adsorbate and adsorbent at the increased flow rate of the drug solution. As a consequence, the low flow rate appropriately favors the adsorbate adsorption due to the adequate residence time. Adsorption capacity, breakthrough time and saturation time were decreased at a higher flow rate due to the low duration of contact between adsorbate and adsorbent (Saadi et al., 2020). Under the condition of lower flow rate, the column adsorption of cephalexin (CFX) was more efficient (Saadi et al., 2020). The results clearly showed that the breakthrough time and exhaustion time decreased with increasing the flow rate because of the less residence time of the solute in the column (Yan et al., 2020). It was observed that an increase in the flow rate significantly reduces the breakthrough time and exhaustion time because the adsorbate molecule has less time to diffuse into the adsorbent pores (Ahmad & Hameed, 2010).

4.2.3. Effect of the bed height

The performance of adsorption is impacted by bed height. The extent of adsorption depends on the amount of adsorbent within the column, which provides the appropriate adsorption sites for the best performance. The impact of the amount of biochar on the adsorption of pollutants was studied by varying the bed depth in the range of 3 and 4 cm, while the initial concentration and flow rate were kept constant at 10 mg/L and 2 mL/min, respectively. The results are shown in Tables 28 and 29.

Table 28 Breakthrough and exhaustion points at the bed depth of 3 cm

Point	t (min)	q (mg/g)	Y (%)
Breakthrough	5	0.8	90
Exhaustion	31	0.55	10

Note: $C_0 = 10$ mg/L and $Q = 2$ mL/min

Table 29 Breakthrough and exhaustion points at the bed depth of 4 cm

Point	t (min)	q (mg/g)	Y (%)
Breakthrough	31	3.72	90
Exhaustion	170	2.266	10

Note: $C_0 = 10$ mg/L and $Q = 2$ mL/min

Loading behavior of different concentrations of venlafaxine to be eliminated from the solution in the laboratory-scale column is indicated by the breakthrough curves (Fig. 15 and 16).

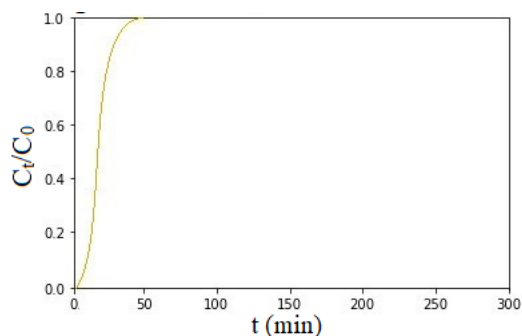


Fig. 15 Breakthrough curve at the bed depth of 3 cm

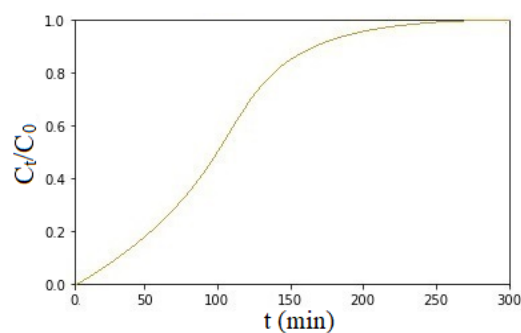


Fig. 16 Breakthrough curve at the bed depth of 4 cm

According to Tables 28 and 29 and Fig. 15 and 16, increasing the bed depth from 3 cm to 4 cm caused the breakthrough time and exhaustion time to increase from 5 to 31 min and 31 to 170 min, respectively.

90% of venlafaxine was eliminated at the breakthrough point where the adsorption capacity was increased from 0.8 mg/g to 3.72 mg/g due to increasing the bed height. Moreover, the removal efficiency of 10% occurred at the exhaustion point in which the adsorption capacity of venlafaxine was increased from 0.55 mg/g to 2.226 mg/g due to increasing the bed depth. Such results are attributed to the additional binding sites which increase the adsorption area of the adsorbent. As a result, late breakthrough and exhaustion can be observed at high bed length. The results showed an improvement of adsorption capacity with an increase of the bed height in the column (Patel et al., 2019). With respect to the identical initial concentration and flow rate of adsorbate, when the bed depth is increased, the adsorbate molecules have adequate time to diffuse into the pores of the adsorbent particles which leads to increase in the number of adsorbate molecules adsorbed by the adsorbent (Marzbali et al., 2017; Patel et al., 2019). At the higher adsorbent bed depth, the column adsorption of cephalexin (CFX) was more efficient (Saadi et al., 2020). The breakthrough time

was increased for higher bed depth due to increasing the residence time (Dubey et al., 2014). The breakthrough time was increased at higher bed depth which resulted in a rapid mass transfer zone (Rafat et al., 2019). Rapid breakthrough was observed at the higher bed depth due to better interactions between adsorbent and adsorbate (Lonappan et al., 2019).

4.2.4. Comparison the effect of different factors on the adsorption capacity

The cluster analysis of the effect of initial concentration, flow rate and bed depth variations on the adsorption capacity at the breakthrough point was represented by the MVSP model (Fig. 17 to 19).

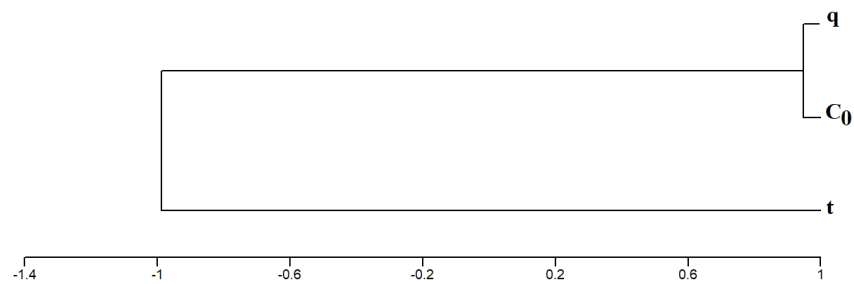


Fig. 17 Cluster analysis of the initial concentration variations at the breakthrough point

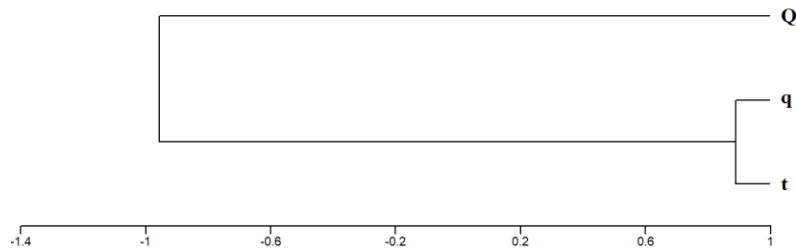


Fig. 18 Cluster analysis of the flow rate variations at the breakthrough point

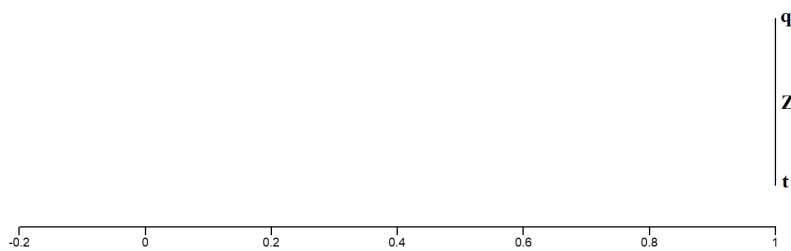


Fig. 19 Cluster analysis of the bed depth variations at the breakthrough point

According to Fig. 17 to 19, the adsorption capacity (q) at the breakthrough point was controlled by initial concentration, flow rate and bed depth with similarity coefficient of 0.95, 0.88 and 1, respectively. As a result, the effects of different factors on the adsorption capacity increased in the sequence of flow rate < initial concentration < bed depth. Fig. 20 to 22 show the cluster analysis of the effect of such factors on the adsorption capacity at the exhaustion point.

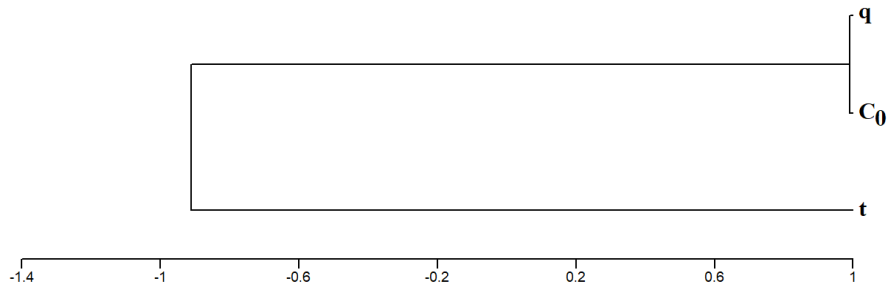


Fig. 20 Cluster analysis of the initial concentration variations at the exhaustion point

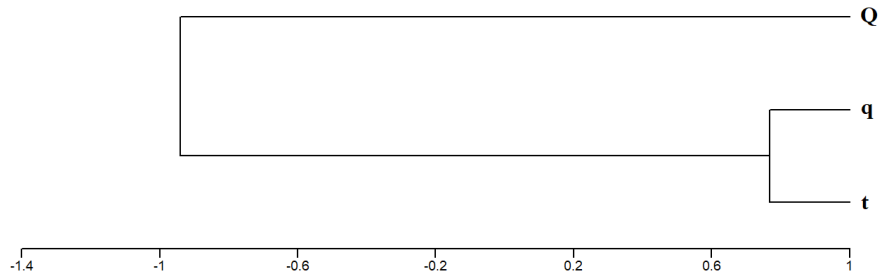


Fig. 21 Cluster analysis of the flow rate variations at the exhaustion point

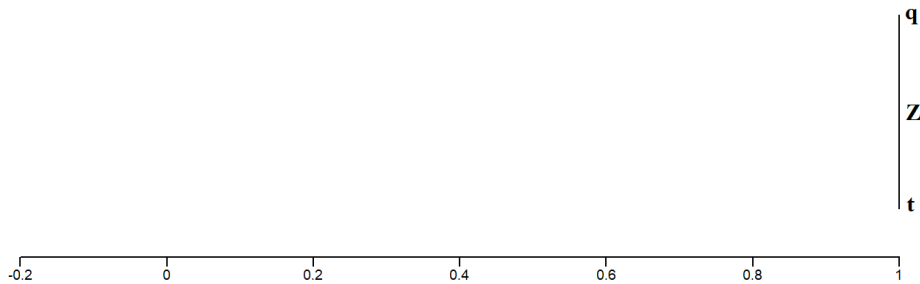


Fig. 22 Cluster analysis of the bed depth variations at the exhaustion point

Based on Fig. 20 to 22, the adsorption capacity at the exhaustion point was joined to initial concentration, flow rate and bed depth with similarity coefficient of 0.99, 0.76 and 1, respectively.

As a result, the effect of such factors on the adsorption capacity could be arranged in the increasing order of flow rate < initial concentration < bed depth.

The results of cluster analysis of initial concentration, flow rate and bed depth confirmed that the driving parameter for adsorption column design is bed depth.

4.3. Design the large-scale PVC column (venlafaxine)

The Adams–Bohart model was used to evaluate the efficiency and applicability of the novel biochar in the large-scale column. Based on the results of section 4.2.3, the bed depth variations (cm) with time (min) are shown in Table 30 and Fig. 23.

Table 30 Bed-depth service time (BDST) at the removal efficiency of 90%

Bed depth (cm)	Breakthrough time (min)	q (mg/g)	Y (%)
3	5	0.8	90
4	31	3.72	90

Note: $C_0 = 10 \text{ mg/L}$ and $Q = 2 \text{ mL/min}$

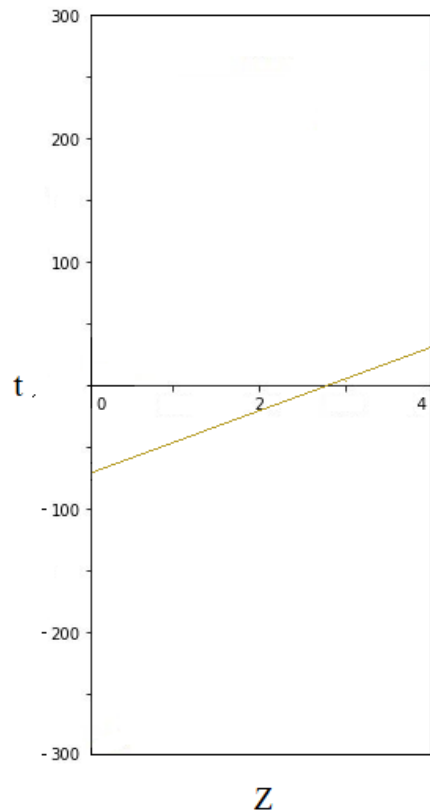


Fig. 23 Bed-depth service time (BDST) curve at the removal efficiency of 90%

In Fig. 23, the line can be represented by the Bohart-Adams equation (LaGrega et al., 2010). The large-scale PVC column can be designed as follows:

$$\text{Area of the laboratory column} = \pi r^2 = 0.785 \times 10^{-4} \text{ m}^2$$

Studying the fixed-bed adsorption column under various experimental conditions indicated that the low flow rate appropriately favors the adsorbate adsorption due to the adequate residence time. As a result, the flow rate equal to 2 mL/min was used to determine the loading rate in the laboratory column.

Loading rate in the laboratory column:

$$V = (0.2 \times 10^{-5} \text{ m}^3 / \text{min}) / 0.785 \times 10^{-4} \text{ m}^2 = 0.03 \text{ m}^3 / (\text{m}^2 \cdot \text{min})$$

Based on the Adams–Bohart model the same loading rate was used for the full-scale unit yields (LaGrega et al., 2010):

$$\text{Area of the large-scale column} = Q/V = (0.001 \text{ m}^3 / \text{min}) / (0.03 \text{ m}^3 / (\text{m}^2 \cdot \text{min})) = 0.03 \text{ m}^2$$

$$\text{Diameter of the large-scale column} = 0.2 \text{ m}$$

BDST equation for 90% removal of venlafaxine can be shown as follows:

$$\text{Slope } a = 3 \text{ days} / 2.13 \text{ m} = 1.81 \text{ days} / \text{m}$$

$$\text{Intercept } b = -0.05 \text{ days}$$

$$\text{Equation of line (formula 3-1): } t = 1.81x - 0.05$$

$$\text{Velocity of adsorption zone in large-scale column} = 1 / a = 0.55 \text{ m} / \text{day}$$

$$\text{Adsorbent utilization in large-scale column (formula 3-4)} = \text{area} \times (1/a) \times \text{unit weight} = 0.03 \text{ m}^2 \times 0.55 \text{ m/day} \times 50 \text{ kg/m}^3 = 0.825 \text{ kg/day}$$

According to the obtained results, the large-scale PVC column was installed (Fig. 8).

The results of passing wastewater effluent from the large-scale column are shown in Table 31.

Table 31 Removal efficiency of venlafaxine in the large-scale column

Sample	Concentration (ng/L)	Y (%)
The effluent of column (first day)	117.558073	95
The effluent of column (second day)	1765.8652294	25
The effluent of column (third day)	2116.22931	10

Note: the initial concentration of venlafaxine in wastewater effluent is 2354.48 ng/L

Based on the Table 31, the concentration of venlafaxine in wastewater effluent was decreased from 2354 ng / L to 117.70 ng / L within first day. The obtained results confirmed the feasibility of using

biochar to remove venlafaxine by 95%, within one day from wastewater effluent. Decreasing the removal efficiency of venlafaxine from 95 to 10% approved the result of designing the column by Adams-Bohart model which shows the adsorbent utilization in the large-scale column is 0.825 kg/day.

Considering the industrial applications of the adsorption process, plotting the breakthrough curve is of key importance, since it accurately reveals the operational limit of the column (Suzaki et al., 2017). Loading behavior of venlafaxine to be eliminated from the wastewater in a fixed-bed column can be indicated by the breakthrough curve (Gupta et al., 2016; Mojiri et al., 2019; Qian et al., 2019). The breakthrough curve of the large-scale column was drawn by plotting the relative concentration of venlafaxine, which is the ratio of the venlafaxine concentration in the effluent of column to the concentration of venlafaxine in wastewater with respect to time (Fig. 24). Moreover, the exhaustion and breakthrough points are shown in Table 32.

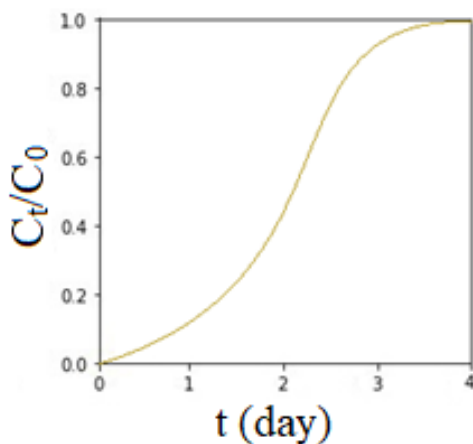


Fig. 24 Breakthrough curve for large-scale PVC column

Table 32 Breakthrough and exhaustion points of venlafaxine in the large-scale column

Point	t (day)	q (ng/g)	Y (%)
Breakthrough	1	3051.406	95
Exhaustion	3	1017.135	10

Note: $Q = 0.001 \text{ m}^3/\text{min}$, the amount of biochar = 1000 g, and $C_0 = 2354.48 \text{ ng/L}$

According to Table 32 and Fig. 24, the breakthrough time and exhaustion time were 1 and 3 days, respectively. 95% of venlafaxine was eliminated at the breakthrough point where the adsorption

capacity was 3051.406 ng/g. Moreover, the removal efficiency of 10% occurred at the exhaustion point in which the adsorption capacity of venlafaxine was 1017.135.

The results of other studies revealed that primary treatment and trickling filter/solids contact are not capable of eliminating antidepressants from sewage (Lajeunesse et al., 2012). Nevertheless, the capacity of activated sludge, biological aerated filter, and biological nutrient removal processes in the elimination of antidepressants from sewage is 30% (Lajeunesse et al., 2012). Venlafaxine was not totally eliminated in the wastewater treatment plants and remained in the effluents entering river water (Alonso et al., 2010; Rúa-Gómez and Püttmann 2012; Zhou et al., 2010) and even groundwater (Einsiedl et al., 2010; Rúa-Gómez and Püttmann 2012). 79 % of venlafaxine was eliminated from wastewater by advanced biological activated carbon filter in a fixed-bed column (Sbardella et al., 2018). Casas et al. (2015) showed that the removal efficiency of sulfamethoxazole, venlafaxine, iopromide, tramadol, and diatrizoic is lower than 20 %. Near 60% of diclofenac was eliminated through using microbiochar in a fixed-bed column (Lonappan et al., 2019).

Municipal wastewater treatment plants eliminate some of the pharmaceuticals and other complex substances. Nevertheless, a huge percentage of such pharmaceuticals can still be found in the treatment plant final effluent, which is released into receiving waterways, especially Saint-Lowrance River (Blaise et al., 2006; Grill et al., 2016; Marcogliese et al., 2014). Grill et al. (2016) revealed that pharmaceuticals pose a serious threat to various aquatic organisms due to higher MEC concentration in comparison with the PNEC concentration. Based on the obtained results from the utilization of large-scale PVC column, the risk of venlafaxine to the aquatic and marine organisms can be evaluated as follows:

$$RQ_{freshwater} = \frac{117.558073 \text{ ng/L}}{141 \text{ ng/L}} = 0.834 < 1$$

$$RQ_{marine\ water} = \frac{117.558073 \frac{\text{ng}}{\text{L}}}{120 \frac{\text{ng}}{\text{L}}} = 0.978 < 1$$

The values of RQ clearly indicated that the risk of presence of venlafaxine for freshwater and marine water is converted from high risk to low risk to aquatic and marine organisms. The results

acknowledged this fact that the novel biochar in the fixed-bed column gave aid to eliminate venlafaxine from wastewater effluent. Utilization of novel biochar in full-scale facility will provide a proper position for eliminating pharmaceuticals from the effluent of wastewater treatment plant. As a consequence, it is expected that such a novel biochar plays a vital role in enriching the condition of Saint Lawrence River.

4.4. Laboratory-scale fixed-bed adsorption column (Ni, Pb and Cu)

4.4.1 Effect of the initial concentration

The initial concentration of adsorbate is considered as an important factor which influences on the efficiency of the adsorption system. This parameter adequately determined helps to provide an appropriate driving force for the transport of adsorbate molecules toward the adsorbent bed. As a result, the effect of initial concentration on the column performance should be evaluated in an accurate manner.

The impact of different initial concentrations of Ni, Pb and Cu on the adsorption were studied by varying the concentration of each metal in the range of 60, 70 and 80 $\mu\text{g/L}$, while the bed depth and flow rate were kept constant at 4 cm and 2 mL/min, respectively. The results are shown in Tables 33 to 41.

Table 33 Breakthrough and exhaustion points of Ni at the initial concentration of 60 $\mu\text{g/L}$

Point	t (min)	q ($\mu\text{g/g}$)	Y (%)
Breakthrough	24	17.28	90
Exhaustion	150	12	10

Note: Q = 2 mL/min and Z = 4 cm

Table 34 Breakthrough and exhaustion points of Ni at the initial concentration of 70 $\mu\text{g/L}$

Point	t (min)	q ($\mu\text{g/g}$)	Y (%)
Breakthrough	21	17.64	90
Exhaustion	130	12.13	10

Note: Q = 2 mL/min and Z = 4 cm

Table 35 Breakthrough and exhaustion points of Ni at the initial concentration of 80 $\mu\text{g/L}$

Point	t (min)	q ($\mu\text{g/g}$)	Y (%)
Breakthrough	19	18.24	90
Exhaustion	114	12.16	10

Note: Q = 2 mL/min and Z = 4 cm

Table 36 Breakthrough and exhaustion points of Pb at the initial concentration of 60 µg/L

Point	t (min)	q (µg/g)	Y (%)
Breakthrough	40	28.8	90
Exhaustion	180	14.4	10

Note: Q = 2 mL/min and Z = 4 cm

Table 37 Breakthrough and exhaustion points of Pb at the initial concentration of 70 µg/L

Point	t (min)	q (µg/g)	Y (%)
Breakthrough	35	29.4	90
Exhaustion	158	14.47	10

Note: Q = 2 mL/min and Z = 4 cm

Table 38 Breakthrough and exhaustion points of Pb at the initial concentration of 80 µg/L

Point	t (min)	q (µg/g)	Y (%)
Breakthrough	32	30.72	90
Exhaustion	145	15.46	10

Note: Q = 2 mL/min and Z = 4 cm

Table 39 Breakthrough and exhaustion points of Cu at the initial concentration of 60 µg/L

Point	t (min)	q (µg/g)	Y (%)
Breakthrough	34	23	90
Exhaustion	161	12.8	10

Note: Q = 2 mL/min and Z = 4 cm

Table 40 Breakthrough and exhaustion points of Cu at the initial concentration of 70 µg/L

Point	t (min)	q (µg/g)	Y (%)
Breakthrough	28	23.52	90
Exhaustion	141	13.16	10

Note: Q = 2 mL/min and Z = 4 cm

Table 41 Breakthrough and exhaustion points of Cu at the initial concentration of 80 µg/L

Point	t (min)	q (µg/g)	Y (%)
Breakthrough	25	24	90
Exhaustion	125	13.3	10

Note: Q = 2 mL/min and Z = 4 cm

Loading behavior of different concentrations of Ni, Pb and Cu to be eliminated from the synthetic wastewater in the laboratory-scale column is indicated by the breakthrough curves (Fig. 25 to 33).

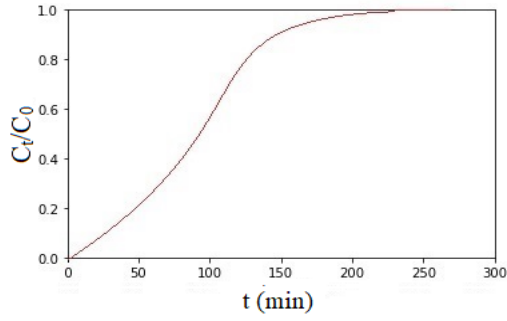


Fig. 25 Breakthrough curve of Ni at the initial concentration of 60 µg/L

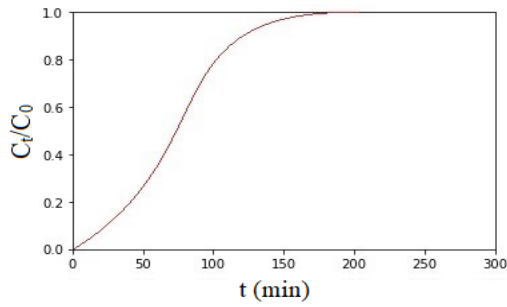


Fig. 26 Breakthrough curve of Ni at the initial concentration of 70 µg/L

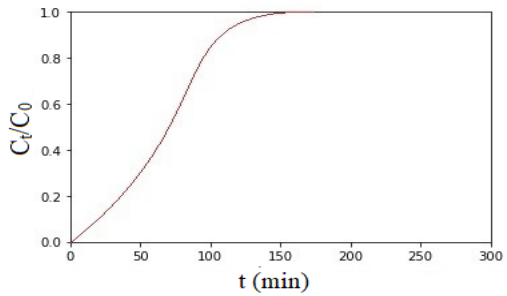


Fig. 27 Breakthrough curve of Ni at the initial concentration of 80 µg/L

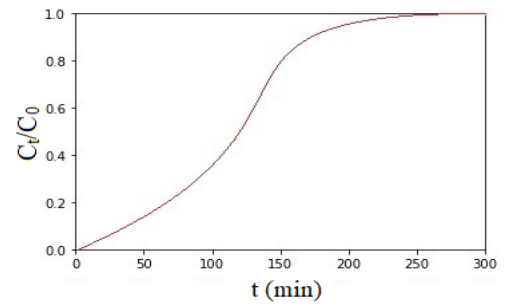


Fig. 28 Breakthrough curve of Pb at the initial concentration of 60 µg/L

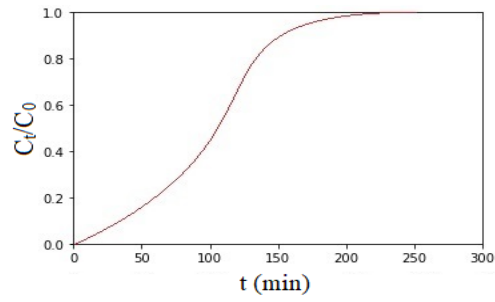


Fig. 29 Breakthrough curve of Pb at the initial concentration of 70 µg/L

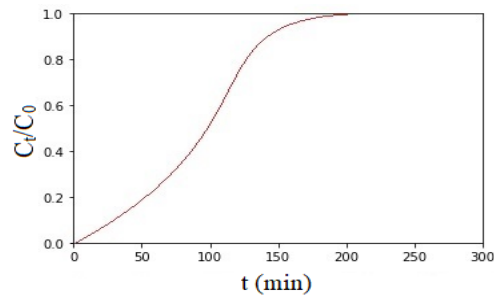


Fig. 30 Breakthrough curve of Pb at the initial concentration of 80 µg/L

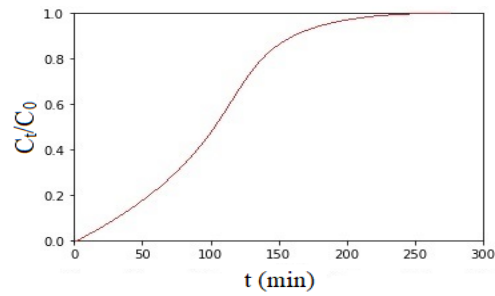


Fig. 31 Breakthrough curve of Cu at the initial concentration of 60 µg/L

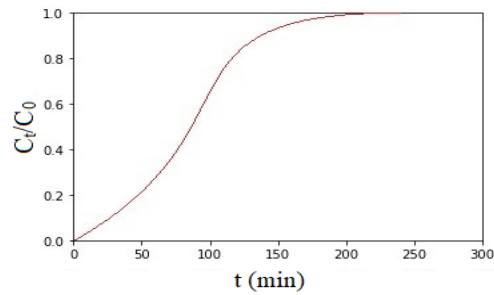


Fig. 32 Breakthrough curve of Cu at the initial concentration of 70 µg/L

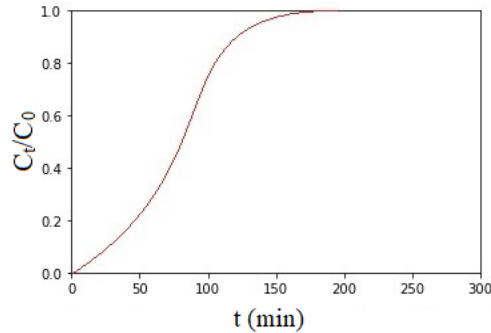


Fig. 33 Breakthrough curve of Cu at the initial concentration of 80 µg/L

According to the Tables 33 to 41 and Fig. 25 to 33, increasing the initial concentration of each metal from 60 to 80 µg/L caused the breakthrough time to decrease from 24 to 19 min for Ni, 40 to 32 min for Pb and 34 to 25 min for Cu. Furthermore, the exhaustion time was decreased from 150 to 114 min for Ni, 180 to 145 min for Pb and 161 to 125 min for Cu because of increasing the initial concentration. 90% of Ni, Pb and Cu was eliminated at the breakthrough point where the adsorption capacity was increased from 17.28 to 18.24, 28.8 to 30.72 and 23 to 24 µg/g, respectively. The removal efficiency of 10% occurred at the exhaustion point in which the adsorption capacity was increased from 12 to 12.16 µg/g for Ni, 14.4 to 15.46 µg/g for Pb and 12.8 to 13.3 µg/g for Cu. The adsorption capacity could be arranged in the order of Pb > Cu > Ni.

Increasing the initial concentration of adsorbate caused the adsorption capacity to be on the increase because of providing a larger driving force (Abdolali et al., 2017). In the adsorption process, the main driving force can be defined as the difference between the concentration of solute on the sorbent and concentration of solute in the solution (Patel 2019; Volesky and Prasetyo 1994). Increasing the initial concentration of metal provides a greater driving force of adsorption because of the high concentration difference facilitated by high mass transfer coefficient values (Patel 2019; Volesky and Prasetyo 1994). As a consequence, higher adsorption capacity can be achieved at higher adsorbate concentration. The acceleration of the adsorption rate leads to an early saturation of the column. Increasing the initial concentration of heavy metals in a fixed-bed column leads to an increase in the total removal (%) (Sankararamakrishnan et al., 2008). At higher initial concentration, greater concentration gradient and smaller mass transfer resistance reduce the breakthrough and exhaustion time, and thus the adsorbent reached saturation more quickly (Zhang et al., 2019c). Rapid exhaustion and breakthrough were observed due to greater concentration

gradient along with smaller mass transfer resistance (Abdolali et al., 2017). Increasing the initial concentration of contaminants caused the breakthrough time and exhaustion time to increase because of the availability of more adsorption sites (Chatterjee and Abraham 2019; Han et al., 2006).

4.4.2. Effect of the flow rate

The efficiency of the adsorption system is influenced by the volumetric flow rate. In other words, the flow rate as a significant factor determines the adequate contact between adsorbate and adsorbent.

The impact of the flow rate of Ni, Pb and Cu on the adsorption was studied by varying the flow rate of each metal in the range of 2, 5 and 10 mL/min, while the bed depth and initial concentration were kept constant at 4 cm and 60 µg/L, respectively. The results are represented in Tables 42 to 50.

Table 42 Breakthrough and exhaustion points of Ni at the flow rate of 2 mL/min

Point	t (min)	q (µg/g)	Y (%)
Breakthrough	24	17.28	90
Exhaustion	150	12	10

Note: $C_0 = 60 \mu\text{g/L}$ and $Z = 4 \text{ cm}$

Table 43 Breakthrough and exhaustion points of Ni at the flow rate of 5 mL/min

Point	t (min)	q (µg/g)	Y (%)
Breakthrough	9	16.2	90
Exhaustion	56	11.2	10

Note: $C_0 = 60 \mu\text{g/L}$ and $Z = 4 \text{ cm}$

Table 44 Breakthrough and exhaustion points of Ni at the flow rate of 10 mL/min

Point	t (min)	q (µg/g)	Y (%)
Breakthrough	3	10.8	90
Exhaustion	25	10	10

Note: $C_0 = 60 \mu\text{g/L}$ and $Z = 4 \text{ cm}$

Table 45 Breakthrough and exhaustion points of Pb at the flow rate of 2 mL/min

Point	t (min)	q (µg/g)	Y (%)
Breakthrough	40	28.8	90
Exhaustion	180	14.4	10

Note: $C_0 = 60 \mu\text{g/L}$ and $Z = 4 \text{ cm}$

Table 46 Breakthrough and exhaustion points of Pb at the flow rate of 5 mL/min

Point	t (min)	q (µg/g)	Y (%)
Breakthrough	14	25.2	90
Exhaustion	70	14	10

Note: $C_0 = 60 \mu\text{g/L}$ and $Z = 4 \text{ cm}$

Table 47 Breakthrough and exhaustion points of Pb at the flow rate of 10 mL/min

Point	t (min)	q (µg/g)	Y (%)
Breakthrough	6	21.6	90
Exhaustion	34	13.6	10

Note: $C_0 = 60 \mu\text{g/L}$ and $Z = 4 \text{ cm}$

Table 48 Breakthrough and exhaustion points of Cu at the flow rate of 2 mL/min

Point	t (min)	q (µg/g)	Y (%)
Breakthrough	34	23	90
Exhaustion	161	12.8	10

Note: $C_0 = 60 \mu\text{g/L}$ and $Z = 4 \text{ cm}$

Table 49 Breakthrough and exhaustion points of Cu at the flow rate of 5 mL/min

Point	t (min)	q (µg/g)	Y (%)
Breakthrough	11	19.8	90
Exhaustion	61	12.2	10

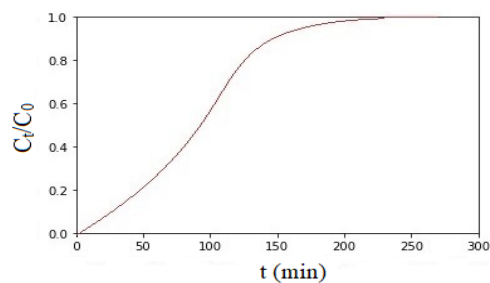
Note: $C_0 = 60 \mu\text{g/L}$ and $Z = 4 \text{ cm}$

Table 50 Breakthrough and exhaustion points of Cu at the flow rate of 10 mL/min

Point	t (min)	q (µg/g)	Y (%)
Breakthrough	4	14.4	90
Exhaustion	29	11.6	10

Note: $C_0 = 60 \mu\text{g/L}$ and $Z = 4 \text{ cm}$

Loading behavior of concentrations of Ni, Pb and Cu to be eliminated from the solution in the laboratory-scale column is represented by the breakthrough curves (Fig. 34 to 42).

**Fig. 34 Breakthrough curve of Ni at the volumetric flow rate of 2 mL/min**

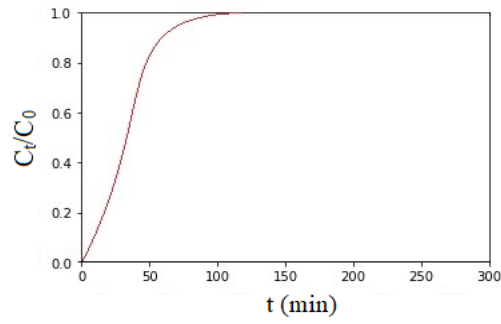


Fig. 35 Breakthrough curve of Ni at the volumetric flow rate of 5 mL/min

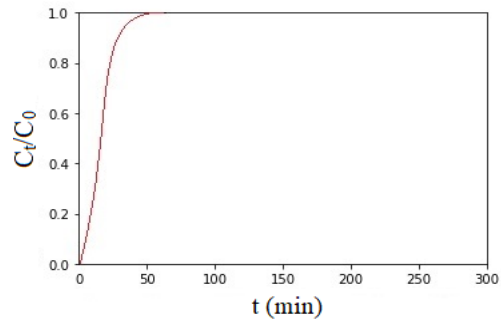


Fig. 36 Breakthrough curve of Ni at the volumetric flow rate of 10 mL/min

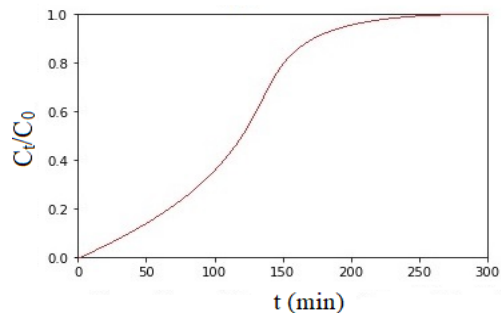


Fig. 37 Breakthrough curve of Pb at the volumetric flow rate of 2 mL/min

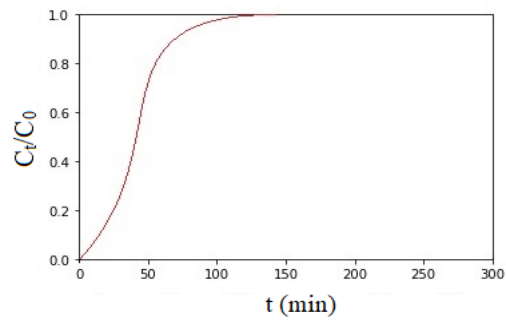


Fig. 38 Breakthrough curve of Pb at the volumetric flow rate of 5 mL/min

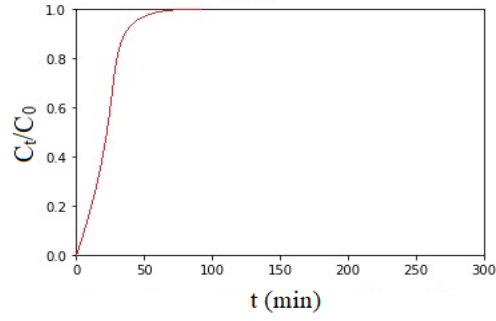


Fig. 39 Breakthrough curve of Pb at the volumetric flow rate of 10 mL/min

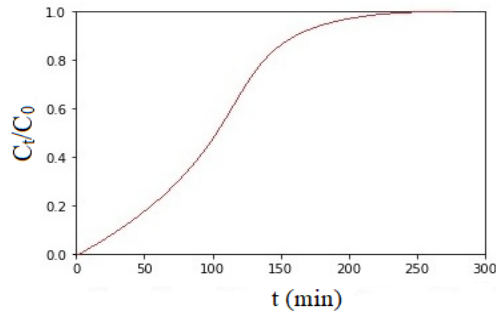


Fig. 40 Breakthrough curve of Cu at the volumetric flow rate of 2 mL/min

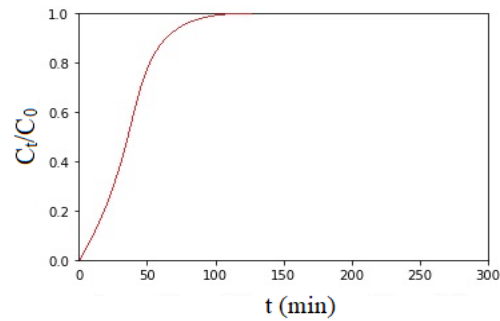


Fig. 41 Breakthrough curve of Cu at the volumetric flow rate of 5 mL/min

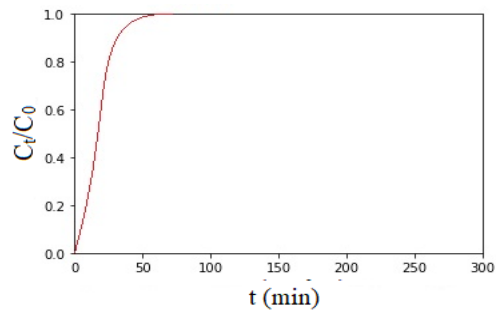


Fig. 42 Breakthrough curve of Cu at the volumetric flow rate of 10 mL/min

Based on the Tables 42 to 50 and Fig. 34 to 42, increasing the volumetric flow rate of each metal from 2 to 10 ml/min caused the breakthrough time to decrease from 24 to 3 min for Ni, 40 to 6 min for Pb and 34 to 4 min for Cu. Furthermore, the exhaustion time was decreased from 150 to 25 min for Ni, 180 to 34 min for Pb and 161 to 29 min for Cu because of increasing the flow rate. 90% of Ni, Pb and Cu was eliminated at the breakthrough point where the adsorption capacity was decreased from 17.28 to 10.8, 28.8 to 21.6 and 23 to 14.4 $\mu\text{g/g}$, respectively. The removal efficiency of 10% occurred at the exhaustion point in which the adsorption capacity was decreased from 12 to 10 $\mu\text{g/g}$ for Ni, 14.4 to 13.6 $\mu\text{g/g}$ for Pb and 12.8 to 11.6 $\mu\text{g/g}$ for Cu. The adsorption capacity could be arranged in the order of $\text{Pb} > \text{Cu} > \text{Ni}$.

Such results are related to the inadequate contact between adsorbate and adsorbent at the increased flow rate. As a consequence, the low flow rate appropriately favors the adsorbate adsorption due to the adequate residence time. The results showed that adsorption capacity, breakthrough time and saturation time are decreased at a higher flow rate due to the low duration of contact between adsorbate and adsorbent (Yusuf et al., 2020). Increasing the flow rate in a fixed-bed column leads to a reduction in the total removal (%) (Futalan et al., 2011). Decreasing the flow rate provides more residence time for mass transfer into the pores, consequently allowing heavy metals to access more active sites within the adsorbent (Abdolali et al., 2017). Increasing the flow rate caused breakthrough and exhaustion points to occur faster because of a reduction in the external film diffusion mass transfer resistance (Renu et al., 2020). At advanced flow rate, steeper breakthrough curve was observed in a dumpier mass transfer region due to inadequate interaction time between the adsorbent and adsorbate (Yusuf et al., 2020). Since the contact time between heavy metal and adsorbent in a packed-bed column is increased by decreasing influent flow rate, it causes the breakthrough and exhaustion time to be on the increase (Yusuf et al., 2020).

4.4.3. Effect of the bed depth

The performance of adsorption is impacted by bed height. The extent of adsorption depends on the amount of adsorbent within the column, which provides the appropriate adsorption sites for the best performance. In other words, bed depth as an important factor affect the surface area and the number of binding sites available for adsorption. The impact of bed depth or amount of biochar on the adsorption was studied by varying the bed depth in the range of 3 and 4 cm, while the

volumetric flow rate and initial concentration were kept constant at 2 mL/min and 60 µg/L, respectively. The results are shown in Tables 51 to 56.

Table 51 Breakthrough and exhaustion points of Ni at the bed depth of 3 cm

Point	t (min)	q (µg/g)	Y (%)
Breakthrough	2	1.92	90
Exhaustion	16	1.7	10

Note: $C_0 = 60 \mu\text{g/L}$ and $Q = 2 \text{ mL/min}$

Table 52 Breakthrough and exhaustion points of Ni at the bed depth of 4 cm

Point	t (min)	q (µg/g)	Y (%)
Breakthrough	24	17.28	90
Exhaustion	150	12	10

Note: $C_0 = 60 \mu\text{g/L}$ and $Q = 2 \text{ mL/min}$

Table 53 Breakthrough and exhaustion points of Pb at the bed depth of 3 cm

Point	t (min)	q (µg/g)	Y (%)
Breakthrough	4	3.84	90
Exhaustion	33	3.52	10

Note: $C_0 = 60 \mu\text{g/L}$ and $Q = 2 \text{ mL/min}$

Table 54 Breakthrough and exhaustion points of Pb at the bed depth of 4 cm

Point	t (min)	q (µg/g)	Y (%)
Breakthrough	40	28.8	90
Exhaustion	180	14.4	10

Note: $C_0 = 60 \mu\text{g/L}$ and $Q = 2 \text{ mL/min}$

Table 55 Breakthrough and exhaustion points of Cu at the bed depth of 3 cm

Point	t (min)	q (µg/g)	Y (%)
Breakthrough	3	2.88	90
Exhaustion	18	1.92	10

Note: $C_0 = 60 \mu\text{g/L}$ and $Q = 2 \text{ mL/min}$

Table 56 Breakthrough and exhaustion points of Cu at the bed depth of 4 cm

Point	t (min)	q (µg/g)	Y (%)
Breakthrough	34	23	90
Exhaustion	161	12.8	10

Note: $C_0 = 60 \mu\text{g/L}$ and $Q = 2 \text{ mL/min}$

Loading behavior of different concentrations of Ni, Pb and Cu to be eliminated from the solution in the laboratory-scale column is indicated by the breakthrough curves (Fig. 43 and 48).

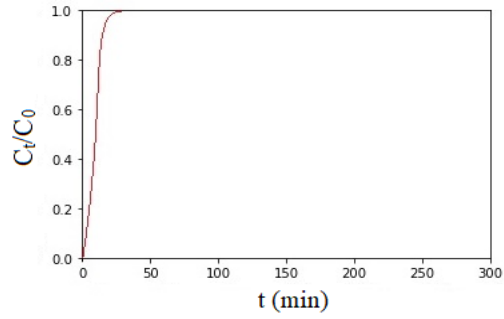


Fig. 43 Breakthrough curve of Ni at the bed depth of 3 cm

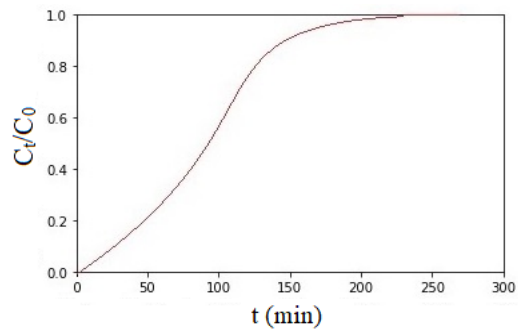


Fig. 44 Breakthrough curve of Ni at the bed depth of 4 cm

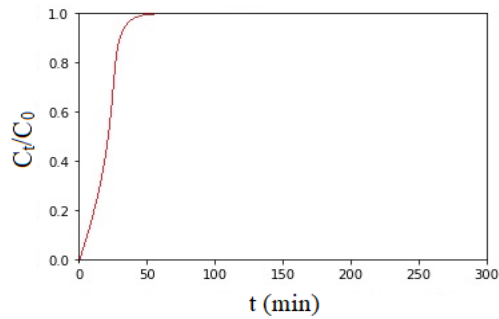


Fig. 45 Breakthrough curve of Pb at the bed depth of 3 cm

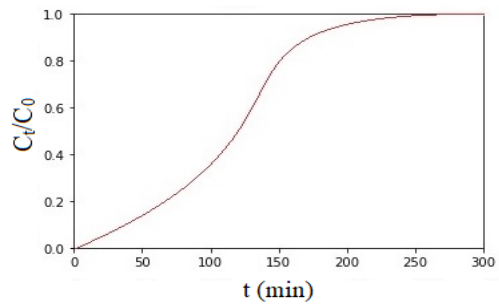


Fig. 46 Breakthrough curve of Pb at the bed depth of 4 cm

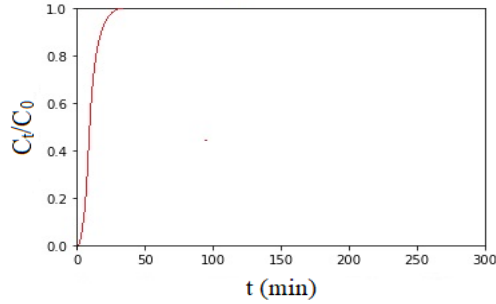


Fig. 47 Breakthrough curve of Cu at the bed depth of 3 cm

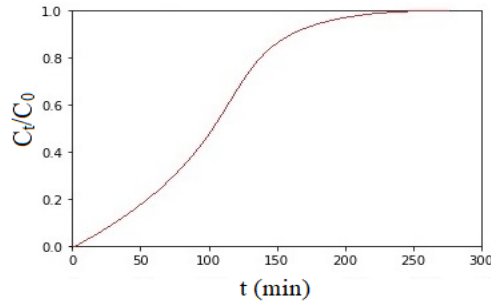


Fig. 48 Breakthrough curve of Cu at the bed depth of 4 cm

According to the Tables 51 to 56 and Fig. 43 to 48, increasing the bed depth of biochar from 3 to 4 cm caused the breakthrough time to increase from 2 to 24 min for Ni, 4 to 40 min for Pb and 3 to 34 min for Cu. Furthermore, the exhaustion time was increased from 16 to 150 min for Ni, 33 to 180 min for Pb and 18 to 161 min for Cu because of increasing the bed depth. 90% of Ni, Pb and Cu was eliminated at the breakthrough point where the adsorption capacity was increased from 1.92 to 17.28, 3.84 to 28.8 and 2.88 to 23 $\mu\text{g/g}$, respectively. The removal efficiency of 10% occurred at the exhaustion point in which the adsorption capacity was increased from 1.7 to 12 $\mu\text{g/g}$ for Ni, 3.52 to 14.4 $\mu\text{g/g}$ for Pb and 1.92 to 12.8 $\mu\text{g/g}$ for Cu. The adsorption capacity could be arranged in the order of $\text{Pb} > \text{Cu} > \text{Ni}$.

Such results are attributed to the additional binding sites which increase the adsorption area of the adsorbent. As a result, late breakthrough and more adsorption capacity for heavy metals can be observed at high bed length. The extent of adsorption depends on the amount of adsorbent within the column, which provides the appropriate adsorption sites for the best performance (Abdolali et al., 2017). Increasing bed depth in a fixed-bed column leads to an increase in the total removal (%) (Futalan et al., 2011). Increasing the bed depth of adsorbent caused the breakthrough time along

with exhaustion time to increase due to the availability of binding site for adsorption (Rodrigues et al., 2020). Since increasing the bed height results in a wide mass transfer zone, more specific surface and more available binding sites, it caused the breakthrough time and exhaustion time to increase (Abdolali et al., 2017). Slower breakthrough and exhaustion occurred at a higher bed height (Kavianinia et al., 2012).

4.4.4. Comparison the effect of different factors on the adsorption capacity

The cluster analysis of the effect of initial concentration, flow rate and bed depth variations on the adsorption capacity at the breakthrough points of Ni, Pb and Cu is shown by the MVSP (Fig. 49 to 57).

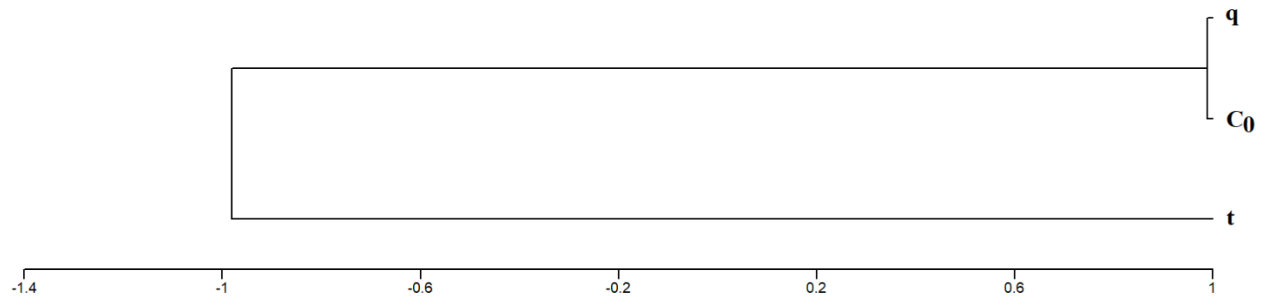


Fig. 49 Cluster analysis of the initial concentration variations at the breakthrough point of Ni

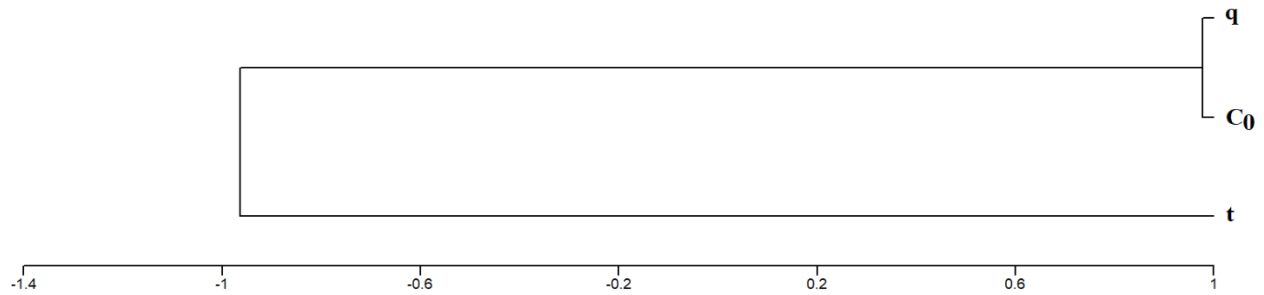


Fig. 50 Cluster analysis of the initial concentration variations at the breakthrough point of Pb

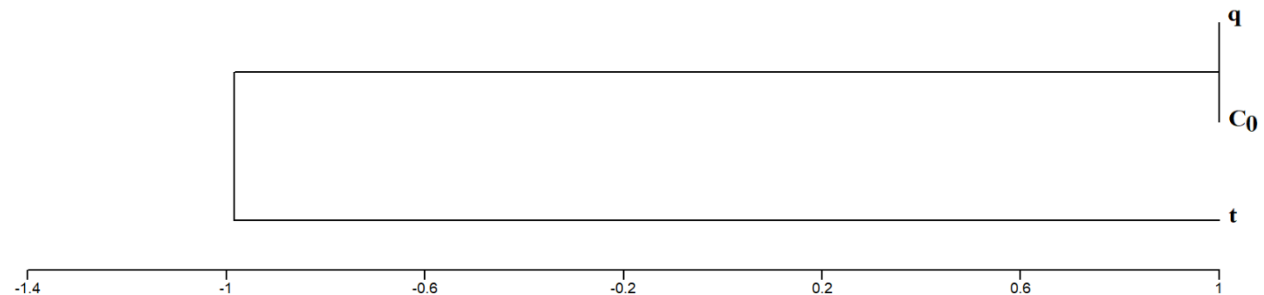


Fig. 51 Cluster analysis of the initial concentration variations at the breakthrough point of Cu

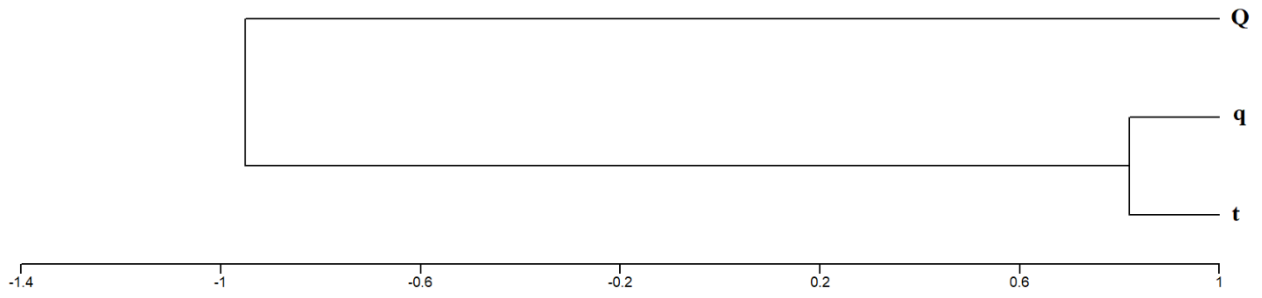


Fig. 52 Cluster analysis of the flow rate variations at the breakthrough point of Ni

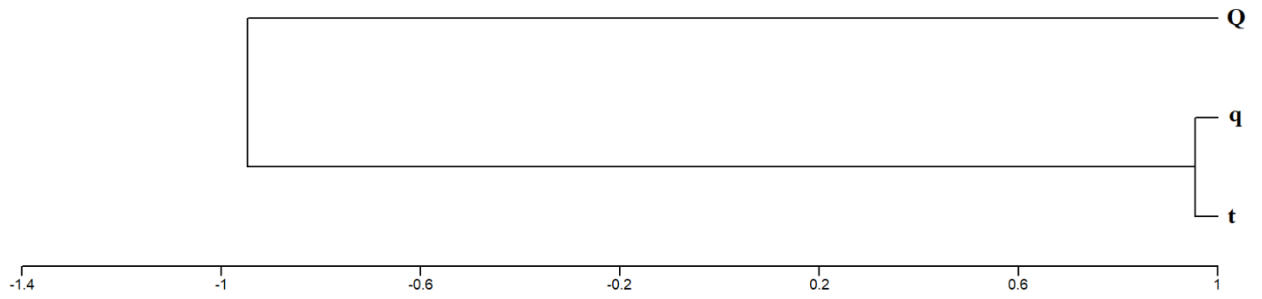


Fig. 53 Cluster analysis of the flow rate variations at the breakthrough point of Pb

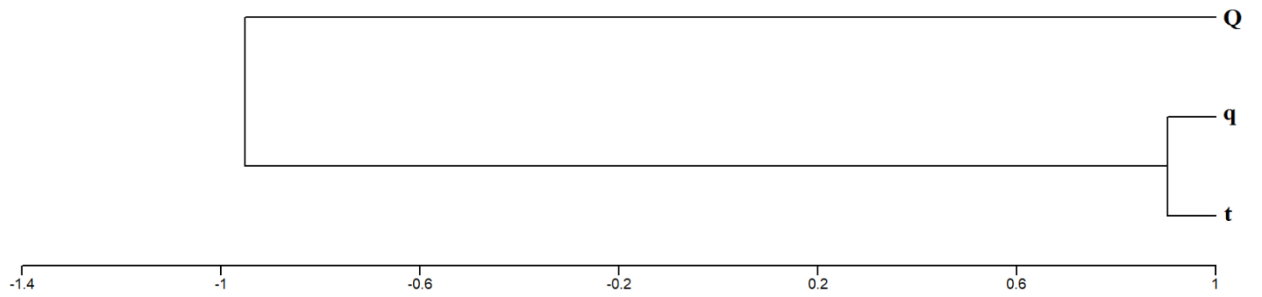


Fig. 54 Cluster analysis of the flow rate variations at the breakthrough point of Cu

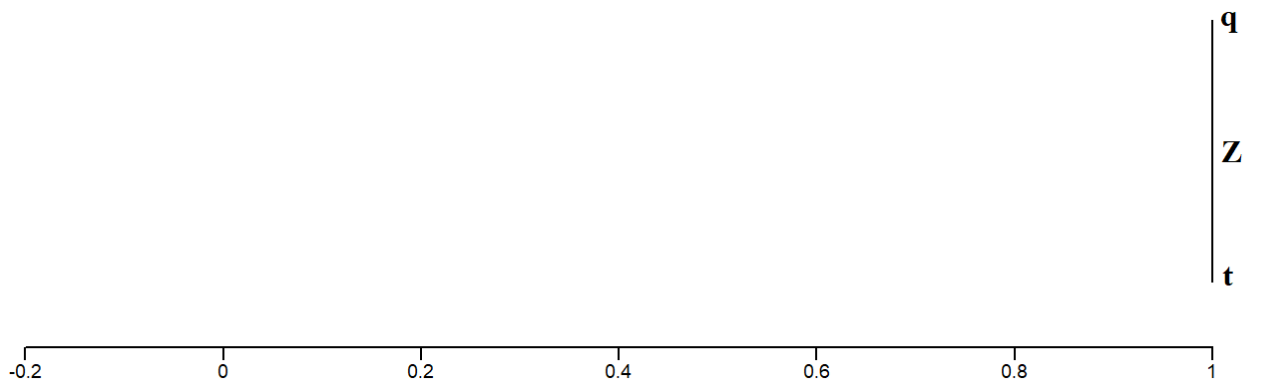


Fig. 55 Cluster analysis of the bed depth variations at the breakthrough point of Ni

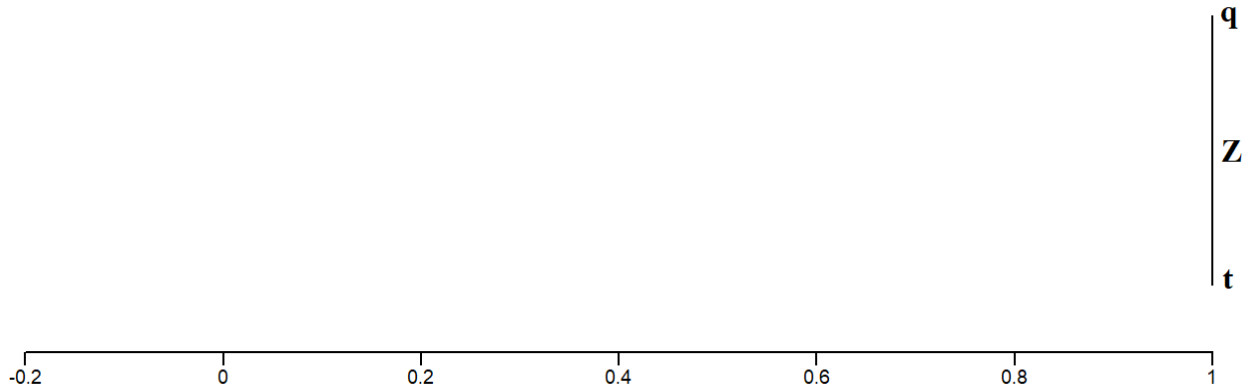


Fig. 56 Cluster analysis of the bed depth variations at the breakthrough point of Pb

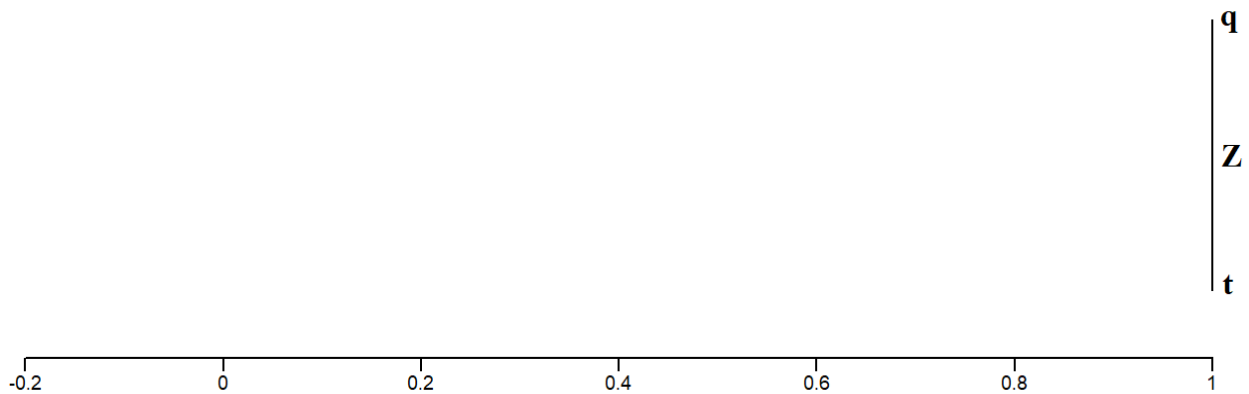


Fig. 57 Cluster analysis of the bed depth variations at the breakthrough point of Cu

According to Fig. 49 to 57, the adsorption capacity (q) at the breakthrough points of Ni, Pb and Cu was controlled by initial concentration with similarity coefficient of 0.99, 0.97 and 0.999, respectively. Moreover, adsorption capacity at the breakthrough points of Ni, Pb and Cu was joined to the flow rate with similarity coefficient of 0.82, 0.95 and 0.9, respectively.

Due to high similarity coefficient of 1, the adsorption capacity at the breakthrough points of Ni, Pb and Cu was governed by the bed depth. Consequently, the effect of such factors on the adsorption capacity could be arranged in the increasing order of flow rate < initial concentration < bed depth.

Fig. 58 to 66 show the cluster analysis of the effect of such factors on the adsorption capacity at the exhaustion points of Ni, Pb and Cu.

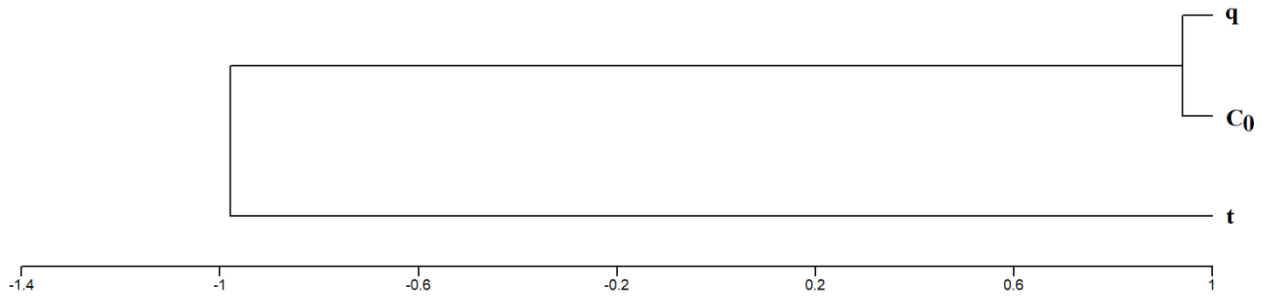


Fig. 58 Cluster analysis of the initial concentration variations at the exhaustion point of Ni

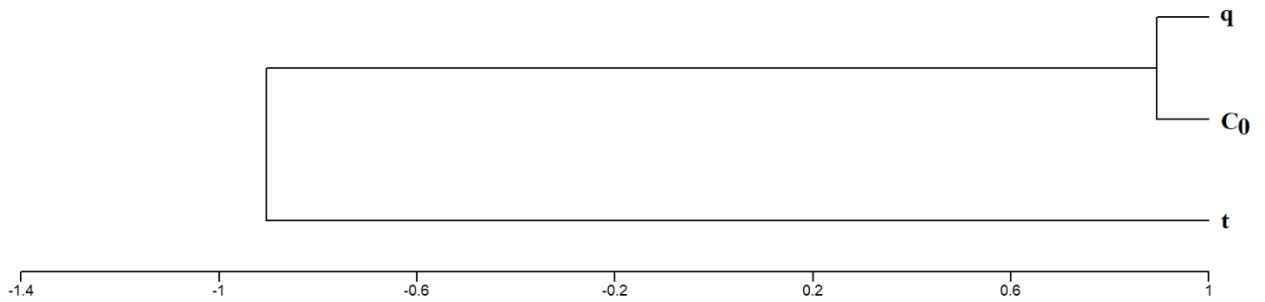


Fig. 59 Cluster analysis of the initial concentration variations at the exhaustion point of Pb

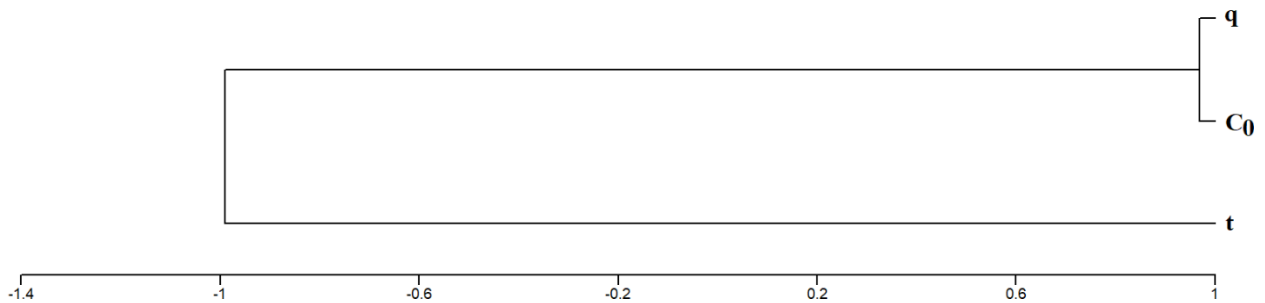


Fig. 60 Cluster analysis of the initial concentration variations at the exhaustion point of Cu

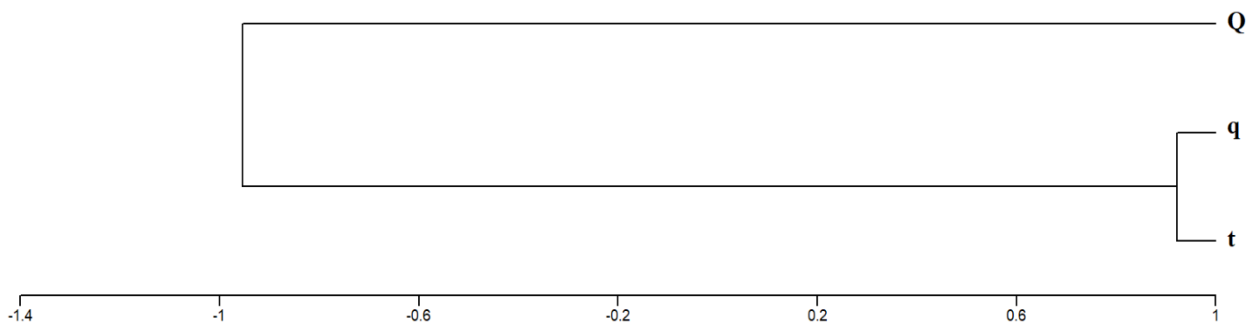


Fig. 61 Cluster analysis of the flow rate variations at the exhaustion point of Ni

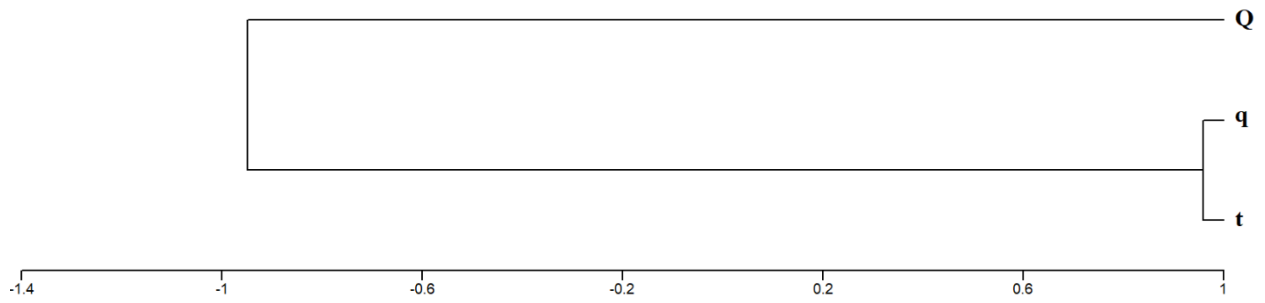


Fig. 62 Cluster analysis of the flow rate variations at the exhaustion point of Pb

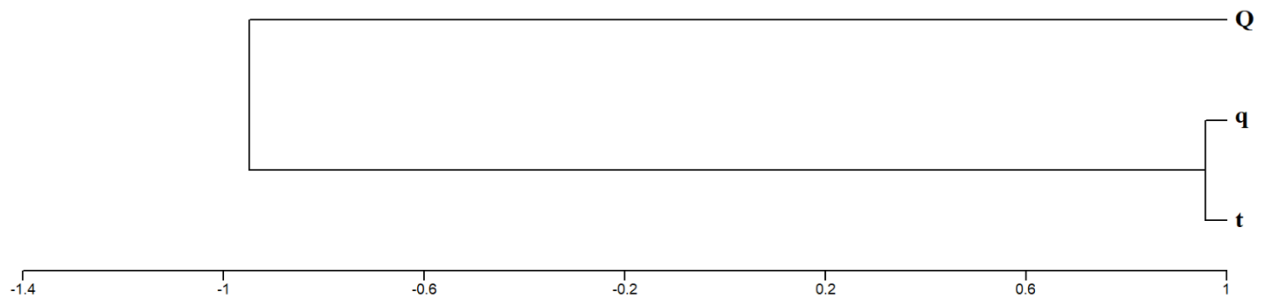


Fig. 63 Cluster analysis of the flow rate variations at the exhaustion point of Cu

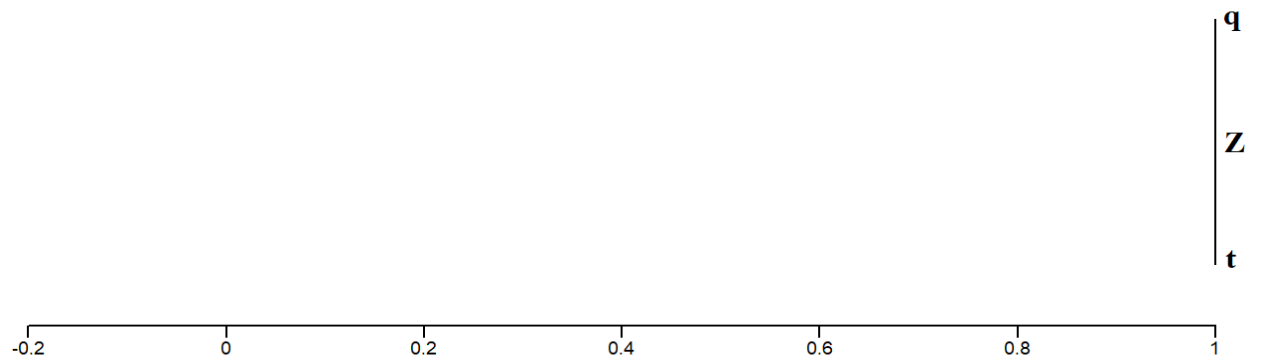


Fig. 64 Cluster analysis of the bed depth variations at the exhaustion point of Ni

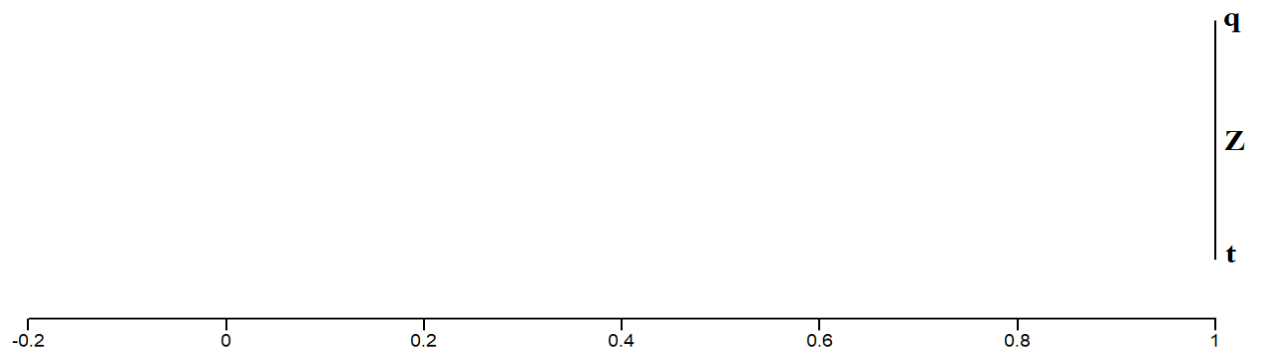


Fig. 65 Cluster analysis of the bed depth variations at the exhaustion point of Pb

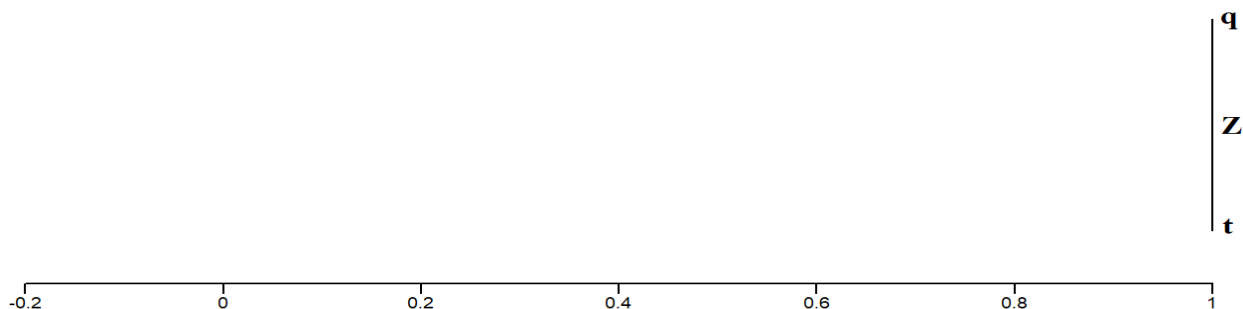


Fig. 66 Cluster analysis of the bed depth variations at the exhaustion point of Cu

Based on Fig. 58 to 66, the adsorption capacity (q) at the exhaustion points of Ni, Pb and Cu was controlled by initial concentration with similarity coefficient of 0.94, 0.98 and 0.96, respectively. Furthermore, adsorption capacity at the exhaustion points of Ni, Pb and Cu was joined to the flow rate with similarity coefficient of 0.92, 0.96 and 0.95, respectively. Due to high similarity coefficient of 1, the adsorption capacity at the exhaustion points of Ni, Pb and Cu was governed by the bed depth. As a consequence, the effect of such factors on the adsorption capacity could be arranged in the increasing order of flow rate < initial concentration < bed depth.

The results of cluster analysis of initial concentration, flow rate and bed depth confirmed that the driving parameter for adsorption column design is bed depth.

4.5. Design the large-scale PVC column (Ni, Pb and Cu)

The Adams–Bohart model was used to evaluate the efficiency and applicability of the novel biochar in the large-scale column. Based on the results of section 4.4.3, the bed depth variations (cm) with time (min) are shown in Tables 57 to 59 and Fig. 67 to 69.

Table 57 Bed-depth service time (BDST) for Ni at the removal efficiency of 90%

Bed depth (cm)	Breakthrough time (min)	q (mg/g)	Y (%)
3	2	1.92	90
4	24	17.28	90

Note: $C_0 = 60 \mu\text{g/L}$ and $Q = 2 \text{ mL/min}$

Table 58 Bed-depth service time (BDST) for Pb at the removal efficiency of 90%

Bed depth (cm)	Breakthrough time (min)	q (mg/g)	Y (%)
3	4	3.84	90
4	40	28.8	90

Note: $C_0 = 60 \mu\text{g/L}$ and $Q = 2 \text{ mL/min}$

Table 59 Bed-depth service time (BDST) for Cu at the removal efficiency of 90%

Bed depth (cm)	Breakthrough time (min)	q (mg/g)	Y (%)
3	3	2.88	90
4	34	23	90

Note: $C_0 = 60 \mu\text{g/L}$ and $Q = 2 \text{ mL/min}$

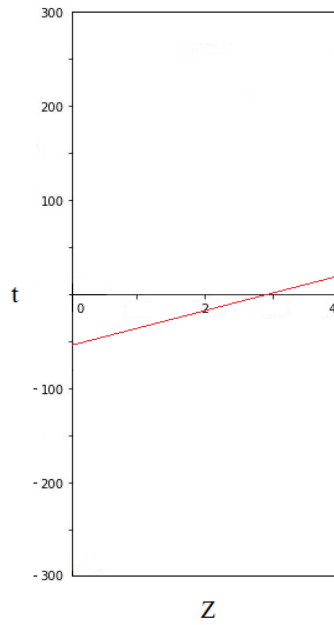


Fig. 67 Bed-depth service time (BDST) curves at the 90% removal of Ni

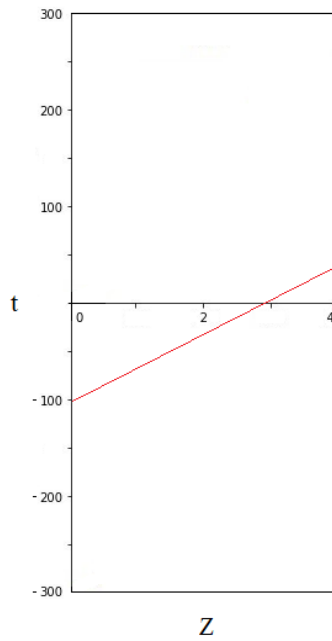


Fig. 68 Bed-depth service time (BDST) curves at the 90% removal of Pb

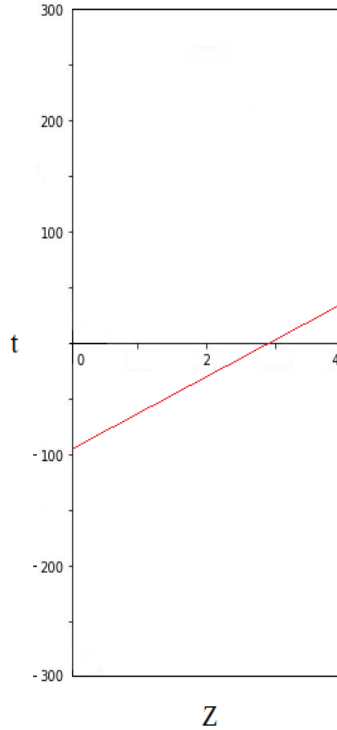


Fig. 69 Bed-depth service time (BDST) curves at the 90% removal of Cu

In Fig. 67, 68 and 69, the line can be represented by the Bohart-Adams equation (LaGrega et al., 2010). The large-scale PVC column can be designed as follows:

$$\text{Area of laboratory column} = \pi r^2 = 0.785 \times 10^{-4} \text{ m}^2$$

Studying fixed-bed adsorption column under various experimental conditions indicated that the low flow rate appropriately favors the adsorbate adsorption due to the adequate residence time. As a result, flow rate equal to 2 mL/min is used to determine loading rate in laboratory column.

Loading rate in laboratory column:

$$V = (0.2 \times 10^{-5} \text{ m}^3 / \text{min}) / 0.785 \times 10^{-4} \text{ m}^2 = 0.03 \text{ m}^3 / (\text{m}^2 \cdot \text{min})$$

Based on the Adams–Bohart model the same loading rate was used for the full-scale unit yields (LaGrega et al., 2010):

$$\text{Area of large-scale column} = Q/V = (0.001 \text{ m}^3 / \text{min}) / (0.03 \text{ m}^3 / (\text{m}^2 \cdot \text{min})) = 0.03 \text{ m}^2$$

$$\text{Diameter of large-scale column} = 0.2 \text{ m}$$

BDST equation for the removal efficiency of 90% and adsorbent utilization are shown in Table 60 and 61, respectively.

Table 60 Equation of Bed-depth service time (BDST) curve at the removal efficiency of 90%

Heavy metal	Slop of the line (a) (day/m)	Intercept (b) (day)	Equation of line
Ni	1.53	0.04	$t = 1.53 X - 0.04$
Pb	2.5	0.07	$t = 2.5 X - 0.07$
Cu	2.15	0.06	$t = 2.15 X - 0.06$

Note: Formula 3-1 was used to represent the equation of line

Table 61 Adsorbent utilization in the large-scale column

Heavy metal	Velocity of adsorption zone (1/a) (day/m)	Unit weight (kg/m ³)	Area (m ²)	Adsorbent utilization (kg/day)
Ni	0.65	50	0.03	0.975
Pb	0.4	50	0.03	0.6
Cu	0.47	50	0.03	0.705

Note: Formula 3-4 was used to evaluate the adsorbent utilization

According to the obtained results, the large-scale PVC column was installed (Fig. 8). The results of passing the effluent of RABEL wastewater treatment plant from the large-scale column are shown in Tables 62 to 64.

Table 62 Removal efficiency of Ni in the large-scale column

Sample	Concentration (µg/L)	Y (%)
The effluent of column (first day)	1.88332	90
The effluent of column (second day)	14.0987	25
The effluent of column (third day)	16.9187	10

Note: $C_0 = 18.8 \mu\text{g/g}$, $Q = 0.001 \text{ m}^3/\text{min}$ and the amount of biochar = 1000 g

Table 63 Removal efficiency of Pb in the large-scale column

Sample	Concentration (µg/L)	Y (%)
The effluent of column (first day)	0.01	90
The effluent of column (second day)	0.0675	32.5
The effluent of column (third day)	0.0897	10

Note: $C_0 = 0.1 \mu\text{g/g}$, $Q = 0.001 \text{ m}^3/\text{min}$ and the amount of biochar = 1000 g

Table 64 Removal efficiency of Cu in the large-scale column

Sample	Concentration (µg/L)	Y (%)
The effluent of column (first day)	0.5489	90
The effluent of column (second day)	3.9802	27.5
The effluent of column (third day)	4.9413	10

Note: $C_0 = 5.49 \mu\text{g/g}$, $Q = 0.001 \text{ m}^3/\text{min}$ and the amount of biochar = 1000 g

Based on the Tables 62 to 64, the concentration of Ni, Pb and Cu in wastewater effluent was decreased from 18.8 to 1.88332, 0.1 to 0.01 and 5.49 to 0.5489 $\mu\text{g/L}$, respectively. Such results confirmed the feasibility of using biochar to remove Ni, Pb and Cu by 90%, within one day from wastewater effluent. Decreasing the removal efficiency of studied metals from 90 to 10% within 3 days approved the result of designing the column by Adams-Bohart model which shows the adsorbent utilization in the large-scale column is 0.975 kg/day for Ni, 0.6 kg/day for Pb and 0.705 kg/day for Cu.

Considering the industrial applications of the adsorption process, plotting the breakthrough curve is of leading importance, since it accurately reveals the operational limit of the column (Suzaki et al., 2017). Loading behavior of Ni, Pb and Cu to be eliminated from the wastewater in a fixed-bed column can be indicated by the breakthrough curve (Gupta et al., 2016; Mojiri et al., 2019; Qian et al., 2019).

The breakthrough curves of the large-scale column were drawn by plotting the relative concentration of heavy metals, which is the ratio of the studied metals concentration in the effluent of column to the concentration of studied metals in wastewater with respect to time (Fig. 70, 71 and 72). Moreover, the exhaustion and breakthrough points are shown in Tables 65 to 67.

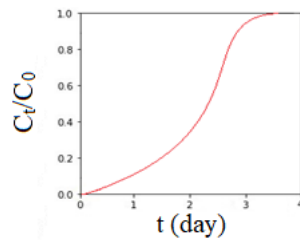


Fig. 70 Breakthrough curve of Ni for large-scale PVC column

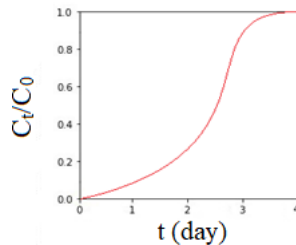


Fig. 71 Breakthrough curve of Pb for large-scale PVC column

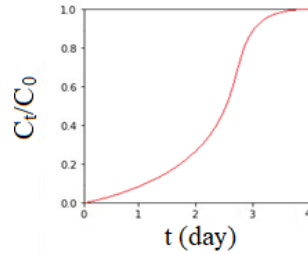


Fig. 72 Breakthrough curve of Cu for large-scale PVC column

Table 65 Breakthrough and exhaustion points of Ni in the large-scale column

Point	t (day)	q (µg/g)	Y (%)
Breakthrough	1	24.364	90
Exhaustion	3	8.1216	10

Note: $C_0 = 18.8 \mu\text{g/g}$, $Q = 0.001 \text{ m}^3/\text{min}$ and the amount of biochar = 1000 g

Table 66 Breakthrough and exhaustion points of Pb in the large-scale column

Point	t (day)	q (µg/g)	Y (%)
Breakthrough	1	0.1296	90
Exhaustion	3	0.0432	10

Note: $C_0 = 0.1 \mu\text{g/g}$, $Q = 0.001 \text{ m}^3/\text{min}$ and the amount of biochar = 1000 g

Table 67 Breakthrough and exhaustion points of Cu in the large-scale column

Point	t (day)	q (µg/g)	Y (%)
Breakthrough	1	7.115	90
Exhaustion	3	2.372	10

Note: $C_0 = 5.49 \mu\text{g/g}$, $Q = 0.001 \text{ m}^3/\text{min}$ and the amount of biochar = 1000 g

According to the Tables 65 to 67 and Fig. 70 to 72, the breakthrough time and exhaustion time for Ni, Pb and Cu were 1 and 3 days, respectively. 90% of Ni, Pb and Cu were eliminated at the breakthrough point where the adsorption capacity was 24.364 µg/g for Ni, 0.1296 µg/g for Pb and 7.115 µg/g for Cu. Moreover, the removal efficiency of 10% occurred at the exhaustion point in which the adsorption capacity of Ni, Pb and Cu was 8.1216, 0.0432 and 2.372 µg/g, respectively.

Physical–chemical primary treatment of effluents have given aid to reduce the concentration of heavy metals in Saint Lawrence River (Gobeil et al., 2005). High percentage of heavy metals was eliminated from municipal wastewater treatment plant effluents because of using activated sludge treatment (Carletti et al., 2008; Nielsen and Hrudey 1983). Li and Champagne (2009) showed that 42.7% of Ni can be adsorbed on the crushed shells and Sphagnum peat moss in a fixed-bed column.

65 % of nickel was eliminated from wastewater using untreated and treated rice straw (Spurthi et al., 2015). Maximum nickel adsorption onto boiled sunflower head (BSH) and formaldehyde sunflower head (FSH) was 65.5 and 75.9%, respectively (Jain et al., 2014).

Pandey and Sharma (2017) showed that the adsorption capacity and removal efficiency of Pb is 8.896 mg/g and 89%, respectively due to utilization of zeoliteNaX in the fixed-bed column. The removal efficiency of Cu by chicken bone-derived biochar in a fixed-bed column was 17% (Park et al., 2015).

In Montreal, where chemically enhanced primary treatment is utilized, municipal wastewater plays an important role in loading a huge percentage of heavy metals into the Saint Lawrence River (Marcogliese et al., 2015). The significant contribution of urban effluents to the total metal fluxes carried into the sea by the Saint Lawrence River was demonstrated by measuring heavy metals at the Montreal wastewater treatment plant (Gobeil et al., 2005). The high risk of heavy metals in wild freshwater mussels of Grand River (Ontario) was observed due to high concentration of metals in effluents from municipal wastewater treatment plants (Gillis 2012). Based on the obtained results from utilization of the large-scale PVC column, the risk of heavy metals to the aquatic and marine organisms are summarized in Table 68.

Table 68 Risk assessment of heavy metals

Metals	C _t (µg/L)	S _i (µg/L)	W _i	Q _i	W _i x Q _i	HPI	Class of risk
Cu	0.5489	1000	0.001	0.05489	0.00005489	3.185	Low
Ni	1.88332	20	0.05	9.42	0.471		
Pb	0.01	10	0.1	0.1	0.01		
			Σ W_i = 0.151		Σ W_i x Q_i = 0.481		

Note: the concentration of Ni, Pb and Cu in wastewater effluent was 1.88332, 0.01 and 0.5489 µg/L, respectively

According to the Table 68, the value of HPI index was decreased from 31.669 to 3.185. In other words, the pollution intensity of Ni, Pb and Cu was decreased from high risk to low risk to aquatic and marine organisms. The results acknowledged this fact that the novel biochar in the fixed-bed column gave aid to eliminate heavy metals from wastewater effluent. Utilization of novel biochar in full-scale facility will provide a proper position for eliminating heavy metals. As a consequence, it is expected that such a novel biochar plays a vital role in enriching the condition of Saint Lawrence River.

Chapter 5: Conclusion and future work

5.1. Conclusion

This work demonstrated the feasibility of applying newly produced biochar to adsorption columns in the wastewater treatment plants. The results showed that biochar which was produced in a sustainable way from a combination of municipal sludge, wood waste and KOH was able to adsorb pharmaceuticals (venlafaxine) and inorganic (lead, nickel, and copper) compounds from effluent of wastewater. Utilization of the waste materials as the primary materials along with the availability of materials onsite led to the preparation of novel biochar at lower costs. The efficiency of the novel biochar was confirmed in 3 steps including using biochar in laboratory-scale column and large-scale column along with risk assessment.

1- The application of biochar in the laboratory-scale column (inner diameter of 1 cm and height of 10 cm) was influenced by a wide variety factors including initial concentration of pollutants, volumetric flow rate of pollutants and the amount of biochar. Thus, increasing the initial concentration from 10 to 30 mg/L for venlafaxine and 60 to 80 $\mu\text{g/L}$ for heavy metals caused the adsorption of pollutants on biochar in the column to be on the increase due to providing a greater driving force. Moreover, increasing the effective bed depth from 3 to 4 cm and decreasing flow rate from 10 to 2 mL/min led to higher adsorption capacity due to providing additional binding sites and adequate contact between adsorbate and adsorbent, respectively. The effect of different factors on the adsorption capacity at the breakthrough and exhaustion points could be arranged in the increasing order of flow rate < initial concentration < bed depth. As a result, bed depth should be considered as the most appropriate factor in designing the full-scale facility. 90% of venlafaxine, Ni, Pb and Cu was eliminated at the breakthrough point where the adsorption capacity was increased from 0.8 to 5.4 mg/g for venlafaxine, from 1.92 to 18.24 $\mu\text{g/g}$ for Ni, from 3.84 to 30.72 $\mu\text{g/g}$ for Pb, and from 2.88 to 24 $\mu\text{g/g}$ for Cu. The adsorption capacity of heavy metals could be arranged in the order of Pb > Cu > Ni.

2- Based on the very low concentration and high flow rate of studied pollutants in the effluent of wastewater treatment, the results of variation of biochar amount were used in the Adams-Bohart model to design the large-scale column. Applying the large-scale column with area of 0.03 m² and biochar utilization of 1 kg/day clearly showed that the effects of lower concentration and higher flow rate on the adsorption capacity can be compensated by appropriate amount of adsorbent. Elimination of 95% of venlafaxine and 90% of Ni, Pb and Cu at the breakthrough point within one

day from wastewater effluent confirmed the feasibility of using biochar in the large-scale column. The adsorption capacity at the breakthrough point was 3051.406 ng/g for venlafaxine, 24.364 µg/g for Ni, 0.1296 µg/g for Pb, and 7.115 µg/g for Cu.

3- RQ and HPI as the proper indexes were used to risk assessment of studied pollutants. $RQ > 1$ and $HPI > 30$ showed that the low concentration of venlafaxine and heavy metals in the effluent of wastewater treatment might pose a serious threat to aquatic and marine organisms and thus human health. The pollution intensity of venlafaxine, Ni, Pb and Cu to aquatic and marine organisms was decreased from high risk to low risk due to application of the novel biochar in the fixed-bed column.

According to the obtained results, utilization of the novel biochar in full-scale facility might be cost-effective in eliminating organic and inorganic trace pollutants from effluent of wastewater treatment plant. Thus, it is expected that such a novel biochar plays a vital role in enriching the condition of water bodies, especially Saint Lawrence River properly.

5.2. Contribution

The contribution of conducting such a project is as follows:

- Risk assessment permitted to be identified that organic and inorganic compounds in the RABL wastewater treatment plant effluent might be responsible for some irreversible damages to biota, even at low concentrations. However, application of fixed-bed adsorption column with novel biochar decreased the pollution intensity of such trace pollutants from a high risk to low risk.
- This study showed that the most appropriate factor in designing the fixed-bed adsorption column is bed depth of biochar which influences on the adsorption capacity. Consequently, bed depth should be considered as the most appropriate factor in designing the full-scale facility.
- Exposing the large-scale adsorption column to the natural fluctuation of effluent components contributed to confirm the feasibility of the novel biochar in high removal efficiency. It was found that the capability of the novel biochar in high removal efficiency is persistent even at high flow rates and low concentrations.

- The study demonstrated that biochar, which was not always produced in optimal operation conditions at a large scale, preserved its high performance properties. The effluent treated at large-scale showed as high quality as effluent from small lab treatment of synthetic wastewater. As a consequence, the sustainable combination of municipal sludge, hardwood and KOH as the novel biochar can be used in the full-scale facility. Since both types of waste (municipal sludge and hardwood) are generated in large amounts in Canada, the elimination of pollutants by using the novel biochar in the full-scale facility will be remarkably cost effective.
- It is expected that the utilization of the novel biochar in the full-scale facility plays a vital role in enriching the condition of water bodies, especially Saint Lawrence River appropriately.

5.3. Future work

The future work might concentrate on the following tasks:

Making use of optimizing methods such as genetic algorithm (GA) in identifying the most appropriate dimensions for column.

Applying life cycle assessment for assessing environmental impacts associated with all the stages of utilizing such a column in industrial applications.

Verifying a capacity of the novel biochar at full-scale facility to reduce pharmaceuticals and heavy metals risks to aquatic and marine organisms

References

- Abbas, S., & Javed, M. (2016). Growth performance of *Labeo rohita* under chronic dual exposure of water-borne and dietary cobalt. *Pakistan Journal of Zoology*, 48(1), 257-264.
- Abdel-Tawwab, M., Sharafeldin, K. M., & Ismaiel, N. E. M. (2018). Interactive effects of coffee bean supplementation and waterborne zinc toxicity on growth performance, biochemical variables, antioxidant activity and zinc bioaccumulation in whole body of common carp, *Cyprinus carpio* L. *Aquaculture Nutrition*, 24(1), 123-130.
- Abadi, M., Zamani, A., Parizanganeh, A., Khosravi, Y., & Badiee, H. (2018). Heavy metals and arsenic content in water along the southern Caspian coasts in Iran. *Environmental Science and Pollution Research*, 25(24), 23725-23735.
- Abdolali, A., Ngo, H.H., Guo, W., Zhou, J.L., Zhang, J., Liang, S., Chang, S.W., Nguyen, D.D. and Liu, Y. (2017). Application of a breakthrough biosorbent for removing heavy metals from synthetic and real wastewaters in a lab-scale continuous fixed-bed column. *Bioresource Technology*, 229, 78-87.
- Abazari, R., Mahjoub, A. R., & Shariati, J. (2019). Synthesis of a nanostructured pillar MOF with high adsorption capacity towards antibiotics pollutants from aqueous solution. *Journal of Hazardous Materials*, 366, 439-451.
- Abdullah, E. J. (2013). Quality assessment for Shatt Al-Arab river using heavy metal pollution index and metal index. *Journal of Environment and Earth Science*, 3(5), 114-120.
- adel Abdel-Khalek, A., Kadry, M., Hamed, A., & Marie, M. A. (2015). Ecotoxicological impacts of zinc metal in comparison to its nanoparticles in Nile tilapia; *Oreochromis niloticus*. *The Journal of Basic & Applied Zoology*, 72, 113-125.
- Adeyemi, J. A., da Cunha Martins-Junior, A., & Barbosa Jr, F. (2015). Teratogenicity, genotoxicity and oxidative stress in zebrafish embryos (*Danio rerio*) co-exposed to arsenic and atrazine. *Comparative Biochemistry and Physiology Part C: Toxicology & Pharmacology*, 172, 7-12.
- Afzal, M. Z., Sun, X. F., Liu, J., Song, C., Wang, S. G., & Javed, A. (2018). Enhancement of ciprofloxacin sorption on chitosan/biochar hydrogel beads. *Science of the Total Environment*, 639, 560-569.
- Agrafioti, E., Bouras, G., Kalderis, D., & Diamadopoulou, E. (2013). Biochar production by sewage sludge pyrolysis. *Journal of Analytical and Applied Pyrolysis*, 101, 72-78.
- Ahmed, M. J., & Theydan, S. K. (2012). Adsorption of cephalixin onto activated carbons from *Albizia lebeck* seed pods by microwave-induced KOH and K₂CO₃ activations. *Chemical Engineering Journal*, 211, 200-207.
- Ahmed, S., Pan, J., Ashiq, M. N., Li, D., Tang, P., & Feng, Y. (2019). Ethylene glycol-assisted fabrication and superb adsorption capacity of hierarchical porous flower-like magnesium oxide microspheres for phosphate. *Inorganic Chemistry Frontiers*, 6(8), 1952-1961.
- Ahmed, M. J., & Hameed, B. H. (2018a). Removal of emerging pharmaceutical contaminants by adsorption in a fixed-bed column: a review. *Ecotoxicology and Environmental Safety*, 149, 257-266.
- Ahmad, A. A., & Hameed, B. H. (2010). Fixed-bed adsorption of reactive azo dye onto granular activated carbon prepared from waste. *Journal of Hazardous Materials*, 175(1-3), 298-303.
- Ahmed, M. B., Zhou, J. L., Ngo, H. H., Guo, W., Thomaidis, N. S., & Xu, J. (2017a) Progress in the biological and chemical treatment technologies for emerging contaminant removal from wastewater: a critical review. *Journal of Hazardous Materials*, 323, 274-298.

- Ahmed, M. B., Zhou, J. L., Ngo, H. H., Guo, W., Johir, M. A. H., & Sornalingam, K. (2017b). Single and competitive sorption properties and mechanism of functionalized biochar for removing sulfonamide antibiotics from water. *Chemical Engineering Journal*, 311, 348-358.
- Ahmed, M. B., Zhou, J. L., Ngo, H. H., Guo, W., Johir, M. A. H., & Belhaj, D. (2017c). Competitive sorption affinity of sulfonamides and chloramphenicol antibiotics toward functionalized biochar for water and wastewater treatment. *Bioresource Technology*, 238, 306-312.
- Alalwan, H. A., Abbas, M. N., & Alminshid, A. H. (2020). Uptake of cyanide compounds from aqueous solutions by lemon peel with utilising the residue absorbent as rodenticide. *Indian Chemical Engineer*, 62(1), 40-51.
- Al-Ghanim, K. A. (2011). Impact of nickel (Ni) on hematological parameters and behavioral changes in *Cyprinus carpio* (common carp). *African Journal of Biotechnology*, 10(63), 13860-13866.
- Alimohammadi, Z., Younesi, H., & Bahramifar, N. (2016). Batch and column adsorption of reactive red 198 from textile industry effluent by microporous activated carbon developed from walnut shells. *Waste and Biomass Valorization*, 7(5), 1255-1270.
- Alinovi, R., Goldoni, M., Pinelli, S., Campanini, M., Aliatis, I., Bersani, D., Lottici, P.P., Iavicoli, S., Petyx, M., Mozzoni, P. and Mutti, A. (2015). Oxidative and pro-inflammatory effects of cobalt and titanium oxide nanoparticles on aortic and venous endothelial cells. *Toxicology in Vitro*, 29(3), 426-437.
- Alonso, S. G., Catalá, M., Maroto, R. R., Gil, J. L. R., de Miguel, Á. G., & Valcárcel, Y. (2010). Pollution by psychoactive pharmaceuticals in the Rivers of Madrid metropolitan area (Spain). *Environment International*, 36(2), 195-201.
- AnvariFar, H., Amirkolaie, A.K., Jalali, A.M., Miandare, H.K., Sayed, A.H., Üçüncü, S.İ., Ouraji, H., Ceci, M. and Romano, N. (2018). Environmental pollution and toxic substances: Cellular apoptosis as a key parameter in a sensible model like fish. *Aquatic Toxicology*, 204, 144-159.
- Appavu, B., Thiripuranthagan, S., Ranganathan, S., Erusappan, E., & Kannan, K. (2018). BiVO₄/N-rGO nano composites as highly efficient visible active photocatalyst for the degradation of dyes and antibiotics in eco system. *Ecotoxicology and Environmental Safety*, 151, 118-126.
- Apul, O. G., & Karanfil, T. (2015). Adsorption of synthetic organic contaminants by carbon nanotubes: a critical review. *Water Research*, 68, 34-55.
- Aslam, S., & Yousafzai, A. M. (2017). Chromium toxicity in fish: A review article. *Journal of Entomology and Zoology Studies*, 5(3), 1483-1488.
- Ashfaq, M., Khan, K.N., Rehman, M.S.U., Mustafa, G., Nazar, M.F., Sun, Q., Iqbal, J., Mulla, S.I. and Yu, C.P. (2017). Ecological risk assessment of pharmaceuticals in the receiving environment of pharmaceutical wastewater in Pakistan. *Ecotoxicology and Environmental Safety*, 136, 31-39.
- Assadian, E., Zarei, M. H., Gilani, A. G., Farshin, M., Degampanah, H., & Pourahmad, J. (2018). Toxicity of copper oxide (CuO) nanoparticles on human blood lymphocytes. *Biological Trace Element Research*, 184(2), 350-357.
- Assi, M. A., Hezmee, M. N. M., Haron, A. W., Sabri, M. Y. M., & Rajion, M. A. (2016). The detrimental effects of lead on human and animal health. *Veterinary World*, 9(6), 660.
- Authman, M. M., Zaki, M. S., Khallaf, E. A., & Abbas, H. H. (2015). Use of fish as bio-indicator of the effects of heavy metals pollution. *Journal of Aquaculture Research & Development*, 6(4), 1-13.
- Azmat, H., Javed, M., Abdullah, S., Javid, A., & Hussain, S. M. (2018). Growth responses of major carps reared under chronic stress of chromium. *Journal of Animal and Plant Sciences*, 28(2), 604-609.

- Backhaus, T., & Faust, M. (2012). Predictive environmental risk assessment of chemical mixtures: a conceptual framework. *Environmental Science & Technology*, 46(5), 2564-2573.
- Bakar, A., Haslija, A., Abdullah, L. C., Zahri, M., Amirah, N., & Alkhatib, M. A. (2019). Column Efficiency of Fluoride Removal Using Quaternized Palm Kernel Shell (QPKS). *International Journal of Chemical Engineering*, 2019, 1-13.
- Bakshi, A., & Panigrahi, A. K. (2018). A comprehensive review on chromium induced alterations in fresh water fishes. *Toxicology Reports*, 5, 440-447.
- Baker, C. O., Huang, X., Nelson, W., & Kaner, R. B. (2017). Polyaniline nanofibers: broadening applications for conducting polymers. *Chemical Society Reviews*, 46(5), 1510-1525.
- Banerjee, M., Basu, R. K., & Das, S. K. (2019). Cu (II) removal using green adsorbents: kinetic modeling and plant scale-up design. *Environmental Science and Pollution Research*, 26(12), 11542-11557.
- Basu, M., Guha, A. K., & Ray, L. (2019). Adsorption of Lead on Lentil Husk in Fixed Bed Column Bioreactor. *Bioresource Technology*, 283, 86-95.
- Bebianno, M. J., & da Fonseca, T. G. (2020). Fate and Effects of Cytostatic Pharmaceuticals in the Marine Environment. In *Fate and Effects of Anticancer Drugs in the Environment* (pp. 295-330). Springer, Cham, Switzerland AG.
- Beckers, F., & Rinklebe, J. (2017). Cycling of mercury in the environment: Sources, fate, and human health implications: A review. *Critical Reviews in Environmental Science and Technology*, 47(9), 693-794.
- Beesley, L., Moreno-Jiménez, E., Gomez-Eyles, J. L., Harris, E., Robinson, B., & Sizmur, T. (2011). A review of biochars' potential role in the remediation, revegetation and restoration of contaminated soils. *Environmental Pollution*, 159(12), 3269-3282.
- Beji, R., Hamdi, W., Kesraoui, A., & Seffen, M. (2018). Adsorption of phosphorus by alkaline Tunisian soil in a fixed bed column. *Water Science and Technology*, 78(4), 751-763.
- Benaduce, A. P. S., Kochhann, D., Flores, E. M., Dressler, V. L., & Baldissotto, B. (2008). Toxicity of cadmium for silver catfish *Rhamdia quelen* (Heptapteridae) embryos and larvae at different alkalinities. *Archives of Environmental Contamination and Toxicology*, 54(2), 274-282.
- Bhowmick, S., Pramanik, S., Singh, P., Mondal, P., Chatterjee, D., & Nriagu, J. (2018). Arsenic in groundwater of West Bengal, India: a review of human health risks and assessment of possible intervention options. *Science of the Total Environment*, 612, 148-169.
- Billah, M. M., Kamal, A. H. M., Idris, M. H., & Ismail, J. (2017). Mangrove macroalgae as biomonitors of heavy metal contamination in a tropical estuary, Malaysia. *Water, Air, & Soil Pollution*, 228(9), 347.
- Bikkini, A., & Nanda, P. (2016). Vanadium toxicity to fish *Heteropneustes fossilis* (Bloch). *International Journal of Fisheries and Aquatic Studies*, 4(5), 316-317.
- Biswas, J. K., Rai, M., Mondal, M., & Ingle, A. P. (2018). The flip side of using heavy metal (oids) s in the traditional medicine: toxic insults and injury to human health. In *Biomedical Applications of Metals* (pp. 257-276). Springer, Cham, Switzerland AG.
- Blair Crawford, C., Quinn, B. (2017). The interactions of microplastics and chemical pollutants. *Microplastic Pollutants*, 131-157.
- Blaise, C., Gagné, F., Eullaffroy, P., & Féraud, J. F. (2006). Ecotoxicity of selected pharmaceuticals of urban origin discharged to the Saint-Lawrence river (Québec, Canada): a review. *Ecotoxicity of selected pharmaceuticals of urban*

origin discharged to the Saint-Lawrence river (Québec, Canada): a review. *Brazilian Journal of Aquatic Science and Technology*, 10, 29-51.

Blewett, T. A., & Leonard, E. M. (2017). Mechanisms of nickel toxicity to fish and invertebrates in marine and estuarine waters. *Environmental Pollution*, 223, 311-322.

Blewett, T. A., Ransberry, V. E., McClelland, G. B., & Wood, C. M. (2016). Investigating the mechanisms of Ni uptake and sub-lethal toxicity in the Atlantic killifish *Fundulus heteroclitus* in relation to salinity. *Environmental Pollution*, 211, 370-381.

Boni, M. R., Chiavola, A., & Marzeddu, S. (2020). Remediation of Lead-Contaminated Water by Virgin Coniferous Wood Biochar Adsorbent: Batch and Column Application. *Water, Air, & Soil Pollution*, 231, 1-16.

Bonnefille, B., Gomez, E., Courant, F., Escande, A., & Fenet, H. (2018). Diclofenac in the marine environment: a review of its occurrence and effects. *Marine Pollution Bulletin*, 131, 496-506.

Boran, H., & Şaffak, S. (2018). Comparison of Dissolved Nickel and Nickel Nanoparticles Toxicity in Larval Zebrafish in Terms of Gene Expression and DNA Damage. *Archives of Environmental Contamination and Toxicology*, 74(1), 193-202.

Borgia, V. F., Thatheyus, A. J., Murugesan, A. G., Alexander, S. C. P., & Geetha, I. (2018). Effects of effluent from electroplating industry on the immune response in the freshwater fish, *Cyprinus carpio*. *Fish & Shellfish Immunology*, 79, 86-92.

Bosch, A. C., O'Neill, B., Sigge, G. O., Kerwath, S. E., & Hoffman, L. C. (2016). Heavy metals in marine fish meat and consumer health: a review. *Journal of the Science of Food and Agriculture*, 96(1), 32-48.

Bozich, J., Hang, M., Hamers, R., & Klaper, R. (2017). Core chemistry influences the toxicity of multicomponent metal oxide nanomaterials, lithium nickel manganese cobalt oxide, and lithium cobalt oxide to *Daphnia magna*. *Environmental Toxicology and Chemistry*, 36(9), 2493-2502.

Brassesco, M. E., Valetti, N. W., & Picó, G. (2019). Prediction of breakthrough curves in packed-bed column as tool for lysozyme isolation using a green bed. *Polymer Bulletin*, 76(11), 5831-5847.

Buekers, J., De Brouwere, K., Lefebvre, W., Willems, H., Vandenbroele, M., Van Sprang, P., Eliat-Eliat, M., Hicks, K., Schlekot, C.E. and Oller, A.R. (2015). Assessment of human exposure to environmental sources of nickel in Europe: Inhalation exposure. *Science of the Total Environment*, 521, 359-371.

Bueno, M. M., Boillot, C., Munaron, D., Fenet, H., Casellas, C., & Gomez, E. (2014). Occurrence of venlafaxine residues and its metabolites in marine mussels at trace levels: development of analytical method and a monitoring program. *Analytical and Bioanalytical Chemistry*, 406(2), 601-610.

Byeon, E., Park, J. C., Hagiwara, A., Han, J., & Lee, J. S. (2020). Two antidepressants fluoxetine and sertraline cause growth retardation and oxidative stress in the marine rotifer *Brachionus koreanus*. *Aquatic Toxicology*, 218, 105337.

Çanlı, M. (2018). A new perspective to aberrations caused by barium and vanadium ions on *Lens culinaris* Medik. *Ecotoxicology and Environmental Safety*, 160, 19-23.

Carletti, G., Fatone, F., Bolzonella, D., & Cecchi, F. (2008). Occurrence and fate of heavy metals in large wastewater treatment plants treating municipal and industrial wastewaters. *Water Science and Technology*, 57(9), 1329-1336.

Carson, B. L. (2018). *Toxicology biological monitoring of metals in humans*. Chapman & Hall, Productivity Press, Auerbach Publications. Boca Raton, Florida, United States of America.

Casas, M. E., Chhetri, R. K., Ooi, G., Hansen, K. M., Litty, K., Christensson, M., Kragelund, C., Andersen, H.R & Bester, K. (2015). Biodegradation of pharmaceuticals in hospital wastewater by a hybrid biofilm and activated sludge system (Hybas). *Science of the Total Environment*, 530, 383-392.

Castro, D., Mieiro, C.L., Coelho, J.P., Guilherme, S., Marques, A., Santos, M.A., Duarte, A.C., Pereira, E. and Pacheco, M. (2018). Addressing the impact of mercury estuarine contamination in the European eel (*Anguilla anguilla* L., 1758)–An early diagnosis in glass eel stage based on erythrocytic nuclear morphology. *Marine Pollution Bulletin*, 127, 733-742.

Cazan, A. M., & Klerks, P. L. (2015). Effects from a short-term exposure to copper or cadmium in gravid females of the livebearer fish (*Gambusia affinis*). *Ecotoxicology and Environmental Safety*, 118, 199-203.

Cengiz, M. F., Kilic, S., Yalcin, F., Kilic, M., & Yalcin, M. G. (2017). Evaluation of heavy metal risk potential in Bogacayi River water (Antalya, Turkey). *Environmental Monitoring and Assessment*, 189(6), 248.

Chatterjee, A., & Abraham, J. (2019). Desorption of heavy metals from metal loaded sorbents and e-wastes: A review. *Biotechnology Letters*, 41(3), 319-333.

Chen, H., Guo, Z., Zhou, Y., Li, D., Mu, L., Klerks, P. L., Luo, Y. and Xie, L. (2018). Accumulation, depuration dynamics and effects of dissolved hexavalent chromium in juvenile Japanese medaka (*Oryzias latipes*). *Ecotoxicology and Environmental Safety*, 148, 254-260.

Chen, T., Luo, L., Deng, S., Shi, G., Zhang, S., Zhang, Y., eng, O., Wang, L., Zhang, J. and Wei, L. (2018a). Sorption of tetracycline on H₃PO₄ modified biochar derived from rice straw and swine manure. *Bioresource Technology*, 267, 431-437.

Chen, S., Yue, Q., Gao, B., Li, Q., Xu, X., & Fu, K. (2012). Adsorption of hexavalent chromium from aqueous solution by modified corn stalk: a fixed-bed column study. *Bioresource Technology*, 113, 114-120.

Chin, J. H., & Vora, N. (2014). The global burden of neurologic diseases. *Neurology*, 83(4), 349-351.

Chiou, Y. H., Wong, R. H., Chao, M. R., Chen, C. Y., Liou, S. H., & Lee, H. (2014). Nickel accumulation in lung tissues is associated with increased risk of p53 mutation in lung cancer patients. *Environmental and Molecular Mutagenesis*, 55(8), 624-632.

Cipro, C. V., Cherel, Y., Bocher, P., Caurant, F., Miramand, P., & Bustamante, P. (2018). Trace elements in invertebrates and fish from Kerguelen waters, southern Indian Ocean. *Polar Biology*, 41(1), 175-191.

Corcoll, N., Yang, J., Backhaus, T., Zhang, X., & Eriksson, K. M. (2019). Copper affects composition and functioning of microbial communities in marine biofilms at environmentally relevant concentrations. *Frontiers in Microbiology*, 9, 3248.

Coppola, F., Almeida, Â., Henriques, B., Soares, A. M., Figueira, E., Pereira, E., & Freitas, R. (2018). Biochemical responses and accumulation patterns of *Mytilus galloprovincialis* exposed to thermal stress and Arsenic contamination. *Ecotoxicology and Environmental Safety*, 147, 954-962.

Costigan, M., Cary, R., Dobson, S., & World Health Organization. (2001). Vanadium pentoxide and other inorganic vanadium compounds. World Health Organization, Geneva, Switzerland.

Cruz, M. A. P., Guimarães, L. C. M., da Costa Júnior, E. F., Rocha, S. D. F., & Mesquita, P. D. L. (2020). Adsorption of crystal violet from aqueous solution in continuous flow system using bone char. *Chemical Engineering Communications*, 207(3), 372-381.

Dabbagh, R., Mirkamali, M. S., & Vafajoo, L. (2019). Removal of Antimony Metalloid From Synthetic Effluent Using Seaweed as a Low-Cost Natural Sorbent: Adsorption on a Fixed-Bed Column. *Journal of Water Chemistry and Technology*, 41(1), 21-28.

- Dai, L., Wang, Y., Liu, Y., Ruan, R., Duan, D., Zhao, Y., Yu, Z. and Jiang, L. (2019). Catalytic fast pyrolysis of torrefied corn cob to aromatic hydrocarbons over Ni-modified hierarchical ZSM-5 catalyst. *Bioresource Technology*, 272, 407-414.
- Das R., Das Tuhi S., Zaidi S.M.J. (2018) Adsorption. In: Das R. (eds) Carbon Nanotubes for Clean Water. Carbon Nanostructures. Springer, Cham, Switzerland AG.
- da Silva Aires, M., Paganini, C. L., & Bianchini, A. (2018). Biochemical and physiological effects of nickel in the euryhaline crab *Neohelice granulata* (Dana, 1851) acclimated to different salinities. *Comparative Biochemistry and Physiology Part C: Toxicology & Pharmacology*, 204, 51-62.
- de Angelis, C., Galdiero, M., Pivonello, C., Salzano, C., Gianfrilli, D., Piscitelli, P., Lenzi, A., Colao, A. and Pivonello, R. (2017). The environment and male reproduction: The effect of cadmium exposure on reproductive function and its implication in fertility. *Reproductive Toxicology*, 73, 105-127.
- de Franco, M. A. E., de Carvalho, C. B., Bonetto, M. M., de Pelegrini Soares, R., & Féris, L. A. (2017). Removal of amoxicillin from water by adsorption onto activated carbon in batch process and fixed bed column: Kinetics, isotherms, experimental design and breakthrough curves modelling. *Journal of Cleaner Production*, 161, 947-956.
- de Namor, A. F. D., El Gamouz, A., Frangie, S., Martinez, V., Valiente, L., & Webb, O. A. (2012). Turning the volume down on heavy metals using tuned diatomite. A review of diatomite and modified diatomite for the extraction of heavy metals from water. *Journal of Hazardous Materials*, 241, 14-31.
- Deng, Y., Zhang, T., & Wang, Q. (2017). Biochar adsorption treatment for typical pollutants removal in livestock wastewater: a review. *Engineering Applications of Biochar*, 71.
- de Water, E., Proal, E., Wang, V., Medina, S.M., Schnaas, L., Téllez-Rojo, M.M., Wright, R.O., Tang, C.Y. and Horton, M.K. (2018). Prenatal manganese exposure and intrinsic functional connectivity of emotional brain areas in children. *Neurotoxicology*, 64, 85-93.
- Deokar, S. K., & Mandavgane, S. A. (2015). Estimation of packed-bed parameters and prediction of breakthrough curves for adsorptive removal of 2, 4-dichlorophenoxyacetic acid using rice husk ash. *Journal of Environmental Chemical Engineering*, 3(3), 1827-1836.
- Dew, W. A., Azizishirazi, A., & Pyle, G. G. (2014). Contaminant-specific targeting of olfactory sensory neuron classes: Connecting neuron class impairment with behavioural deficits. *Chemosphere*, 112, 519-525.
- Ding, X., Ye, S., Yuan, H., & Krauss, K. W. (2018). Spatial distribution and ecological risk assessment of heavy metals in coastal surface sediments in the Hebei Province offshore area, Bohai Sea, China. *Marine Pollution Bulletin*, 131, 655-661.
- Dong, W. Q., Sun, H. J., Zhang, Y., Lin, H. J., Chen, J. R., & Hong, H. C. (2018). Impact on growth, oxidative stress, and apoptosis-related gene transcription of zebrafish after exposure to low concentration of arsenite. *Chemosphere*, 211, 648-652.
- Doufene, N., Berrama, T., Nekaa, C., & Dadou, S. (2019). Determination of adsorption operating conditions in dynamic mode on basis of batch study: Application for Dimethylphthalate elimination on activated carbon prepared from *Arundo donax*. *Chemical Engineering Communications*, 206(8), 1015-1034.
- Du, L., Yang, J., & Xu, X. (2019). Highly enhanced adsorption of dimethyl disulfide from model oil on MOF-199/attapulgite composites. *Industrial & Engineering Chemistry Research*, 58(5), 2009-2016.
- Dubey, S. P., Dwivedi, A. D., Lee, C., Kwon, Y. N., Sillanpaa, M., & Ma, L. Q. (2014). Raspberry derived mesoporous carbon-tubules and fixed-bed adsorption of pharmaceutical drugs. *Journal of Industrial and Engineering Chemistry*, 20(3), 1126-1132.

- Duan, Y., Han, D. S., Batchelor, B., & Abdel-Wahab, A. (2016). Application of a reactive adsorbent-coated support system for removal of mercury (II). *Colloids and Surfaces A: Physicochemical and Engineering Aspects*, 509, 623-630.
- Duarte, I.A., Reis-Santos, P., Novais, S.C., Rato, L.D., Lemos, M.F., Freitas, A., Pouca, A.S.V., Barbosa, J., Cabral, H.N. and Fonseca, V.F. (2020). Depressed, hypertense and sore: Long-term effects of fluoxetine, propranolol and diclofenac exposure in a top predator fish. *Science of The Total Environment*, 712, 136564.
- Edosa, O., Captain, V. E., Festus, N., Brian, M. S., Gadaffi, L., & Kaspar, S. (2019). Assessment of copper levels along the Namibian marine coastline. *GSC Biological and Pharmaceutical Sciences*, 7(3), 048-055.
- Elbeshti, R. T. A., Elderwish, N. M., Abdelali, K. M. K., & Tastan, Y. (2018). Effects of Heavy Metals on Fish. *Menba Journal of Fisheries Faculty*, 2147-2254.
- Elia, A.C., Magara, G., Caruso, C., Masoero, L., Prearo, M., Arsieni, P., Caldaroni, B., Dörr, A.J.M., Scoparo, M., Salvati, S. and Brizio, P. (2018). A comparative study on subacute toxicity of arsenic trioxide and dimethylarsinic acid on antioxidant status in Crandell Rees feline kidney (CRFK), human hepatocellular carcinoma (PLC/PRF/5), and epithelioma papulosum cyprini (EPC) cell lines. *Journal of Toxicology and Environmental Health, Part A*, 81(10), 333-348.
- Einsiedl, F., Radke, M., & Maloszewski, P. (2010). Occurrence and transport of pharmaceuticals in a karst groundwater system affected by domestic wastewater treatment plants. *Journal of Contaminant Hydrology*, 117(1-4), 26-36.
- Ermolli, M., Menné, C., Pozzi, G., Serra, M. Á., & Clerici, L. A. (2001). Nickel, cobalt and chromium-induced cytotoxicity and intracellular accumulation in human hacat keratinocytes. *Toxicology*, 159(1-2), 23-31.
- Erşan, M., Bağda, E., & Bağda, E. (2013). Investigation of kinetic and thermodynamic characteristics of removal of tetracycline with sponge like, tannin based cryogels. *Colloids and surfaces B: Biointerfaces*, 104, 75-82.
- Espejo, W., Padilha, J.D.A., Gonçalves, R.A., Dorneles, P.R., Barra, R., Oliveira, D., Malm, O., Chiang, G. and Celis, J.E. (2019). Accumulation and potential sources of lead in marine organisms from coastal ecosystems of the Chilean Patagonia and Antarctic Peninsula area. *Marine Pollution Bulletin*, 140, 60-64.
- Estévez-Calvar, N., Canesi, L., Montagna, M., Faimali, M., Piazza, V., & Garaventa, F. (2017). Adverse effects of the SSRI antidepressant sertraline on early life stages of marine invertebrates. *Marine Environmental Research*, 128, 88-97.
- Fabbri, E., & Franzellitti, S. (2016). Human pharmaceuticals in the marine environment: focus on exposure and biological effects in animal species. *Environmental Toxicology and Chemistry*, 35(4), 799-812.
- Fadzil, F., Ibrahim, S., & Hanafiah, M. A. K. M. (2016). Adsorption of lead (II) onto organic acid modified rubber leaf powder: batch and column studies. *Process Safety and Environmental Protection*, 100, 1-8.
- Karbassi, A., Fakhraee, M., Vaezi, A., Bashiri, A., & Heidari, M. (2015). An investigation on flocculation, adsorption and desorption process during mixing of saline water with fresh water (Caspian Sea). *Journal of Environmental Studies*, 41(2), 11.
- Fakhri, A., & Behrouz, S. (2015). Comparison studies of adsorption properties of MgO nanoparticles and ZnO–MgO nanocomposites for linezolid antibiotic removal from aqueous solution using response surface methodology. *Process Safety and Environmental Protection*, 94, 37-43.
- Fang, L., Li, L., Qu, Z., Xu, H., Xu, J., & Yan, N. (2018). A novel method for the sequential removal and separation of multiple heavy metals from wastewater. *Journal of Hazardous Materials*, 342, 617-624.
- Farajnejad H, Karbassi A, Heidari M (2017) Fate of toxic metals during estuarine mixing of fresh water with saline water. *Environmental Science and Pollution Research* 24(35):27430-27435.

Faucher, K., Fichet, D., Miramand, P., & Lagardere, J. P. (2008). Impact of chronic cadmium exposure at environmental dose on escape behaviour in sea bass (*Dicentrarchus labrax* L.; Teleostei, Moronidae). *Environmental Pollution*, 151(1), 148-157.

Fernandes, J., Chandler, J. D., Liu, K. H., Uppal, K., Go, Y. M., & Jones, D. P. (2018). Putrescine as indicator of manganese neurotoxicity: Dose-response study in human SH-SY5Y cells. *Food and Chemical Toxicology*, 116, 272-280.

Fernandes, J., Hao, L., Bijli, K.M., Chandler, J.D., Orr, M., Hu, X., Jones, D.P. and Go, Y.M. (2016). From the cover: manganese stimulates mitochondrial H₂O₂ production in SH-SY5Y human neuroblastoma cells over physiologic as well as toxicologic range. *Toxicological Sciences*, 155(1), 213-223.

Filler, G., Kobrzynski, M., Sidhu, H. K., Belostotsky, V., Huang, S. H. S., McIntyre, C., & Yang, L. (2017). A cross-sectional study measuring vanadium and chromium levels in paediatric patients with CKD. *BMJ open*, 7(5), 1-10.

Fox, K. A., Phillips, T. M., Yanta, J. H., & Abesamis, M. G. (2016). Fatal cobalt toxicity after total hip arthroplasty revision for fractured ceramic components. *Clinical Toxicology*, 54(9), 874-877.

Fuentes-Gandara, F., Pinedo-Hernández, J., Marrugo-Negrete, J., & Díez, S. (2018). Human health impacts of exposure to metals through extreme consumption of fish from the Colombian Caribbean Sea. *Environmental Geochemistry and Health*, 40(1), 229-242.

Ferreira, C. I., Calisto, V., Otero, M., Nadais, H., & Esteves, V. I. (2017). Fixed-bed adsorption of Tricaine Methanesulfonate onto pyrolysed paper mill sludge. *Aquacultural Engineering*, 77, 53-60.

Fong, J. J., Sreedhara, K., Deng, L., Varki, N. M., Angata, T., Liu, Q., Nizet, V. & Varki, A. (2015). Immunomodulatory activity of extracellular Hsp70 mediated via paired receptors Siglec-5 and Siglec-14. *The EMBO Journal*, 34(22), 2775-2788.

Fong, P. P., & Hoy, C. M. (2012). Antidepressants (venlafaxine and citalopram) cause foot detachment from the substrate in freshwater snails at environmentally relevant concentrations. *Marine and Freshwater Behaviour and Physiology*, 45(2), 145-153.

Frontalini, F., Greco, M., Di Bella, L., Lejzerowicz, F., Reo, E., Caruso, A., Cosentino, C., Maccotta, A., Scopelliti, G., Nardelli, M.P. and Losada, M.T. (2018). Assessing the effect of mercury pollution on cultured benthic foraminifera community using morphological and eDNA metabarcoding approaches. *Marine Pollution Bulletin*, 129(2), 512-524.

Fu, Z., Guo, W., Dang, Z., Hu, Q., Wu, F., Feng, C., Zhao, X., Meng, W., Xing, B. and Giesy, J.P. (2017). Refocusing on nonpriority toxic metals in the aquatic environment in China. *Environmental Science and Technology*, 51, 3117–3118.

Fu, Z., & Xi, S. (2020). The effects of heavy metals on human metabolism. *Toxicology Mechanisms and Methods*, 30(3), 167-176.

Futalan, C. M., Kan, C. C., Dalida, M. L., Pascua, C., & Wan, M. W. (2011). Fixed-bed column studies on the removal of copper using chitosan immobilized on bentonite. *Carbohydrate Polymers*, 83(2), 697-704.

Gautam, G. J., & Chaube, R. (2018). Differential Effects of Heavy Metals (Cadmium, Cobalt, Lead and Mercury) On Oocyte Maturation and Ovulation of the Catfish *Heteropneustes fossilis*: an In Vitro Study. *Turkish Journal of Fisheries and Aquatic Sciences*, 18(10), 1205-1214.

Georgin, J., Franco, D. S., Grassi, P., Tonato, D., Piccilli, D. G., Meili, L., & Dotto, G. L. (2019). Potential of *Cedrella fissilis* bark as an adsorbent for the removal of red 97 dye from aqueous effluents. *Environmental Science and Pollution Research*, 1-13.

Ghosh, A., Kaviraj, A., & Saha, S. (2018). Deposition, acute toxicity, and bioaccumulation of nickel in some freshwater organisms with best-fit functions modeling. *Environmental Science and Pollution Research*, 25(4), 3588-3595.

Gobeil, C., Rondeau, B., & Beaudin, L. (2005). Contribution of municipal effluents to metal fluxes in the St. Lawrence River. *Environmental Science & Technology*, 39(2), 456-464.

Gokulan, R., Ganesh Prabhu, G., & Jegan, J. (2019). A novel sorbent *Ulva lactuca*-derived biochar for remediation of Remazol Brilliant Orange 3R in packed column. *Water Environment Research*, 91(7), 642-649.

Gong, J.L., Zhang, Y.L., Jiang, Y., Zeng, G.M., Cui, Z.H., Liu, K., Deng, C.H., Niu, Q.Y., Deng, J.H. and Huan, S.Y. (2015). Continuous adsorption of Pb (II) and methylene blue by engineered graphite oxide coated sand in fixed-bed column. *Applied Surface Science*, 330, 148-157.

Goodnough, L. H., Bala, A., Huddleston III, J. I., Goodman, S. B., Maloney, W. J., & Amanatullah, D. F. (2018). Metal-on-metal total hip arthroplasty is not associated with cardiac disease. *The Bone & Joint Journal*, 100(1), 28-32.

Gouran-Orimi, R., Mirzayi, B., Nematollahzadeh, A., & Tardast, A. (2018). Competitive adsorption of nitrate in fixed-bed column packed with bio-inspired polydopamine coated zeolite. *Journal of Environmental Chemical Engineering*, 6(2), 2232-2240.

Green, A. J., & Planchart, A. (2018). The neurological toxicity of heavy metals: A fish perspective. *Comparative Biochemistry and Physiology Part C: Toxicology & Pharmacology*, 208, 12-19.

Grill, G., Khan, U., Lehner, B., Nicell, J., & Ariwi, J. (2016). Risk assessment of down-the-drain chemicals at large spatial scales: Model development and application to contaminants originating from urban areas in the Saint Lawrence River Basin. *Science of the Total Environment*, 541, 825-838.

Gillis, P. L. (2012). Cumulative impacts of urban runoff and municipal wastewater effluents on wild freshwater mussels (*Lasmigona costata*). *Science of the Total Environment*, 431, 348-356.

Gros, M., Rodríguez-Mozaz, S., & Barceló, D. (2012). Fast and comprehensive multi-residue analysis of a broad range of human and veterinary pharmaceuticals and some of their metabolites in surface and treated waters by ultra-high-performance liquid chromatography coupled to quadrupole-linear ion trap tandem mass spectrometry. *Journal of Chromatography A*, 1248, 104-121.

Guocheng, L.Ü., Jiao, H., Liu, L., Hongwen, M.A., Qinfang, F.A.N.G., Limei, W.U., Mingquan, W.E.I. and Zhang, Y. (2011). The adsorption of phenol by lignite activated carbon. *Chinese Journal of Chemical Engineering*, 19(3), 380-385.

Gupta, A., & Garg, A. (2019). Adsorption and oxidation of ciprofloxacin in a fixed bed column using activated sludge derived activated carbon. *Journal of Environmental Management*, 250, 109474.

Gupta, V. K., Tyagi, I., Agarwal, S., Singh, R., Chaudhary, M., Harit, A., & Kushwaha, S. (2016). Column operation studies for the removal of dyes and phenols using a low-cost adsorbent. *Global Journal of Environmental Science and Management*, 2(1), 1-10.

Hadavifar, M., Bahramifar, N., Younesi, H., & Li, Q. (2014). Adsorption of mercury ions from synthetic and real wastewater aqueous solution by functionalized multi-walled carbon nanotube with both amino and thiolated groups. *Chemical Engineering Journal*, 237, 217-228.

Hajilari, M., Shariati, A., & Khosravi-Nikou, M. (2019). Equilibrium and Dynamic Adsorption of Bioethanol on Activated Carbon in the Liquid Phase. *Chemical Engineering & Technology*, 42(2), 343-354.

Halm-Lemeille, M. P., & Gomez, E. (2016). Pharmaceuticals in the environment. *Environmental Science and Pollution Research*, 23, 4961-4963.

Hamilton, P. B., Rolshausen, G., Uren Webster, T. M., & Tyler, C. R. (2017). Adaptive capabilities and fitness consequences associated with pollution exposure in fish. *Philosophical Transactions of the Royal Society B: Biological Sciences*, 372(1712), 20160042.

Han, R., Zhang, J., Zou, W., Xiao, H., Shi, J., & Liu, H. (2006). Biosorption of copper (II) and lead (II) from aqueous solution by chaff in a fixed-bed column. *Journal of Hazardous Materials*, 133(1-3), 262-268.

Hanbali, M., Holail, H., & Hammud, H. (2014). Remediation of lead by pretreated red algae: adsorption isotherm, kinetic, column modeling and simulation studies. *Green Chemistry Letters and Reviews*, 7(4), 342-358.

Has-Schön, E., Bogut, I., Vuković, R., Galović, D., Bogut, A., & Horvatić, J. (2015). Distribution and age-related bioaccumulation of lead (Pb), mercury (Hg), cadmium (Cd), and arsenic (As) in tissues of common carp (*Cyprinus carpio*) and European catfish (*Sylurus glanis*) from the Buško Blato reservoir (Bosnia and Herzegovina). *Chemosphere*, 135, 289-296.

Hayati, A., Giarti, K., Winarsih, Y., & Amin, M. H. F. (2017). The Effect of Cadmium on Sperm Quality and Fertilization Of *Cyprinus carpio* L. *Journal of Tropical Biodiversity and Biotechnology*, 2(2), 45-50.

Heidari, M. (2019). Role of Natural Flocculation in Eliminating Toxic Metals. *Archives of Environmental Contamination and Toxicology*, 76: 366.

Heidari F, Heidari M (2015) Effectiveness of Management of Environmental Education on Improving Knowledge for Environmental protection (case study: teachers at Tehran's Elementary School), *International Journal of Environmental Research* 9: 1225-1232.

Heidari F, Dabiri F, Heidari M (2017) Legal System Governing on Water Pollution in Iran. *Journal of Geoscience and Environment Protection* 5: 36-59.

Hernando, M. D., Mezcuca, M., Fernández-Alba, A. R., & Barceló, D. (2006). Environmental risk assessment of pharmaceutical residues in wastewater effluents, surface waters and sediments. *Talanta*, 69(2), 334-342.

Hethnawi, A., Nassar, N. N., Manasrah, A. D., & Vitale, G. (2017). Polyethylenimine-functionalized pyroxene nanoparticles embedded on Diatomite for adsorptive removal of dye from textile wastewater in a fixed-bed column. *Chemical Engineering Journal*, 320, 389-404.

Hodkovicova, N., Schonova, P., Blahova, J., Faldyna, M., Marsalek, P., Mikula, P., Chloupek, P., Dobsikova, R., Vecerek, V., Vicenova, M. and Vosmerova, P. (2020). The effect of the antidepressant venlafaxine on gene expression of biotransformation enzymes in zebrafish (*Danio rerio*) embryos. *Environmental Science and Pollution Research*, 27(2), 1686-1696.

Hu, J., Peng, Y., Zheng, T., Zhang, B., Liu, W., Wu, C., Jiang, M., Braun, J.M., Liu, S., Buka, S.L. and Zhou, A. (2018). Effects of trimester specific exposure to vanadium on ultrasound measures of fetal growth and birth size: a longitudinal prospective prenatal cohort study. *The Lancet Planetary Health*, 2(10), e427-e437.

Huggins, T. M., Haeger, A., Biffinger, J. C., & Ren, Z. J. (2016). Granular biochar compared with activated carbon for wastewater treatment and resource recovery. *Water Research*, 94, 225-232.

Igberase, E., & Osifo, P. O. (2019). Mathematical modelling and simulation of packed bed column for the efficient adsorption of Cu (II) ions using modified bio-polymeric material. *Journal of Environmental Chemical Engineering*, 7(3), 103129.

Ikert, H., & Craig, P. M. (2020). Chronic exposure to venlafaxine and increased water temperature reversibly alters microRNA in zebrafish gonads (*Danio rerio*). *Comparative Biochemistry and Physiology Part D: Genomics and Proteomics*, 33, 100634.

Ingle, A. P., Paralikar, P., Shende, S., Gupta, I., Biswas, J. K., da Silva Martins, L. H., & Rai, M. (2018). Copper in Medicine: Perspectives and Toxicity. In *Biomedical Applications of Metals* (pp. 95-112). Springer, Cham, Switzerland AG.

- Inyang, M.I., Gao, B., Yao, Y., Xue, Y., Zimmerman, A., Mosa, A., Pullammanappallil, P., Ok, Y.S. and Cao, X. (2016). A review of biochar as a low-cost adsorbent for aqueous heavy metal removal. *Critical Reviews in Environmental Science and Technology*, 46(4), 406-433.
- Izah, S. C., Chakrabarty, N., & Srivastav, A. L. (2016). A review on heavy metal concentration in potable water sources in Nigeria: Human health effects and mitigating measures. *Exposure and Health*, 8(2), 285-304.
- Jain, M., Garg, V. K., & Kadirvelu, K. (2014). Removal of Ni (II) from aqueous system by chemically modified sunflower biomass. *Desalination and Water Treatment*, 52(28-30), 5681-5695.
- Jain, M., Garg, V. K., & Kadirvelu, K. (2013). Cadmium (II) sorption and desorption in a fixed bed column using sunflower waste carbon calcium-alginate beads. *Bioresource Technology*, 129, 242-248.
- Jaishankar, M., Tseten, T., Anbalagan, N., Mathew, B. B., & Beeregowda, K. N. (2014). Toxicity, mechanism and health effects of some heavy metals. *Interdisciplinary Toxicology*, 7(2), 60-72.
- Jang, J., & Lee, D. S. (2019). Effective phosphorus removal using chitosan/Ca-organically modified montmorillonite beads in batch and fixed-bed column studies. *Journal of Hazardous Materials*, 375, 9-18.
- Jang, J., Miran, W., Divine, S. D., Nawaz, M., Shahzad, A., Woo, S. H., & Lee, D. S. (2018). Rice straw-based biochar beads for the removal of radioactive strontium from aqueous solution. *Science of the Total Environment*, 615, 698-707.
- Jaria, G., Calisto, V., Silva, C. P., Gil, M. V., Otero, M., & Esteves, V. I. (2019). Fixed-bed performance of a waste-derived granular activated carbon for the removal of micropollutants from municipal wastewater. *Science of The Total Environment*, 683, 699-708.
- Jin, M., Ji, X., Zhang, B., Sheng, W., Wang, R., & Liu, K. (2019). Synergistic effects of Pb and repeated heat pulse on developmental neurotoxicity in zebrafish. *Ecotoxicology and Environmental Safety*, 172, 460-470.
- Jing, X. R., Wang, Y. Y., Liu, W. J., Wang, Y. K., & Jiang, H. (2014). Enhanced adsorption performance of tetracycline in aqueous solutions by methanol-modified biochar. *Chemical Engineering Journal*, 248, 168-174.
- Jose, C. C., Jagannathan, L., Tanwar, V. S., Zhang, X., Zang, C., & Cuddapah, S. (2018). Nickel exposure induces persistent mesenchymal phenotype in human lung epithelial cells through epigenetic activation of ZEB1. *Molecular Carcinogenesis*, 57(6), 794-806.
- Karbassi, A. R., Fakhraee, M., Heidari, M., Vaezi, A. R., & Samani, A. V. (2015). Dissolved and particulate trace metal geochemistry during mixing of Karganrud River with Caspian Sea water. *Arabian Journal of Geosciences*, 8(4), 2143-2151.
- Karbassi AR, Heidari M (2015) An investigation on role of salinity, pH and DO on heavy metals elimination throughout estuarial mixture. *Global Journal of Environmental Science and Management*, 1(1), 41-46.
- Karbassi, A. R., Heidari, M., Vaezi, A. R., Samani, A. V., Fakhraee, M., & Heidari, F. (2014). Effect of pH and salinity on flocculation process of heavy metals during mixing of Aras River water with Caspian Sea water. *Environmental Earth Sciences*, 72(2), 457-465.
- Karbassi AR, Heidari M, Afsari F, Heidari F, Behzadian B (2016) The Individual Effects of Salinity, Voltage and NaClO on Elimination Efficiency of Metals in Estuary. *Academia Journal of Environmental Science* 4(11), 201-2012.
- Kavianinia, I., Plieger, P. G., Kandile, N. G., & Harding, D. R. (2012). Fixed-bed column studies on a modified chitosan hydrogel for detoxification of aqueous solutions from copper (II). *Carbohydrate Polymers*, 90(2), 875-886.
- Kaya, H., Aydın, F., Gürkan, M., Yılmaz, S., Ates, M., Demir, V., & Arslan, Z. (2015). Effects of zinc oxide nanoparticles on bioaccumulation and oxidative stress in different organs of tilapia (*Oreochromis niloticus*). *Environmental Toxicology and Pharmacology*, 40(3), 936-947.

- Khan, R. K., & Strand, M. A. (2018). Road dust and its effect on human health: a literature review. *Epidemiology and Health*, 40, e2018013.
- Khairul, I., Wang, Q. Q., Jiang, Y. H., Wang, C., & Naranmandura, H. (2017). Metabolism, toxicity and anticancer activities of arsenic compounds. *Oncotarget*, 8(14), 23905.
- Khobragade, M. U., & Pal, A. (2016). Fixed-bed column study on removal of Mn (II), Ni (II) and Cu (II) from aqueous solution by surfactant bilayer supported alumina. *Separation Science and Technology*, 51(8), 1287-1298.
- Khoshdel, Z., Naghibalhossaini, F., Abdollahi, K., Shojaei, S., Moradi, M., & Malekzadeh, M. (2016). Serum copper and zinc levels among Iranian colorectal cancer patients. *Biological Trace Element Research*, 170(2), 294-299.
- Kim, T. H., Choi, J. Y., Jung, M. M., Oh, S. Y., & Choi, C. Y. (2018). Effects of waterborne copper on toxicity stress and apoptosis responses in red seabream, *Pagrus major*. *Molecular & Cellular Toxicology*, 14(2), 201-210.
- Kim, K. H., Kim, J. Y., Cho, T. S., & Choi, J. W. (2012). Influence of pyrolysis temperature on physicochemical properties of biochar obtained from the fast pyrolysis of pitch pine (*Pinus rigida*). *Bioresource Technology*, 118, 158-162.
- Kim, H. S., Kim, Y. J., & Seo, Y. R. (2015). An overview of carcinogenic heavy metal: molecular toxicity mechanism and prevention. *Journal of Cancer Prevention*, 20(4), 232.
- Klatte, S., Schaefer, H. C., & Hempel, M. (2017). Pharmaceuticals in the environment—a short review on options to minimize the exposure of humans, animals and ecosystems. *Sustainable Chemistry and Pharmacy*, 5, 61-66.
- Kohzadi, S., Shahmoradi, B., Ghaderi, E., Loqmani, H., & Maleki, A. (2018). Concentration, Source, and Potential Human Health Risk of Heavy Metals in the Commonly Consumed Medicinal Plants. *Biological Trace Element Research*, 187(1), 41-50.
- Komjarova, I., & Bury, N. R. (2014). Evidence of common cadmium and copper uptake routes in zebrafish *Danio rerio*. *Environmental Science & Technology*, 48(21), 12946-12951.
- Kosma, C. I., Lambropoulou, D. A., & Albanis, T. A. (2014). Investigation of PPCPs in wastewater treatment plants in Greece: occurrence, removal and environmental risk assessment. *Science of the Total Environment*, 466, 421-438.
- Kovach, W. L. (1999). MVSP-A multivariate statistical Package for Windows, ver. 3.1. Kovach Computing Services, Pentraeth, Wales, UK, 137.
- Kumar, J.A., Amarnath, D.J., Sathish, S., Jabasingh, S.A., Saravanan, A., Hemavathy, R.V., Anand, K.V. and Yaashikaa, P.R. (2019). Enhanced PAHs removal using pyrolysis-assisted potassium hydroxide induced palm shell activated carbon: Batch and column investigation. *Journal of Molecular Liquids*, 279, 77-87.
- Kumar, N., Krishnani, K. K., Brahmane, M. P., Gupta, S. K., Kumar, P., & Singh, N. P. (2018). Temperature induces lead toxicity in *Pangasius hypophthalmus*: an acute test, antioxidative status and cellular metabolic stress. *International Journal of Environmental Science and Technology*, 15(1), 57-68.
- Kumar, P., & Singh, A. (2010). Cadmium toxicity in fish: An overview. *GERF Bulletin of Biosciences*, 1(1), 41-47.
- Kumpanenko, I. V., Ivanova, N. A., Dyubanov, M. V., Shapovalova, O. V., Solov'yanov, A. A., & Roshchin, A. V. (2019). Analysis of Breakthrough Curves of Dynamic Adsorptive Removal of Pollutants from Water. *Russian Journal of Physical Chemistry B*, 13(2), 328-338.
- La, H., Hettiaratchi, J. P. A., & Achari, G. (2019). The influence of biochar and compost mixtures, water content, and gas flow rate, on the continuous adsorption of methane in a fixed bed column. *Journal of Environmental Management*, 233, 175-183.

- LaGrega, M. D., Buckingham, P. L., & Evans, J. C. (2010). Hazardous waste management. Waveland Press, Long Grove, Illinois, United States of America.
- Lajeunesse, A., Smyth, S. A., Barclay, K., Sauv e, S., & Gagnon, C. (2012). Distribution of antidepressant residues in wastewater and biosolids following different treatment processes by municipal wastewater treatment plants in Canada. *Water Research*, 46(17), 5600-5612.
- Lari, E., Bogart, S. J., & Pyle, G. G. (2018). Fish can smell trace metals at environmentally relevant concentrations in freshwater. *Chemosphere*, 203, 104-108.
- Lau, L. C., Mohamad Nor, N., Lee, K. T., & Mohamed, A. (2016). Adsorption isotherm, kinetic, thermodynamic and breakthrough curve models of H₂S removal using CeO₂/NaOH/PSAC. *Petrochemical Science & Engineering*, 1(2), 1-10.
- Lawal, I. A., & Moodley, B. (2018). Fixed-Bed and Batch Adsorption of Pharmaceuticals from Aqueous Solutions on Ionic Liquid-Modified Montmorillonite. *Chemical Engineering & Technology*, 41(5), 983-993.
- Lee, J.J., Valeri, L., Kapur, K., Ibne Hasan, M.O.S., Quamruzzaman, Q., Wright, R.O., Bellinger, D.C., Christiani, D.C. and Mazumdar, M. (2018). Growth parameters at birth mediate the relationship between prenatal manganese exposure and cognitive test scores among a cohort of 2-to 3-year-old Bangladeshi children. *International journal of epidemiology*, 47(4), 1169-1179.
- Leysens, L., Vinck, B., Van Der Straeten, C., Wuyts, F., & Maes, L. (2017). Cobalt toxicity in humans—A review of the potential sources and systemic health effects. *Toxicology*, 387, 43-56.
- Li, C., & Champagne, P. (2009). Fixed-bed column study for the removal of cadmium (II) and nickel (II) ions from aqueous solutions using peat and mollusk shells. *Journal of Hazardous Materials*, 171(1-3), 872-878.
- Li, Y., Qu, X., Zhang, M., Peng, W., Yu, Y., & Gao, B. (2018). Anthropogenic Impact and Ecological Risk Assessment of Thallium and Cobalt in Poyang Lake Using the Geochemical Baseline. *Water*, 10(11), 1703.
- Li, G., Liu, Q., Liu, Z., Zhang, Z. C., Li, C., & Wu, W. (2010). Production of calcium carbide from fine biochars. *Angewandte Chemie International Edition*, 49(45), 8480-8483.
- Liao, P., Zhan, Z., Dai, J., Wu, X., Zhang, W., Wang, K., & Yuan, S. (2013). Adsorption of tetracycline and chloramphenicol in aqueous solutions by bamboo charcoal: a batch and fixed-bed column study. *Chemical Engineering Journal*, 228, 496-505.
- Lima, L. F., de Andrade, J. R., da Silva, M. G., & Vieira, M. G. (2017). Fixed bed adsorption of benzene, toluene, and xylene (BTX) contaminants from monocomponent and multicomponent solutions using a commercial organoclay. *Industrial & Engineering Chemistry Research*, 56(21), 6326-6336.
- Liu, M., Li, X., Du, Y., & Han, R. (2019). Adsorption of methyl blue from solution using walnut shell and reuse in a secondary adsorption for Congo red. *Bioresource Technology Reports*, 5, 238-242.
- Liu, A., Wang, C.C., Wang, C.Z., Fu, H.F., Peng, W., Cao, Y.L., Chu, H.Y. and Du, A.F. (2018a). Selective adsorption activities toward organic dyes and antibacterial performance of silver-based coordination polymers. *Journal of Colloid and Interface Science*, 512, 730-739.
- Liu, Y., Liu, G., Yuan, Z., Liu, H., & Lam, P. K. (2018). Heavy metals (As, Hg and V) and stable isotope ratios ($\delta^{13}\text{C}$ and $\delta^{15}\text{N}$) in fish from Yellow River Estuary, China. *Science of the Total Environment*, 613, 462-471.
- Lonappan, L., Rouissi, T., Liu, Y., Brar, S. K., & Surampalli, R. Y. (2019). Removal of diclofenac using microbiochar fixed-bed column bioreactor. *Journal of Environmental Chemical Engineering*, 7(1), 102894.
- L pez-Cervantes, J., S nchez-Machado, D. I., S nchez-Duarte, R. G., & Correa-Murrieta, M. A. (2018). Study of a fixed-bed column in the adsorption of an azo dye from an aqueous medium using a chitosan–glutaraldehyde biosorbent. *Adsorption Science & Technology*, 36(1-2), 215-232.

- Ma, R., Wang, B., Lu, S., Zhang, Y., Yin, L., Huang, J., Deng, S., Wang, Y. and Yu, G. (2016). Characterization of pharmaceutically active compounds in Dongting Lake, China: Occurrence, chiral profiling and environmental risk. *Science of the Total Environment*, 557, 268-275.
- Machoń-Grecka, A., Dobrakowski, M., Kasperczyk, A., Birkner, E., & Kasperczyk, S. (2020). Angiogenesis and lead (Pb): is there a connection?. *Drug and Chemical Toxicology*, 1-5.
- Mahato, M. K., Singh, G., Singh, P. K., Singh, A. K., & Tiwari, A. K. (2017). Assessment of mine water quality using heavy metal pollution index in a coal mining area of Damodar River Basin, India. *Bulletin of Environmental Contamination and Toxicology*, 99(1), 54-61.
- Majumdar, S., Baishya, A., & Mahanta, D. (2019). Kinetic and Equilibrium Modeling of Anionic Dye Adsorption on Polyaniline Emeraldine Salt: Batch and Fixed Bed Column Studies. *Fibers and Polymers*, 20(6), 1226-1235.
- Malandrino, P., Russo, M., Ronchi, A., Minoia, C., Cataldo, D., Regalbuto, C., Giordano, C., Attard, M., Squatrito, S., Trimarchi, F. and Vigneri, R. (2016). Increased thyroid cancer incidence in a basaltic volcanic area is associated with non-anthropogenic pollution and biocontamination. *Endocrine*, 53(2), 471-479.
- Malve, H. (2016). Exploring the ocean for new drug developments: Marine pharmacology. *Journal of Pharmacy & Bioallied Sciences*, 8(2), 83.
- Mandal, M. K., Sharma, M., Pandey, S., & Dubey, K. K. (2019). Membrane Technologies for the Treatment of Pharmaceutical Industry Wastewater. In *Water and Wastewater Treatment Technologies* (pp. 103-116). Springer, Singapore.
- Manyà, J. J., Azuara, M., & Manso, J. A. (2018). Biochar production through slow pyrolysis of different biomass materials: Seeking the best operating conditions. *Biomass and Bioenergy*, 117, 115-123.
- Marcogliese, D.J., Blaise, C., Cyr, D., de Lafontaine, Y., Fournier, M., Gagné, F., Gagnon, C. and Hudon, C. (2015). Effects of a major municipal effluent on the St. Lawrence River: A case study. *Ambio*, 44(4), 257-274.
- Marzbali, M. H., & Esmaili, M. (2017). Fixed bed adsorption of tetracycline on a mesoporous activated carbon: Experimental study and neuro-fuzzy modeling. *Journal of Applied Research and Technology*, 15(5), 454-463.
- Maulvault, A.L., Camacho, C., Barbosa, V., Alves, R., Anacleto, P., Pousão-Ferreira, P., Rosa, R., Marques, A. and Diniz, M.S. (2019). Living in a multi-stressors environment: An integrated biomarker approach to assess the ecotoxicological response of meagre (*Argyrosomus regius*) to venlafaxine, warming and acidification. *Environmental Research*, 169, 7-25.
- Maulvault, A.L., Santos, L.H., Paula, J.R., Camacho, C., Pissarra, V., Fogaça, F., Barbosa, V., Alves, R., Ferreira, P.P., Barceló, D. and Rodriguez-Mozaz, S. (2018). Differential behavioural responses to venlafaxine exposure route, warming and acidification in juvenile fish (*Argyrosomus regius*). *Science of The Total Environment*, 634, 1136-1147.
- McGeer, J. C., Szebedinszky, C., McDonald, D. G., & Wood, C. M. (2000). Effects of chronic sublethal exposure to waterborne Cu, Cd or Zn in rainbow trout. 1: Iono-regulatory disturbance and metabolic costs. *Aquatic Toxicology*, 50(3), 231-243.
- Melby, E.S., Cui, Y., Borgatta, J., Mensch, A.C., Hang, M.N., Chrisler, W.B., Dohnalkova, A., Van Gilder, J.M., Alvarez, C.M., Smith, J.N. and Hamers, R.J. (2018). Impact of lithiated cobalt oxide and phosphate nanoparticles on rainbow trout gill epithelial cells. *Nanotoxicology*, 12(10), 1166-1181.
- Meng, J., Wang, W. X., Li, L., & Zhang, G. (2018). Tissue-specific molecular and cellular toxicity of Pb in the oyster (*Crassostrea gigas*): mRNA expression and physiological studies. *Aquatic Toxicology*, 198, 257-268.
- Menon, N. G., Mohapatra, S., Padhye, L. P., Tatiparti, S. S. V., & Mukherji, S. (2020). Review on Occurrence and Toxicity of Pharmaceutical Contamination in Southeast Asia. In *Emerging Issues in the Water Environment during Anthropocene* (pp. 63-91). Springer, Singapore.

- Metwally, S. S., El-Sherief, E. A., & Mekhamer, H. S. (2019). Fixed-bed column for the removal of cesium, strontium, and lead ions from aqueous solutions using brick kiln waste. *Separation Science and Technology*, 55(4), 635-647.
- Meyer, S., Glaser, B., & Quicker, P. (2011). Technical, economical, and climate-related aspects of biochar production technologies: a literature review. *Environmental Science & Technology*, 45(22), 9473-9483.
- Milivojević, J., Krstić, D., Šmit, B., & Djekić, V. (2016). Assessment of heavy metal contamination and calculation of its pollution index for Uglješnica River, Serbia. *Bulletin of Environmental Contamination and Toxicology*, 97(5), 737-742.
- Minguez, L., Pedelucq, J., Farcy, E., Ballandonne, C., Budzinski, H., & Halm-Lemeille, M. P. (2016). Toxicities of 48 pharmaceuticals and their freshwater and marine environmental assessment in northwestern France. *Environmental Science and Pollution Research*, 23(6), 4992-5001.
- Minguez, L., Ballandonne, C., Rakotomalala, C., Dubreule, C., Kientz-Bouchart, V., & Halm-Lemeille, M. P. (2015). Transgenerational effects of two antidepressants (sertraline and venlafaxine) on *Daphnia magna* life history traits. *Environmental Science & Technology*, 49(2), 1148-1155.
- Misson, B., Garnier, C., Lauga, B., Dang, D.H., Ghiglione, J.F., Mullot, J.U., Duran, R. and Pringault, O. (2016). Chemical multi-contamination drives benthic prokaryotic diversity in the anthropized Toulon Bay. *Science of the Total Environment*, 556, 319-329.
- Mitra, T., Bar, N., & Das, S. K. (2019). Rice husk: green adsorbent for Pb (II) and Cr (VI) removal from aqueous solution—column study and GA–NN modeling. *SN Applied Sciences*, 1(5), 486.
- Mizutani, T., & Mizutani, A. (1978). Estimation of adsorption of drugs and proteins on glass surfaces with controlled pore glass as a reference. *Journal of Pharmaceutical Sciences*, 67(8), 1102-1105.
- Mohan, M. D., & Kasprovicz, M. D. (2016). Identification and Management of Cobalt Toxicity: A Case Report of Rapidly Progressing Toxicity after Hip Arthroplasty Revision. In *The Medicine Forum* (Vol. 17, No. 1, p. 18).
- Mojiri, A., Vakili, M., Farraji, H., & Aziz, S. Q. (2019). Combined ozone oxidation process and adsorption methods for the removal of acetaminophen and amoxicillin from aqueous solution; kinetic and optimisation. *Environmental Technology & Innovation*, 15, 100404.
- Monastero, R., Vacchi-Suzzi, C., Marsit, C., Demple, B., & Meliker, J. (2018). Expression of genes involved in stress, toxicity, inflammation, and autoimmunity in relation to cadmium, mercury, and lead in human blood: a pilot study. *Toxics*, 6(3), 35.
- Mondal, S., Aikat, K., & Halder, G. (2016). Ranitidine hydrochloride sorption onto superheated steam activated biochar derived from mung bean husk in fixed bed column. *Journal of Environmental Chemical Engineering*, 4(1), 488-497.
- Moreira, A., Freitas, R., Figueira, E., Ghirardini, A.V., Soares, A.M., Radaelli, M., Guida, M. and Libralato, G. (2018). Combined effects of arsenic, salinity and temperature on *Crassostrea gigas* embryotoxicity. *Ecotoxicology and Environmental Safety*, 147, 251-259.
- Moreira, A., Figueira, E., Soares, A. M., & Freitas, R. (2016). The effects of arsenic and seawater acidification on antioxidant and biomineralization responses in two closely related *Crassostrea* species. *Science of the Total Environment*, 545, 569-581.
- Moslen, M., & Miebaka, C. A. (2016). Temporal variation of heavy metal concentrations in *Periophthalmus* sp. obtained from Azuabie Creek in the upper bonny estuary, Nigeria. *Curr Stud Comp Educ Sci Technol*, 2, 136-47.
- Mukherjee, S. (2017). Histopathological profile of freshwater teleost, *channa punctatus* exposed to arsenic. *Indian Journal of Scientific Research*, 16 (1): 38-42.

- Nag, S., Bar, N., & Das, S. K. (2019). Sustainable bioremediation of Cd (II) in fixed bed column using green adsorbents: Application of Kinetic models and GA-ANN technique. *Environmental Technology & Innovation*, 13, 130-145.
- Naifar, I., Pereira, F., Zmembra, R., Bouaziz, M., Elleuch, B., & Garcia, D. (2018). Spatial distribution and contamination assessment of heavy metals in marine sediments of the southern coast of Sfax, Gabes Gulf, Tunisia. *Marine Pollution Bulletin*, 131, 53-62.
- Nair, A., DeGheselle, O., Smeets, K., Van Kerkhove, E., & Cuypers, A. (2013). Cadmium-induced pathologies: where is the oxidative balance lost (or not)? *International Journal of Molecular Sciences*, 14(3), 6116-6143.
- Naseri, M., Rahmanikhah, Z., Beiygloo, V., & Ranjbar, S. (2018). Effects of two cooking methods on the concentrations of some heavy metals (cadmium, lead, chromium, nickel and cobalt) in some rice brands available in Iranian Market. *Journal of Chemical Health Risks*, 4(2), 65-72.
- Nasseh, N., Barikbin, B., Taghavi, L., & Nasser, M. A. (2019). Adsorption of metronidazole antibiotic using a new magnetic nanocomposite from simulated wastewater (isotherm, kinetic and thermodynamic studies). *Composites Part B: Engineering*, 159, 146-156.
- Nazari, G., Abolghasemi, H., Esmaili, M., & Pouya, E. S. (2016). Aqueous phase adsorption of cephalexin by walnut shell-based activated carbon: A fixed-bed column study. *Applied Surface Science*, 375, 144-153.
- Niasar, H. S., Das, S., Xu, C. C., & Ray, M. B. (2019). Continuous column adsorption of naphthenic acids from synthetic and real oil sands process-affected water (OSPW) using carbon-based adsorbents. *Chemosphere*, 214, 511-518.
- Nidheesh, P. V., Gandhimathi, R., Ramesh, S. T., & Singh, T. A. (2013). Modeling of crystal violet adsorption by bottom ash column. *Water Environment Research*, 85(6), 495-502.
- Nielsen, J. S., & Hruday, S. E. (1983). Metal loadings and removal at a municipal activated sludge plant. *Water Research*, 17(9), 1041-1052.
- Niu, Y., Ying, D., & Jia, J. (2019). Continuous Adsorption of Copper Ions by Chitosan-Based Fiber in Adsorption Bed. *Journal of Environmental Engineering*, 145(8), 04019041.
- Noor, N., Zong, G., Seely, E. W., Weisskopf, M., & James-Todd, T. (2018). Urinary cadmium concentrations and metabolic syndrome in US adults: The National Health and Nutrition Examination Survey 2001–2014. *Environment International*, 121, 349-356.
- Nordberg, G.F., Bernard, A., Diamond, G.L., Duffus, J.H., Illing, P., Nordberg, M., Bergdahl, I.A., Jin, T. and Skerfving, S. (2018). Risk assessment of effects of cadmium on human health (IUPAC Technical Report). *Pure and Applied Chemistry*, 90(4), 755-808.
- Nourouzi, M. M., Chamani, A., Shirani, M., Malekpouri, P., & Chuah, A. L. (2018). Effect of Cd and Pb pollutions on physiological growth: wavelet neural network (WNN) as a new approach on age determination of *Coenobita scaevola*. *Bulletin of Environmental Contamination and Toxicology*, 101(3), 320-325.
- Nunes, B., Daniel, D., Canelas, G. G., Barros, J., & Correia, A. T. (2020). Toxic effects of environmentally realistic concentrations of diclofenac in organisms from two distinct trophic levels, *Hediste diversicolor* and *Solea senegalensis*. *Comparative Biochemistry and Physiology Part C: Toxicology & Pharmacology*, 231, 108722.
- Nwabanne, J. T., Okoye, A. C., & Lebele-Alawa, B. T. (2012). Packed bed column studies for the removal of lead (ii) using oil palm empty fruit bunch. *European Journal of Scientific Research*, 63(2), 296-305.
- Ocampo-Perez, R., Leyva-Ramos, R., Mendoza-Barron, J., & Guerrero-Coronado, R. M. (2011). Adsorption rate of phenol from aqueous solution onto organobentonite: surface diffusion and kinetic models. *Journal of Colloid and Interface Science*, 364(1), 195-204.

- Officioso, A., Panzella, L., Tortora, F., Alfieri, M. L., Napolitano, A., & Manna, C. (2018). Comparative analysis of the effects of olive oil hydroxytyrosol and its 5-S-lipoyl conjugate in protecting human erythrocytes from mercury toxicity. *Oxidative Medicine and Cellular Longevity*, 2018, 1-9.
- Ojekunle, O. Z., Ojekunle, O. V., Adeyemi, A. A., Taiwo, A. G., Sangowusi, O. R., Taiwo, A. M., & Adekitan, A. A. (2016). Evaluation of surface water quality indices and ecological risk assessment for heavy metals in scrap yard neighbourhood. *SpringerPlus*, 5(1), 560.
- Okoli, C. P., & Ofomaja, A. E. (2019). Development of sustainable magnetic polyurethane polymer nanocomposite for abatement of tetracycline antibiotics aqueous pollution: Response surface methodology and adsorption dynamics. *Journal of Cleaner Production*, 217, 42-55.
- Okpala, C. O. R., Sardo, G., Vitale, S., Bono, G., & Arukwe, A. (2018). Hazardous properties and toxicological update of mercury: From fish food to human health safety perspective. *Critical Reviews in Food Science and Nutrition*, 58(12), 1986-2001.
- Oladipo, A. A., Abureesh, M. A., & Gazi, M. (2016). Bifunctional composite from spent "Cyprus coffee" for tetracycline removal and phenol degradation: Solar-Fenton process and artificial neural network. *International Journal of Biological Macromolecules*, 90, 89-99.
- Olivares, C. I., Field, J. A., Simonich, M., Tanguay, R. L., & Sierra-Alvarez, R. (2016). Arsenic (III, V), indium (III), and gallium (III) toxicity to zebrafish embryos using a high-throughput multi-endpoint in vivo developmental and behavioral assay. *Chemosphere*, 148, 361-368.
- Ololade, I. A., & Oginni, O. (2010). Toxic stress and hematological effects of nickel on African catfish, *Clarias gariepinus*, fingerlings. *Journal of Environmental Chemistry and Ecotoxicology*, 2(2), 014-019.
- Osborne, O.J., Lin, S., Jiang, W., Chow, J., Chang, C.H., Ji, Z., Yu, X., Lin, S., Xia, T. and Nel, A.E. (2017). Differential effect of micron-versus nanoscale III–V particulates and ionic species on the zebrafish gut. *Environmental Science: Nano*, 4(6), 1350-1364.
- Olver, J. S., Burrows, G. D., & Norman, T. R. (2004). The treatment of depression with different formulations of venlafaxine: a comparative analysis. *Human Psychopharmacology: Clinical and Experimental*, 19(1), 9-16.
- Pandey, P. K., & Sharma, S. K. (2017). Removal of Cr (VI) and Pb (II) from Wastewater by ZeoliteNaX in Fixed Bed Column. *Water Conservation Science and Engineering*, 2(3), 61-65.
- Panneerselvam, K., Marigoudar, S. R., & Dhandapani, M. (2018). Toxicity of Nickel on the Selected Species of Marine Diatoms and Copepods. *Bulletin of Environmental Contamination and Toxicology*, 100(3), 331-337.
- Palágyi, Š. (2019). Comparison of several models for fitting breakthrough curves of radionuclides transport in crushed rock: groundwater systems. *Journal of Radioanalytical and Nuclear Chemistry*, 321(3), 1067-1071.
- Park, J.H., Cho, J.S., Ok, Y.S., Kim, S.H., Kang, S.W., Choi, I.W., Heo, J.S., DeLaune, R.D. and Seo, D.C. (2015). Competitive adsorption and selectivity sequence of heavy metals by chicken bone-derived biochar: batch and column experiment. *Journal of Environmental Science and Health, Part A*, 50(11), 1194-1204.
- Pastorelli, A.A., Angeletti, R., Binato, G., Mariani, M.B., Cibin, V., Morelli, S., Ciardullo, S. and Stacchini, P. (2018). Exposure to cadmium through Italian rice (*Oryza sativa* L.): Consumption and implications for human health. *Journal of Food Composition and Analysis*, 69, 115-121.
- Patel, H. (2019). Fixed-bed column adsorption study: a comprehensive review. *Applied Water Science*, 9(3), 45.
- Paul, J. S., & Small, B. C. (2019). Exposure to environmentally relevant cadmium concentrations negatively impacts early life stages of channel catfish (*Ictalurus punctatus*). *Comparative Biochemistry and Physiology Part C: Toxicology & Pharmacology*, 216, 43-51.

- Paz, S., Burgos, A., Gutiérrez, A., Hernández, C., Lozano, G., Rubio, C., Hardisson, A. (2017). The Mercury: a marine and food contaminant, 3 (3), 1-55.
- Pereira, P., Puga, S., Cardoso, V., Pinto-Ribeiro, F., Raimundo, J., Barata, M., Pousão-Ferreira, P., Pacheco, M. and Almeida, A. (2016). Inorganic mercury accumulation in brain following waterborne exposure elicits a deficit on the number of brain cells and impairs swimming behavior in fish (white seabream—*Diplodus sargus*). *Aquatic Toxicology*, 170, 400-412.
- Perrodin, Y., & Orias, F. (2017). Ecotoxicity of Hospital Wastewater. In *Hospital Wastewaters* (pp. 33-47). Springer, Cham, Switzerland AG.
- Philippe, C., Hautekiet, P., Grégoir, A.F., Thoré, E.S., Pinceel, T., Stoks, R., Brendonck, L. and De Boeck, G. (2018). Combined effects of cadmium exposure and temperature on the annual killifish (*Nothobranchius furzeri*). *Environmental toxicology and chemistry*, 37(9), 2361-2371.
- Prichard, E., & Granek, E. F. (2016). Effects of pharmaceuticals and personal care products on marine organisms: from single-species studies to an ecosystem-based approach. *Environmental Science and Pollution Research*, 23(22), 22365-22384.
- Qi, L., Ma, J., Song, J., Li, S., Cui, X., Peng, X., Wang, W., Ren, Z., Han, M. and Zhang, Y. (2017). The physiological characteristics of zebra fish (*Danio rerio*) based on metabolism and behavior: a new method for the online assessment of cadmium stress. *Chemosphere*, 184, 1150-1156.
- Qian, W., Song, Q., Ding, H., & Xie, W. (2019). Computational simulations of the mass transfer zone in GS adsorption column packed with Fe³⁺ type ion exchanger. *Chemosphere*, 215, 507-514.
- Qu, L., Huang, H., Xia, F., Liu, Y., Dahlgren, R. A., Zhang, M., & Mei, K. (2018). Risk analysis of heavy metal concentration in surface waters across the rural-urban interface of the Wen-Rui Tang River, China. *Environmental Pollution*, 237, 639-649.
- Radhika, R., Jayalatha, T., Jacob, S., Rajeev, R., & George, B. K. (2018). Adsorption performance of packed bed column for the removal of perchlorate using modified activated carbon. *Process Safety and Environmental Protection*, 117, 350-362.
- Rafati, L., Ehrampoush, M. H., Rafati, A. A., Mokhtari, M., & Mahvi, A. H. (2019). Fixed bed adsorption column studies and models for removal of ibuprofen from aqueous solution by strong adsorbent nano-clay composite. *Journal of Environmental Health Science and Engineering*, 17(2), 753-765.
- Rajeshkumar, S., Liu, Y., Zhang, X., Ravikumar, B., Bai, G., & Li, X. (2018). Studies on seasonal pollution of heavy metals in water, sediment, fish and oyster from the Meiliang Bay of Taihu Lake in China. *Chemosphere*, 191, 626-638.
- Rashed, M. N. (2013). Adsorption technique for the removal of organic pollutants from water and wastewater. *Organic pollutants-monitoring, risk and treatment*, 167-194.
- Rasinger, J. D., Lundebye, A. K., Penglase, S. J., Ellingsen, S., & Amlund, H. (2017). Methylmercury induced neurotoxicity and the influence of selenium in the brains of adult zebrafish (*danio rerio*). *International Journal of Molecular Sciences*, 18(4), 725.
- Ratn, A., Prasad, R., Awasthi, Y., Kumar, M., Misra, A., & Trivedi, S. P. (2018). Zn²⁺ induced molecular responses associated with oxidative stress, DNA damage and histopathological lesions in liver and kidney of the fish, *Channa punctatus* (Bloch, 1793). *Ecotoxicology and Environmental Safety*, 151, 10-20.
- Rehrah, D., Bansode, R. R., Hassan, O., & Ahmedna, M. (2016). Physico-chemical characterization of biochars from solid municipal waste for use in soil amendment. *Journal of Analytical and Applied Pyrolysis*, 118, 42-53.
- Renault, T. (2015). Immunotoxicological effects of environmental contaminants on marine bivalves. *Fish & Shellfish Immunology*, 46(1), 88-93.

Renu, Agarwal, M., Singh, K., Gupta, R., & Dohare, R. K. (2020). Continuous Fixed-Bed Adsorption of Heavy Metals Using Biodegradable Adsorbent: Modeling and Experimental Study. *Journal of Environmental Engineering*, 146(2), 04019110.

Reynel-Avila, H. E., Mendoza-Castillo, D. I., Bonilla-Petriciolet, A., & Silvestre-Albero, J. (2015). Assessment of naproxen adsorption on bone char in aqueous solutions using batch and fixed-bed processes. *Journal of Molecular Liquids*, 209, 187-195.

Rodrigues, J.A.V., Martins, L.R., Furtado, L.M., Xavier, A.L.P., Almeida, F.T.R.D., Moreira, A.L.D.S.L., Melo, T.M.S., Gil, L.F. and Gurgel, L.V.A. (2020). Oxidized Renewable Materials for the Removal of Cobalt (II) and Copper (II) from Aqueous Solution Using in Batch and Fixed-Bed Column Adsorption. *Advances in Polymer Technology*, 2020, 1-17.

Rodríguez-Moro, G., García-Barrera, T., Trombini, C., Blasco, J., & Gómez-Ariza, J. L. (2018). Combination of HPLC with organic and inorganic mass spectrometry to study the metabolic response of the clam *Scrobicularia plana* to arsenic exposure. *Electrophoresis*, 39(4), 635-644.

Romero-Cano, L. A., García-Rosero, H., del Olmo-Iruela, M., Carrasco-Marín, F., & González-Gutiérrez, L. V. (2019). Amino-functionalized material from a bio-template for silver adsorption: process evaluation in batch and fixed bed. *Journal of Chemical Technology & Biotechnology*, 94(2), 590-599.

Rosales, E., Meijide, J., Pazos, M., & Sanromán, M. A. (2017). Challenges and recent advances in biochar as low-cost biosorbent: from batch assays to continuous-flow systems. *Bioresource Technology*, 246, 176-192.

Rúa-Gómez, P. C., & Püttmann, W. (2012). Occurrence and removal of lidocaine, tramadol, venlafaxine, and their metabolites in German wastewater treatment plants. *Environmental Science and Pollution Research*, 19(3), 689-699.

Saadi, Z., Fazaeli, R., Vafajoo, L., Naser, I., & Mohammadi, G. (2020). Promotion of clinoptilolite adsorption for azithromycin antibiotic by Tween 80 and Triton X-100 surface modifiers under batch and fixed-bed processes. *Chemical Engineering Communications*, 6, 1-21.

Saadi, Z., Fazaeli, R., Vafajoo, L., & Naser, I. (2019). Adsorptive removal of apramycin antibiotic from aqueous solutions using Tween 80-and Triton X-100 modified clinoptilolite: experimental and fixed-bed modeling investigations. *International Journal of Environmental Health Research*, 41, 1-26.

Sancho, J. L. S., Rodríguez, A. R., Torrellas, S. Á., & Rodríguez, J. G. (2012). Removal of an emerging pharmaceutical compound by adsorption in fixed bed column. *Desalination and Water Treatment*, 45(1-3), 305-314.

Sankararamkrishnan, N., Kumar, P., & Chauhan, V. S. (2008). Modeling fixed bed column for cadmium removal from electroplating wastewater. *Separation and Purification Technology*, 63(1), 213-219.

Sangion, A., & Gramatica, P. (2016). Hazard of pharmaceuticals for aquatic environment: prioritization by structural approaches and prediction of ecotoxicity. *Environment International*, 95, 131-143.

Saquib, Q., Siddiqui, M.A., Ahmad, J., Ansari, S.M., Faisal, M., Wahab, R., Alatar, A.A., Al-Khedhairi, A.A. and Musarrat, J. (2018). Nickel Oxide Nanoparticles Induced Transcriptomic Alterations in HEPG2 Cells. In *Cellular and Molecular Toxicology of Nanoparticles* (pp. 163-174). Springer, Cham, Switzerland AG.

Sarkar, S., Mukherjee, S., Chattopadhyay, A., & Bhattacharya, S. (2017). Differential modulation of cellular antioxidant status in zebrafish liver and kidney exposed to low dose arsenic trioxide. *Ecotoxicology and Environmental safety*, 135, 173-182.

Sbardella, L., Comas, J., Fenu, A., Rodriguez-Roda, I., & Weemaes, M. (2018). Advanced biological activated carbon filter for removing pharmaceutically active compounds from treated wastewater. *Science of the Total Environment*, 636, 519-529.

Schiffer, S., & Liber, K. (2017). Estimation of vanadium water quality benchmarks for the protection of aquatic life with relevance to the Athabasca Oil Sands region using species sensitivity distributions. *Environmental toxicology and chemistry*, 36(11), 3034-3044.

Schlesinger, W. H., Klein, E. M., & Vengosh, A. (2017). Global biogeochemical cycle of vanadium. *Proceedings of the National Academy of Sciences*, 114(52), E11092-E11100.

Hasan, S. (2011). Design and performance of a pilot submerged membrane electro-bioreactor (SMEBR) for wastewater treatment (Doctoral dissertation, Concordia University).

Shaheen, S.M., Niazi, N.K., Hassan, N.E., Bibi, I., Wang, H., Tsang, D.C., Ok, Y.S., Bolan, N. and Rinklebe, J. (2019). Wood-based biochar for the removal of potentially toxic elements in water and wastewater: a critical review. *International Materials Reviews*, 64(4), 216-247.

Shahid, M. K., Kim, Y., & Choi, Y. G. (2019). Magnetite synthesis using iron oxide waste and its application for phosphate adsorption with column and batch reactors. *Chemical Engineering Research and Design*, 148, 169-179.

Shahzad, K., Khan, M. N., Jabeen, F., Kosour, N., Chaudhry, A. S., Sohail, M., & Ahmad, N. (2018). Toxicity of zinc oxide nanoparticles (ZnO-NPs) in tilapia (*Oreochromis mossambicus*): tissue accumulation, oxidative stress, histopathology and genotoxicity. *International Journal of Environmental Science and Technology*, 16(4), 1973-1984.

Shanmugam, D., Alagappan, M., & Rajan, R. K. (2016). Bench-scale packed bed sorption of Cibacron blue F3GA using lucrative algal biomass. *Alexandria Engineering Journal*, 55(3), 2995-3003.

Singh, C. B., & Ansari, B. A. (2017). Biochemical markers of oxidative stress in brain of zebra fish *Danio rerio* exposed to different heavy metals lead and Cobalt. *International Journal of Life-Sciences Scientific Research*, 3(6), 1484-1494.

Singh, S. K., Katoria, D., Mehta, D., & Sehgal, D. (2015). Fixed bed column study and adsorption modelling on the adsorption of malachite green dye from wastewater using acid activated sawdust. *International Journal of Advanced Research*, 3(7), 521-529.

Sivarajasekar, N., Balasubramani, K., Mohanraj, N., Maran, J. P., Sivamani, S., Koya, P. A., & Karthik, V. (2017). Fixed-bed adsorption of atrazine onto microwave irradiated *Aegle marmelos* Correa fruit shell: statistical optimization, process design and breakthrough modeling. *Journal of Molecular Liquids*, 241, 823-830.

Sonnack, L., Klawonn, T., Kriehuber, R., Hollert, H., Schäfers, C., & Fenske, M. (2018). Comparative analysis of the transcriptome responses of zebrafish embryos after exposure to low concentrations of cadmium, cobalt and copper. *Comparative Biochemistry and Physiology Part D: Genomics and Proteomics*, 25, 99-108.

Song, Q., & Li, J. (2015). A review on human health consequences of metals exposure to e-waste in China. *Environmental Pollution*, 196, 450-461.

Souza, N. L. N., Carneiro, M. T. W. D., Pimentel, E. F., Frossard, A., Freire, J. B., Endringer, D. C., & Júnior, P. D. F. (2018). Trace elements influence the hatching success and emergence of *Caretta caretta* and *Chelonia mydas*. *Journal of Trace Elements in Medicine and Biology*, 50, 117-122.

Stankovic, S., Kalaba, P., & Stankovic, A. R. (2014). Biota as toxic metal indicators. *Environmental Chemistry Letters*, 12(1), 63-84.

Soto, M. L., Moure, A., Domínguez, H., & Parajó, J. C. (2017). Batch and fixed bed column studies on phenolic adsorption from wine vinasses by polymeric resins. *Journal of Food Engineering*, 209, 52-60.

Spurthi L., Brahmaiah T., Sai Prasad K. S., Chandrika K., Kausalya Chandra L., Yashas S. (2015). Removal of nickel from wastewater using low cost. *European Journal of Biomedical and Pharmaceutical Sciences*, 2(6), 188-192.

Stewart, W. J., Johansen, J. L., & Liao, J. C. (2017). A non-toxic dose of cobalt chloride blocks hair cells of the zebrafish lateral line. *Hearing Research*, 350, 17-21.

Su, Y., Zhao, B., Xiao, W., & Han, R. (2013). Adsorption behavior of light green anionic dye using cationic surfactant-modified wheat straw in batch and column mode. *Environmental Science and Pollution Research*, 20(8), 5558-5568.

Suzaki, P. Y. R., Munaro, M. T., Triques, C. C., Kleinübing, S. J., Klen, M. R. F., Bergamasco, R., & de Matos Jorge, L. M. (2017). Phenomenological mathematical modeling of heavy metal biosorption in fixed-bed columns. *Chemical Engineering Journal*, 326, 389-400.

Swiatkowska, I., Mosselmans, J.F.W., Geraki, T., Wyles, C.C., Maleszewski, J.J., Henckel, J., Sampson, B., Potter, D.B., Osman, I., Trousdale, R.T. and Hart, A.J. (2018). Synchrotron analysis of human organ tissue exposed to implant material. *Journal of Trace Elements in Medicine and Biology*, 46, 128-137.

Swapna Priya, S., & Radha, K. V. (2016). Fixed-bed column dynamics of tetracycline hydrochloride using commercial grade activated carbon: comparison of linear and nonlinear mathematical modeling studies. *Desalination and Water Treatment*, 57(40), 18964-18980.

Tareq, R., Akter, N., & Azam, M. S. (2019). Biochars and biochar composites: low-cost adsorbents for environmental remediation. In *Biochar from Biomass and Waste* (pp. 169-209). Elsevier.

Tsai, W. C., De Luna, M. D. G., Bermillo-Arriegasado, H. L. P., Futralan, C. M., Colades, J. I., & Wan, M. W. (2016). Competitive fixed-bed adsorption of Pb (II), Cu (II), and Ni (II) from aqueous solution using chitosan-coated bentonite. *International Journal of Polymer Science*, 2016, 1-11.

Tien, C. (2018). *Introduction to Adsorption: Basics, Analysis, and Applications*. Elsevier.

Tiwari, A. K., Singh, P. K., & Mahato, M. K. (2017). Assessment of metal contamination in the mine water of the West Bokaro Coalfield, India. *Mine Water and the Environment*, 36(4), 532-541.

ur Rehman, I., Ishaq, M., Ali, L., Khan, S., Ahmad, I., Din, I. U., & Ullah, H. (2018). Enrichment, spatial distribution of potential ecological and human health risk assessment via toxic metals in soil and surface water ingestion in the vicinity of Sewakht mines, district Chitral, Northern Pakistan. *Ecotoxicology and Environmental Safety*, 154, 127-136.

Vaezi AR, Karbassi AR, Habibzadeh SK, Heidari M, ValikhaniSamani AR (2016) Heavy metal contamination and risk assessment in riverine sediments. *Indian Journal of Geo-Marine Sciences* 45(8):1017-1023.

Vaezi AR, Karbassi AR, Fakhraee M, ValikhaniSamani AR, Heidari M (2014) Assessment of Sources and Concentration of Metal Contaminants in Marine Sediments of Musa Estuary, Persian Gulf. *Journal of Environmental Study*, 40 (2), 345-360.

Valcárcel, Y., Alonso, S. G., Rodríguez-Gil, J. L., Gil, A., & Catalá, M. (2011). Detection of pharmaceutically active compounds in the rivers and tap water of the Madrid Region (Spain) and potential ecotoxicological risk. *Chemosphere*, 84(10), 1336-1348.

Valikhani Samani A, Karbassi AR, Fakhraee M, Heidaria M, Vaezia AR, Valikhani Z (2014) Effect of dissolved organic carbon and salinity on flocculation process of heavy metals during mixing of the Navrud River water with Caspian Seawater. *Desalination and Water Treatment* 55(4), 926-934.

Vijaya Bharathi, B., Jaya Prakash, G., Krishna, K. M., Ravi Krishna, C. H., Sivanarayana, T., Madan, K., & Annapurna, A. (2015). Protective effect of alpha glucosyl hesperidin (G-hesperidin) on chronic vanadium induced testicular toxicity and sperm nuclear DNA damage in male Sprague Dawley rats. *Andrologia*, 47(5), 568-578.

Volesky, B., & Prasetyo, I. (1994). Cadmium removal in a biosorption column. *Biotechnology and Bioengineering*, 43(11), 1010-1015.

Wahlberg, K., Love, T.M., Pineda, D., Engström, K., Watson, G.E., Thurston, S.W., Yeates, A.J., Mulhern, M.S., McSorley, E.M., Strain, J.J. and Smith, T.H. (2018). Maternal polymorphisms in glutathione-related genes are

associated with maternal mercury concentrations and early child neurodevelopment in a population with a fish-rich diet. *Environment International*, 115, 142-149.

Wanda, E. M., Gulula, L. C., & Phiri, G. (2012). Determination of characteristics and drinking water quality index in Mzuzu City, Northern Malawi. *Physics and Chemistry of the Earth, Parts A/B/C*, 50, 92-97.

Wang, T., Shen, C., Wang, N., Dai, J., Liu, Z., & Fei, Z. (2019). Adsorption of 3-Aminoacetanilide from aqueous solution by chemically modified hyper-crosslinked resins: Adsorption equilibrium, thermodynamics and selectivity. *Colloids and Surfaces A: Physicochemical and Engineering Aspects*, 575, 346-351.

Wang, J., Yi, H., Tang, X., Zhao, S., & Gao, F. (2019b). Exceptional Adsorptive Capacity and Kinetic of γ -Al₂O₃ for Selective Adsorption of NO assisted by Nonthermal Plasma. *Chemical Engineering Journal*, 378, 122095.

Wang, M., Tong, Y., Chen, C., Liu, X., Lu, Y., Zhang, W., He, W., Wang, X., Zhao, S. and Lin, Y. (2018). Ecological risk assessment to marine organisms induced by heavy metals in China's coastal waters. *Marine Pollution Bulletin*, 126, 349-356.

Wang, W., Li, M., & Zeng, Q. (2015). Adsorption of chromium (VI) by strong alkaline anion exchange fiber in a fixed-bed column: experiments and models fitting and evaluating. *Separation and Purification Technology*, 149, 16-23.

Wang, R. F., Zhu, L. M., Zhang, J., An, X. P., Yang, Y. P., Song, M., & Zhang, L. (2020). Developmental toxicity of copper in marine medaka (*Oryzias melastigma*) embryos and larvae. *Chemosphere*, 125923.

Wazir, S. M., & Ghobrial, I. (2017). Copper deficiency, a new triad: anemia, leucopenia, and myeloneuropathy. *Journal of Community Hospital Internal Medicine Perspectives*, 7(4), 265-268.

Wilk, A., Szypulska-Koziarska, D., & Wiszniewska, B. (2017). The toxicity of vanadium on gastrointestinal, urinary and reproductive system, and its influence on fertility and fetuses malformations. *Advances in Hygiene & Experimental Medicine/Postepy Higieny i Medycyny Doswiadczalnej*, 71: 850-859.

Witeska, M., Jezierska, B., & Chaber, J. (1995). The influence of cadmium on common carp embryos and larvae. *Aquaculture*, 129(1-4), 129-132.

Wold, M., Beckmann, M., Poitra, S., Espinoza, A., Longie, R., Mersereau, E., Darland, D.C. and Darland, T. (2017). The longitudinal effects of early developmental cadmium exposure on conditioned place preference and cardiovascular physiology in zebrafish. *Aquatic Toxicology*, 191, 73-84.

Wu, X., Wang, Y., Liu, J., Ma, J., & Han, R. (2010). Study of malachite green adsorption onto natural zeolite in a fixed-bed column. *Desalination and Water Treatment*, 20(1-3), 228-233.

Wu, Y., & Kong, L. (2020). Advance on toxicity of metal nickel nanoparticles. *Environmental Geochemistry and Health*, 25, 1-10.

Wu, X., Liu, C., Qi, H., Zhang, X., Dai, J., Zhang, Q., Zhang, L., Wu, Y. and Peng, X. (2016). Synthesis and adsorption properties of halloysite/carbon nanocomposites and halloysite-derived carbon nanotubes. *Applied Clay Science*, 119, 284-293.

Xia, W., Hu, J., Zhang, B., Li, Y., Wise Sr, J.P., Bassig, B.A., Zhou, A., Savitz, D.A., Xiong, C., Zhao, J. and Zhou, Y. (2016). A case-control study of maternal exposure to chromium and infant low birth weight in China. *Chemosphere*, 144, 1484-1489.

Xiang, Y., Xu, Z., Wei, Y., Zhou, Y., Yang, X., Yang, Y., Yang, J., Zhang, J., Luo, L. and Zhou, Z. (2019). Carbon-based materials as adsorbent for antibiotics removal: mechanisms and influencing factors. *Journal of Environmental Management*, 237, 128-138.

- Xing, M., Xu, L., & Wang, J. (2016). Mechanism of Co (II) adsorption by zero valent iron/graphene nanocomposite. *Journal of Hazardous Materials*, 301, 286-296.
- Xu, J., Church, S.J., Patassini, S., Begley, P., Waldvogel, H.J., Curtis, M.A., Faull, R.L., Unwin, R.D. and Cooper, G.J. (2017). Evidence for widespread, severe brain copper deficiency in Alzheimer's dementia. *Metallomics*, 9(8), 1106-1119.
- Xu, Q., Zhao, L., Wang, Y., Xie, Q., Yin, D., Feng, X., & Wang, D. (2018). Bioaccumulation characteristics of mercury in fish in the Three Gorges Reservoir, China. *Environmental Pollution*, 243, 115-126.
- Xu, X. Y., Chu, C., Fu, H., Du, X. D., Wang, P., Zheng, W., & Wang, C. C. (2018a). Light-responsive UiO-66-NH₂/Ag₃PO₄ MOF-nanoparticle composites for the capture and release of sulfamethoxazole. *Chemical Engineering Journal*, 350, 436-444.
- Xu, Z., Cai, J. G., & Pan, B. C. (2013). Mathematically modeling fixed-bed adsorption in aqueous systems. *Journal of Zhejiang University Science A*, 14(3), 155-176.
- Yan, Y. Z., Zheng, W., Huang, D. Z., Xiao, Z. Y., Park, S. S., Ha, C. S., & Zhai, S. R. (2020). Hierarchical multi-porous carbonaceous beads prepared with nano-CaCO₃ in-situ encapsulated hydrogels for efficient batch and column removal of antibiotics from water. *Microporous and Mesoporous Materials*, 293, 109830.
- Yan, G., Viraraghavan, T., & Chen, M. (2001). A new model for heavy metal removal in a biosorption column. *Adsorption Science & Technology*, 19(1), 25-43.
- Yang, X., Duan, J., Wang, L., Li, W., Guan, J., Beecham, S., & Mulcahy, D. (2015). Heavy metal pollution and health risk assessment in the Wei River in China. *Environmental Monitoring and Assessment*, 187(3), 111.
- Yargicoglu, E. N., Sadasivam, B. Y., Reddy, K. R., & Spokas, K. (2015). Physical and chemical characterization of waste wood derived biochars. *Waste Management*, 36, 256-268.
- Ye, Y., Jiao, J., Kang, D., Jiang, W., Kang, J., Ngo, H.H., Guo, W. and Liu, Y. (2019). The adsorption of phosphate using a magnesia-pullulan composite: kinetics, equilibrium, and column tests. *Environmental Science and Pollution Research*, 26(13), 13299-13310.
- Yin, Y., Zhang, P., Yue, X., Du, X., Li, W., Yin, Y., Yi, C. and Li, Y. (2018). Effect of sub-chronic exposure to lead (Pb) and *Bacillus subtilis* on *Carassius auratus gibelio*: bioaccumulation, antioxidant responses and immune responses. *Ecotoxicology and Environmental Safety*, 161, 755-762.
- Yu, H. Y., Liu, C., Zhu, J., Li, F., Deng, D. M., Wang, Q., & Liu, C. (2016). Cadmium availability in rice paddy fields from a mining area: the effects of soil properties highlighting iron fractions and pH value. *Environmental Pollution*, 209, 38-45.
- Yu, M., Li, X. J., Ma, Y. X., Liu, R. L., Liu, J. H., & Li, S. M. (2016a). Progress in research on graphene-based composite supercapacitor materials. *Journal of Materials Engineering*, 44, 101-111.
- Yusuf, M., Song, K., & Li, L. (2020). Fixed bed column and artificial neural network model to predict heavy metals adsorption dynamic on surfactant decorated graphene. *Colloids and Surfaces A: Physicochemical and Engineering Aspects*, 585, 124076.
- Zama, E. F., Zhu, Y. G., Reid, B. J., & Sun, G. X. (2017). The role of biochar properties in influencing the sorption and desorption of Pb (II), Cd (II) and As (III) in aqueous solution. *Journal of Cleaner Production*, 148, 127-136.
- Zhang, Y., Jin, F., Shen, Z., Wang, F., Lynch, R., & Al-Tabbaa, A. (2019). Adsorption of methyl tert-butyl ether (MTBE) onto ZSM-5 zeolite: Fixed-bed column tests, breakthrough curve modelling and regeneration. *Chemosphere*, 220, 422-431.

- Zhang, J., Khan, M. A., Xia, M., Abdo, A. M., Lei, W., Liao, C., & Wang, F. (2019b). Facile hydrothermal synthesis of magnetic adsorbent CoFe₂O₄/MMT to eliminate antibiotics in aqueous phase: tetracycline and ciprofloxacin. *Environmental Science and Pollution Research*, 26(1), 215-226.
- Zhang, H., Chang, Q., Han, J., Gao, S., Wu, Z., Hu, J., Yang, Y., Wei, Z., Zhang, D. and Peng, Z. (2019c). A facile synthesis of two engineered poly (vinyl alcohol) macroporous hydrogel beads for the application of Cu (II) and Pb (II) removal: batch and fixed bed column. *Materials Research Express*, 6(9), 095315.
- Zhang, X., Bai, B., Puma, G. L., Wang, H., & Suo, Y. (2016). Novel sea buckthorn biocarbon SBC@ β-FeOOH composites: efficient removal of doxycycline in aqueous solution in a fixed-bed through synergistic adsorption and heterogeneous Fenton-like reaction. *Chemical Engineering Journal*, 284, 698-707.
- Zhang, Y., Geißen, S. U., & Gal, C. (2008). Carbamazepine and diclofenac: removal in wastewater treatment plants and occurrence in water bodies. *Chemosphere*, 73(8), 1151-1161.
- Zhao, Y., Li, R., & Lin, Y. (2015). Allograft inflammatory factor-1 in grass carp (*Ctenopharyngodon idella*): Expression and response to cadmium exposure. *Fish & Shellfish Immunology*, 47(1), 444-449.
- Zheng, J. L., Yuan, S. S., Wu, C. W., & Lv, Z. M. (2016). Acute exposure to waterborne cadmium induced oxidative stress and immunotoxicity in the brain, ovary and liver of zebrafish (*Danio rerio*). *Aquatic Toxicology*, 180, 36-44.
- Zhong, W., Zhang, Y., Wu, Z., Yang, R., Chen, X., Yang, J., & Zhu, L. (2018). Health risk assessment of heavy metals in freshwater fish in the central and eastern North China. *Ecotoxicology and Environmental Safety*, 157, 343-349.
- Zhou, H., Wu, C., Huang, X., Gao, M., Wen, X., Tsuno, H., & Tanaka, H. (2010). Occurrence of selected pharmaceuticals and caffeine in sewage treatment plants and receiving rivers in Beijing, China. *Water Environment Research*, 82(11), 2239-2248.
- Zhu, Z., Wu, P., Liu, G., He, X., Qi, B., Zeng, G., Wang, W., Sun, Y. and Cui, F. (2017). Ultrahigh adsorption capacity of anionic dyes with sharp selectivity through the cationic charged hybrid nanofibrous membranes. *Chemical Engineering Journal*, 313, 957-966.
- Zhu, Z., Li, G., Zeng, G., Chen, X., Hu, D., Zhang, Y., & Sun, Y. (2015). Fast capture of methyl-dyes over hierarchical amino-Co_{0.3}Ni_{0.7}Fe₂O₄@ SiO₂ nanofibrous membranes. *Journal of Materials Chemistry A*, 3(44), 22000-22004.
- Zimmer, A. M., Barcarolli, I. F., Wood, C. M., & Bianchini, A. (2012). Waterborne copper exposure inhibits ammonia excretion and branchial carbonic anhydrase activity in euryhaline guppies acclimated to both fresh water and sea water. *Aquatic Toxicology*, 122, 172-180.
- Zojajy Pourya. 2020. Production of micro-mesoporous alternative carbonaceous adsorbents for high-efficiency sorption of the emerging organic micropollutants from wastewater effluent. MASC thesis, Concordia University
- Zojaji, P., Alhachami, H, Kariminezhad, E., Jauffur, S, Bakhshi, Z., Vaudri, MA., Sauvé, S., and Elektorowicz, M. (2019). Occurrence of organic micropollutants in the Saint Lawrence River. CSCE Conference Proceedings. Laval, QC.
- Zojaji, P., Alhachami, H, Kariminezhad, E., Jauffur, S, Bakhshi, Z., Vaudri, MA., Sauvé, S., and Elektorowicz, M. (2019a). Presence of venlafaxine, a psychiatric drug, in the vicinity of a wastewater treatment plant outfall' 54th Central Canadian Symposium on Water Quality Research, Toronto, Ontario, Canada.
- Zojaji, P., Alhachami, H, Kariminezhad, E., Jauffur, S, Bakhshi, Z., Vaudri, MA., Sauvé, S., and Elektorowicz, M. (2019b). Occurrence of psychiatric drugs in the spring flooding of the Saint Lawrence River, 33th Eastern Canadian Symposium on Water Quality Research, Montreal, Quebec, Canada.
- Zulfadhly, Z., Mashitah, M. D., & Bhatia, S. (2001). Heavy metals removal in fixed-bed column by the macro fungus *Pycnoporus sanguineus*. *Environmental Pollution*, 112(3), 463-470.

Zuo, T. T., Li, Y. L., Jin, H. Y., Gao, F., Wang, Q., Wang, Y. D., & Ma, S. C. (2018). HPLC–ICP-MS speciation analysis and risk assessment of arsenic in *Cordyceps sinensis*. *Chinese Medicine*, 13(1), 19.

Zwolak, I., & Gołębiewska, D. (2018). Protective activity of pyruvate against vanadium-dependent cytotoxicity in Chinese hamster ovary (CHO-K1) cells. *Toxicology and Industrial Health*, 34(5), 283-292.